NUI MAYNOOTH

Ollscoil na hÉireann Má Nuad

Proteomic Profiling of skeletal muscle tissue from the Goto-Kakizaki rat model of type 2 diabetes

Submitted to National University of Ireland Maynooth for the degree of Doctor of Philosophy

Edel Mullen, B.Sc

Head of Department
Professor Kay Ohlendieck
Department of Biology
NUIM
Co. Kildare

Supervisor
Professor Kay Ohlendieck
Department of Biology
NUIM
Co. Kildare

Table of Contents

"I was taught that the way of progress is neither swift nor easy."

Marie Curie

Acknowledgements

I would like to express my thanks to the people who have been very helpful to me during the time it took me to write this thesis.

Many thanks go to Professor Kay Ohlendieck for his guidance throughout the last three years.

I would like to thank Dr. Joan Gannon, Dr. Kathleen O'Connell, Dr. Philip Doran, Dr. Caroline Lewis and Dr. Pamela Donoghue for their advice and assistance in numerous ways. I am also very grateful to Dr. Peter Mowlds for his constant pushing and coercion into remembering how important social outlets are.

To all the members of the muscle lab both past and present, thank you.

I would also like to extend thanks to the staff and members and lecturers of the biology department in NUIM who were always quick to help when asked.

This thesis would not have been possible without the help and indulgence of good friends (Rachel, Emma, Poor Brian, Wayne, Fiachra, Tang, Eimear, Yvonne) who came to realize that for me, science is a way of life and not just a job.

I cannot end without thanking my family, my sisters Louise and Grace and my brother-in-law Clayton, whose encouragement and understanding helped me a lot. I would like to mention my nephew Logan and niece Amelia who make me smile. I would like to thank my Nanny Mullen who is my inspiration and my Nanny Connie for reminding me that youth is precious.

Finally I would like to thank my parents Catherine and Brendan, who helped me when I thought I couldn't do it, who rescued me from myself and who have always been proud of me.

It is to my parents that I dedicate this work.

Declaration

This thesis has not been submitted in whole or part to this or any other university for any degree, and is the original work of the author except where stated.

Signed _____

Date _____

Abbreviations

2D	Two-dimensional
2DGE	Two-dimensional gel electrophoresis
ACN	Acetonitrile
APS	Ammonium persulphate
ATP	Adenosine Triphosphate
Bromophenol Blue	3',3",5',5" tetrabromophenolsulfonphthalien
CA	Carbonic Anhydrase
CCB	Colloidal Coomassie Blue
CHAPS	(3-[(3-Choamidoproply)-Dimethylammonio]-1-Propane sulfonate)
Cy	Cyanine
dH_2O	Distilled water
DHPR	Dihydropyridine receptor

DIGE	Difference in-gel electrophoresis
DMF	Dimethylformamide
DTT	Dithiothreitol
EDTA	Ethylenediamineteraacetic acid
ER	Endoplasmic reticulum
ESI	Electrospray Ionisation
$FADH_2$	Flavin adenine dinucleotide
FFAs	Free Fatty Acids
Gt	Goat
GTP	Guanidine Triphosphate
h	Hour(s)
HB	Homogenisation Buffer
HCl	Hydrochloric acid
Hepes	(N-[2Hydroxyethyl]piperazine-N'-[2-ethanesulfonic acid])
HRP	Horseradish peroxidase
IEF	Isoelectric Focusing
L	Litre
LC	Liquid Chromatography
MALDI	Matrix assisted laser desorption/ionization
MDH	Malate dehydrogenase
Min(s)	minute(s)
MS	Mass spectrometry

Mus	Mouse
Mt	Mitochondrial
ml	Millilitre
NADH	Nicotinamide adenine dinucleotide
ng	Nanograms
PAGE	Polyacrylamide gel electrophoresis
PBS	Phosphate Buffered Saline
PEP	Phosphoenolpyruvate
p*I*	Isoelectric point
PIC	Protease Inhibitor Cocktail
PMF	Peptide Mass Fingerprint
Rb	Rabbit
RPLC	Reverse phase liquid chromatography
RyR	Ryanodine Receptor
s	Second(s)
SERCA	Sarcoplasmic (Endoplasmic) Reticulum Calcium ATPase
SDHA	Succinate dehydrogenase
SDS	Sodium dodecyl sulphate
Shp	Sheep
SR	Sarcoplasmic reticulum
TEMED	N,N,N',N'-tetramethylethylenediamine
TFA	Trifluoroacetic acid

TpC	Troponin C
T-Tubules	Transverse tubules
T2D	Type 2 Diabetes

Abstract

The primary features of type 2 diabetes (T2D) are both insulin resistance and impaired beta cell function. Abnormal glucose handling and variable degrees of peripheral insulin resistance characterise T2D. Skeletal muscle is the largest insulin-regulated glucose sink in the body and represents approximately 80% of whole body insulin-stimulated glucose uptake. As a result a fundamental aspect of T2D is abnormal glucose disposal in contractile tissues triggering metabolic dysregulation and glucotoxic side effects. The significance of skeletal muscle to T2D has prompted research into the perturbed glucose handling mechanisms in suitable animal models, such as muscle tissues from the spontaneously diabetic Goto-Kakizaki rat. Highly sensitive protein analysis techniques such as fluorescence difference in-gel electrophoresis (DIGE) and electrospray ionization liquid chromatography mass spectrometry (ESI LC/MS) were employed to analysis the diabetic muscle tissue proteome and sub-proteome. A differential

expression pattern was observed for proteins involved in glycolysis, the citric acid cycle, oxidative phosphorylation, lipolytic catabolism, the contractile apparatus, cellular detoxification mechanisms and the stress response. These findings demonstrate a perturbed protein expression pattern in diabetic skeletal muscle, which reflects underlying molecular alterations. Over all this study has supplied several potential biomarkers of T2D and adds further knowledge to the mechanism of a complex metabolic disorder.

Chapter 1

Introduction

1 Introduction

1.1 Muscle

Movement is a diverse and fundamental trait of living organisms. In higher organisms muscle contraction is responsible for movement and has evolved to meet a wide variety of functions that require a vast spectrum of differences in execution. Muscle tissue is responsible for providing and facilitating some of the body's most important functions such as contraction, relaxation, metabolism, heat production, and energy conservation. As a result, skeletal muscle accounts for approximately 40% of mammalian body mass and at least 25% of whole body protein turnover occurs in this tissue (Waterlow, J 1976). Muscle can be categorised into four distinct groups (skeletal, cardiac, smooth and myoepithelial) based on morphology, location, and performance and in their mechanisms of activation in order to generate contraction. Both skeletal muscle and cardiac muscle are striated: they have striations, or strips that extend across the width of the muscle fibres. Skeletal muscles are generally attached to bone. It is this tissue that is responsible for short bursts of voluntary movement or prolonged contractions. Continuous activity is the main characteristic of cardiac muscle. It can function continuously as it is highly resistant to fatigue due to its large number of mitochondria. Intercalated disks are unique to cardiac tissue and function in maintaining the synchronised contraction of the short, striated muscle fibres. Both cardiac and smooth muscle are involuntary, as they are not controlled by the somatic nervous system. Unlike cardiac and skeletal muscle fibres, smooth muscle fibres are not striated or rectangular, but spindle shaped.

Smooth muscle fibres are over lapped and layered unlike the bundling experienced by skeletal and cardiac tissues. Myoepithelial cells form the basal layer of the epithelium in mammary glands, lactiferous sinuses and ducts. They can contract and they unequivocally composed of the key fundamental structural proteins involved in muscle contraction. It is the different arrangements of the contractile apparatus in each muscle type that provides their contractile specificity.

1.1.1 Skeletal Muscle

Skeletal muscle is anchored to the skeleton by tendons and is used to affect movement and posture by contraction or relaxation of the muscle. Muscle tissue is created by the formation of bundles of fibres sheathed in connective tissue. Each muscle cell or fibre can vary greatly in size, with human skeletal muscle fibres measuring up to several centimeters in length and 100□m in diameter. Figure 1.1 shows how skeletal muscle is made up of many individual fibres. Each fibre consists of approximately a thousand rectangular rod-like structures, known as myofibrils (Engel, *et al*., 2005). Each fibre is multinucleated cellular structure, formed by the fusion of several myoblast cells during development. The elongation of the growing myofibre navigates towards tendon cells giving rise to stable attachments between muscles, epidermis and cuticle (Schejter *et al.*, 2010) The sarcomere is the core element of the contractile apparatus and is found in the myofibril. The sarcomere is roughly 2.4□m in length and is made up of thick and thin contractile myofilaments, which occur, in an overlapped

arrangement. The thick and thin filaments found in the sarcomere are also known as the myosin and actin filaments, respectively. The overlapped arrangement of these filaments generates a regular pattern of light and dark strips, which results in the striated appearance of skeletal and cardiac muscle.

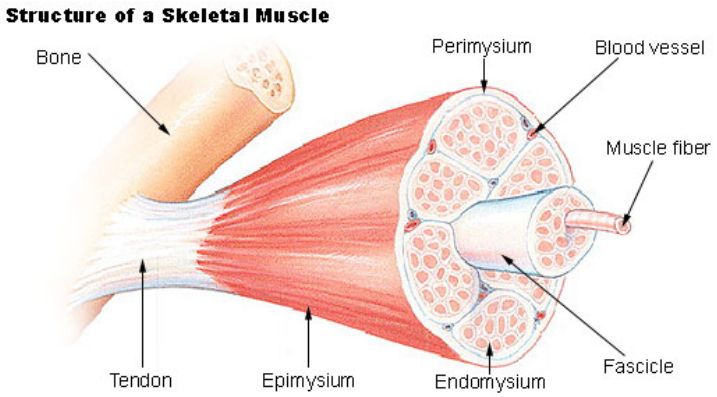

Figure 1.1: The basic structure of muscle. A complex unit comprising of bundles of multinucleate cells called fibres.
http://training.seer.cancer.gov/module_anatomy/

The sarcomere is often divided up into different zones to illustrate how it behaves during muscle contraction. The Z-line separates each sarcomere. The H-zone is the center of the sarcomere and the M-line is where adjacent myosin filaments anchor on to each other. The H-zone appears only when the sarcomere is in a resting state. The darker A-bands are where myosin filaments align and the lighter I-bands are where actin filaments align. When muscle contracts the H-zone and I-band both decrease as the Z-lines are pulled towards each other. Figure 1.2 shows a longitudinal section through skeletal muscle.

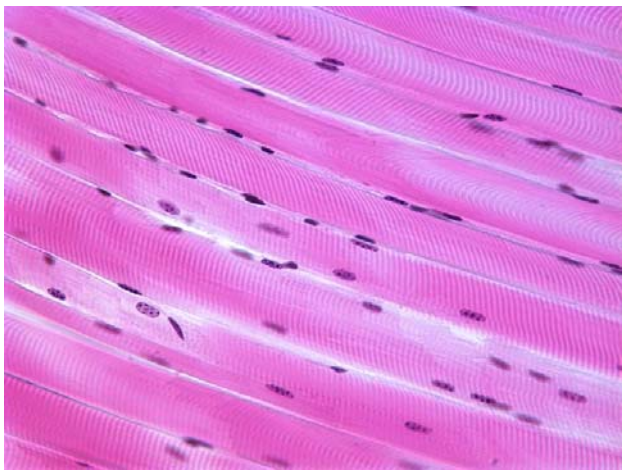

Figure 1.2: Longitudinal section of skeletal muscle.
http://www.drsharma.ca/tag/skeletal-muscle

1.1.2 Sliding Filament Hypothesis

Thin filaments are made up of two actin strands, which intertwine to form an alpha helical structure. Bound to the helix are the proteins tropomyosin and troponin. The protein tropomyosin inhibits muscle contraction by blocking the interaction of myosin with actin. Troponin is a thin-filament protein that regulates the response of myofilaments to calcium. Troponin is a complex composed of TnT (the tropomyosin binding subunit), TnC (the calcium binding subunit) and TnI (prevents the myosin head attachment to F-actin). In 1942 Straub discovered two conformational forms of actin, one as a monomer (globular or G-actin) and the other as a polymer (filamentous or F-actin). F-actin is the type of actin present in skeletal muscle. According to Asakura (1961) polymerisation of the filamentous actin is associated with ATP hydrolysis. Upon stimulation, Ca^{2+} is released from internal stores and binds to troponin, which induces a conformational change of

tropomyosin, moving it from actin allowing actin-myosin interaction (Reedy *et al*., 1965; Moore *et al*., 1970).

The thick filament is composed of a bundle of protein strands called myosin filaments. Myosin is responsible for approximately one third of skeletal muscle mass. Myosin can be separated into two components via tryptic digestion (Szent-Gyorgi, 1953). Light meromyosin (LMM) is the smaller of the two stands and heavy meromyosin (HMM) is the bigger. LMM is utilised during filament formation, and HMM contains the sites for actin interactions. Each myosin filament consists of two globular heads (also known as the myosin head), and a single tail formed by two strands twisted to create a double helical arrangement. The tail of each myosin molecule lies along the axis of the thick filament, and the two globular heads extend out to the sides, to form the cross-bridges that occur during muscle action with specialised active sites in the actin filaments. Each myosin head contains two binding sites, one for ATP and one for actin. The ATP binding site contains ATPase which binds and hydrolyses the ATP (Nigg and Herzog, 1994). The hydrolysis of ATP (the conversion of ATP to ADP via the loss of one phosphate) provides the energy for the cross-bridge to move. In other words the myosin head pivots and pulls the actin filament towards the centre of the sarcomere. This motion is commonly known as the power stroke (Reedy, *et al*., 2000). The ADP, now present in the myosin cleft, is replaced with another ATP molecule which forces the actin and myosin apart. The hydrolysis of this ATP molecule will begin another binding overlapping cycle pushing the actin filament along and resulting in contraction of the cell. When the ATP is released

the myosin head returns to its low energy form configuration. The relaxation changes the angle of the myosin head to the fibrous myosin tail (Huxley, 1954). Shortening of the sarcomere and contraction will continue until there is a lack of calcium ions or ATP (Figure 1.3). The higher the frequency of this shortening of the sarcomere, the shorter the myofibrils become, allowing the entire muscle to contract and also grading the strength of the contraction (Huxley, *et al*., 2004).

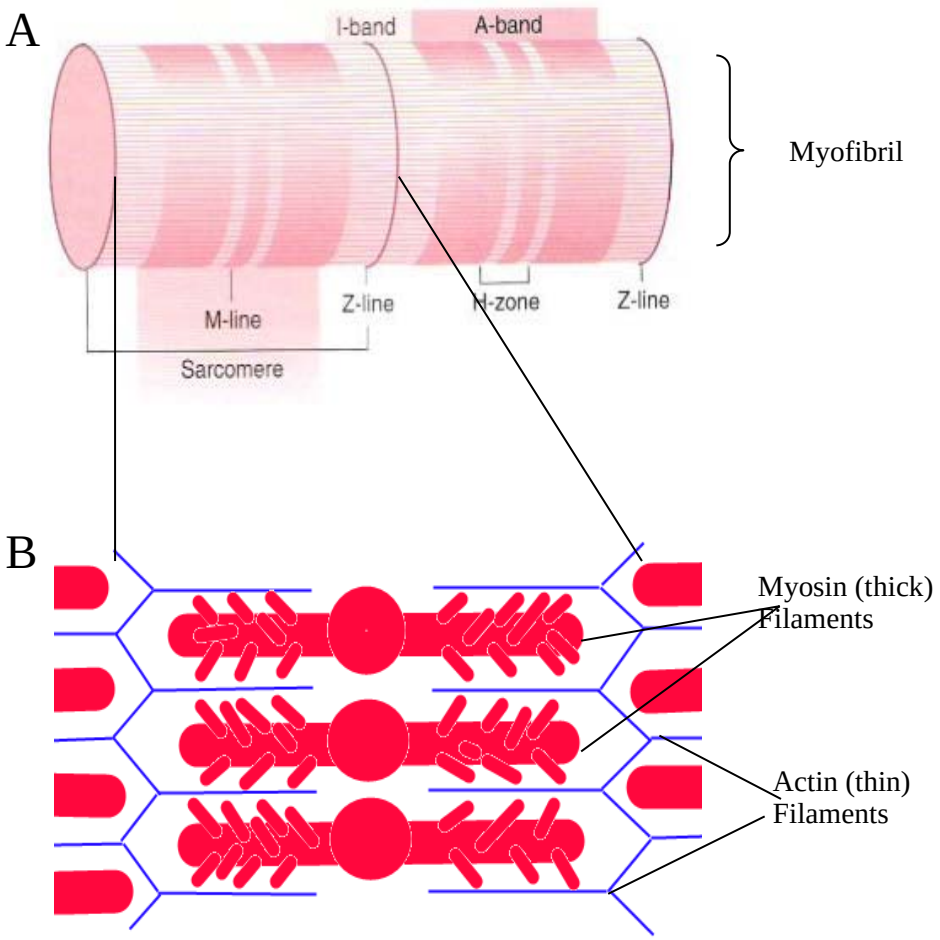

Figure 1.3: A schematic representation of the microstructure of the myofibril. Each Muscle fibre (or cell) is made up of about 75-120 rod-like structures, termed myofibrils. A Illustrates the banding pattern of the contractile unit, the sarcomere. The I-bands of alpha-actinin and desmin mark the borders between the sarcomeres. The Z-lines are made up of actin. The A-band is made from myosin and actin filaments. B shows the arrangement structure of the thick and thin filaments within a single sarcomere.

Adapted from: http://www.sport-fitness-advisor.com/muscle-anatomy.html

1.1.2.1 Excitation Contraction Coupling

The association between excitation of the muscle cell membrane and contraction has been termed excitation-contraction coupling. Voluntary muscle contraction originates in the motor cortex of the brain and is conducted through the somatic nervous system as an electrical signal. Therefore, contraction starts at the neuromuscular junction. The neuromuscular junction is the point at which nerve and muscle meet. Here, the electrical signal must be converted into a chemical one in order for it to pass across the synapse between the motor neuron and the muscle. At the surface of the muscle fibre, the axon splits into a number of short invaginations containing synaptic vesicles. These synaptic vesicles, which can be seen in Figure 1.4, contain the neurotransmitter acetylcholine (ACh), which bridges the gap between the neuron and the muscle. ACh is a chemical substance which transmits nerve impulses across a synapse. The area of the muscle fibre membrane that is located directly beneath the axon is also folded into junctional folds, in a bid to increase the surface area of the membrane exposed to respond to the ACh. An action potential passes down the motor neuron and when it arrives at the axon terminal causes the release Ca^{2+} that in turn affects the release of the stored ACh, which traverses the synapse and binds to the post-synaptic acetylcholine receptors in the junctional folds. Activation of these receptors causes localised depolarisation (Farley *et al*. 1977) leading to the opening of sodium and potassium channels. Since more sodium enters the cytosol than potassium leaves the muscle, the sarcolemma becomes

depolarised (Hodgkin *et al.* 1960), causing an action potential that passes along the membrane into transverse tubules (T-tubules), which are invaginations of the sarcolemma between the termini of two sarcoplasmic reticuli.

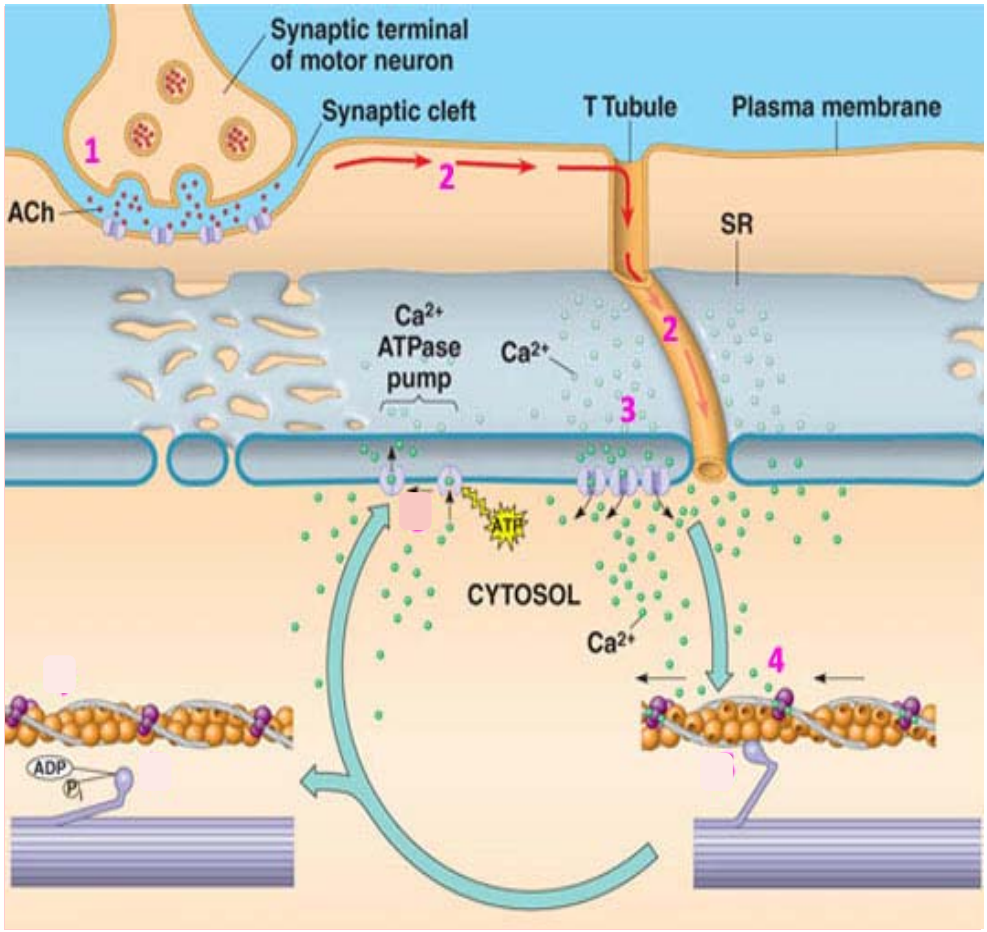

Figure 1.4: Contraction begins at the neuromuscular junction. 1 The neurotransmitter ACh is released from the axon and it then diffuses across the synaptic cleft and attaches to receptors on the sarcolemma. **2** An action potential is propagated along the sarcolemma and down the T-tubules. **3** The action potential triggers the release of Ca^{2+} from the sarcoplasmic reticulum. **4** Ca^{2+} binds to tropomyosin allowing it to bind to actin which inititates contraction.
http://www.bio.miami.edu/~cmallery/150/neuro/c49x36contraction-cycle.htm

The two proteins of central importance in excitation-contraction coupling are the Ryanodine receptor 1 (skeletal isoform) (RyR1) and the α_{1s}-Dihydropyridine receptor (skeletal isoform) (α_{1s}-DHPR). The action potential is sensed by the II-III loop of the voltage sensing α_{1s} subunit of the DHP receptor, which is present in the T-tubules. Once depolarisation is detected the receptor undergoes a conformational change allowing it to interact with the cytoplasmic portion of the RyR1 receptor (Proenza *et al*. 2002), which is on the sarcoplasmic reticulum membrane. This reaction triggers the RyR to open its calcium channels allowing the influx of calcium ions into the cytoplasm of the muscle cell. These calcium ions interact with TpC causing structural changes to tropomyosin allowing for the interaction of the myosin head of the thick filament to interact with the actin of the thin filament (Tao *et al*. 1990). This interaction forms the cross bridges between the filaments (Huxley *et al*. 1954). The more filaments that the cross bridges occur in at any one time the shorter the myofibrils become, allowing not only the entire muscle to contract but also a grading of the strength of contraction. Once the sarcolemma returns to its resting potential the calcium channel RyR closes and various ATPases such as SERCA (sarcoplasmic (endoplasmic) reticulum calcium ATPase) removes calcium back into the sarcoplasmic reticulum (Heegaard *et al*. 1990). Because of the decline in the availability of calcium the calcium ions bound to troponin are released and tropomyosin returns to its normal conformation, which prevents any cross bridges from being formed and the muscle relaxes.

1.2 Glucose Metabolism

Few physiological parameters are more vigilantly regulated in humans than blood glucose concentration. The main cellular mechanism that moderates blood glucose is insulin-stimulated glucose transport into skeletal muscle. Glucose is stored in skeletal muscle as glycogen where it is oxidized to produce energy. GLUT 4 is the paramount transporter protein, which specializes in glucose uptake and therefore plays a key role in regulating whole body glucose homeostasis.

1.2.1 Glycolysis

Glycolysis is the anaerobic catabolism of glucose. The mechanism involves the conversion of one molecule of glucose into two molecules of pyruvate. The C3 pyruvate is then converted to acetyl coenzyme A (CoA), ready for entry into the citric acid cycle. Two ATP molecules are necessary for the reactions that occur in the priming stages of glycolysis. Glucose is phosphorylated to form glucose 6-phosphate by ATP, which becomes ADP. This reaction is catalyzed by the enzyme hexokinase. Phosphoglucoisomerase then mediates the isomerization of glucose 6-phosphate to fructose 6-phosphate which involves the conversion of an aldose to a ketose. The second ATP molecule then phosphorylates fructose 6-phosphate to form fructose 1,6-bisphosphate and ADP. Phosphofructokinase catalyzes this step. The 6 carbon molecule fructose 1,6-bisphosphate is split into two 3 carbon molecules, glyceraldehyde 3-phosphate and dihydroxyacetone phosphate, by the enzyme aldolase. Glyceraldehyde-3-phosphate is converted to 1,3-bisphosphoglycerate. This reaction is catalyzed by glyceraldehyde-3-

phosphate dehydrogenase and uses inorganic phosphate and NAD^+. NADH is the other product of this reaction. The oxidation of the aldehyde group of the glyceraldehyde 3-phosphate generates enough energy to make the conversion to 1,3-bisphosphoglycerate. The energy is utilised in the generation of a new high-energy phosphate bond. This new bond is now used to synthesize ATP. Phosphoglycerate kinase catalyzes the transfer of the phosphoryl group from the 1,3-bisphosphoglycerate to ADP generating ATP and 3-phosphoglycerate. 2-phosphoglycerate is generated from the movement of the phosphate group from carbon 3 to carbon 2 within the same molecule. The enzyme phosphoglycerate mutase is responsible for the shift from 3-phosphoglycerate to 2-phosphoglycerate. The low-energy phosphate ester bond of 2-phosphoglycerate is converted to the high-energy phosphate bond of phosphoenolpyruvate (PEP) by the dehydration action of the enzyme enolase. The last reaction of glycolysis involves pyruvate kinase catalyzing the irreversible transfer of the phosphoryl group from PEP to ADP to form pyruvate and ATP. Glycolysis releases relatively little of the energy present in a glucose molecule, however the high density of glycolytic enzymes present in muscle tissue shows how the system is effective at releasing sufficient energy from the molecule under aerobic conditions. Much more of that trapped energy is released by the subsequent operation of the citric acid cycle and oxidative phosphorylation.

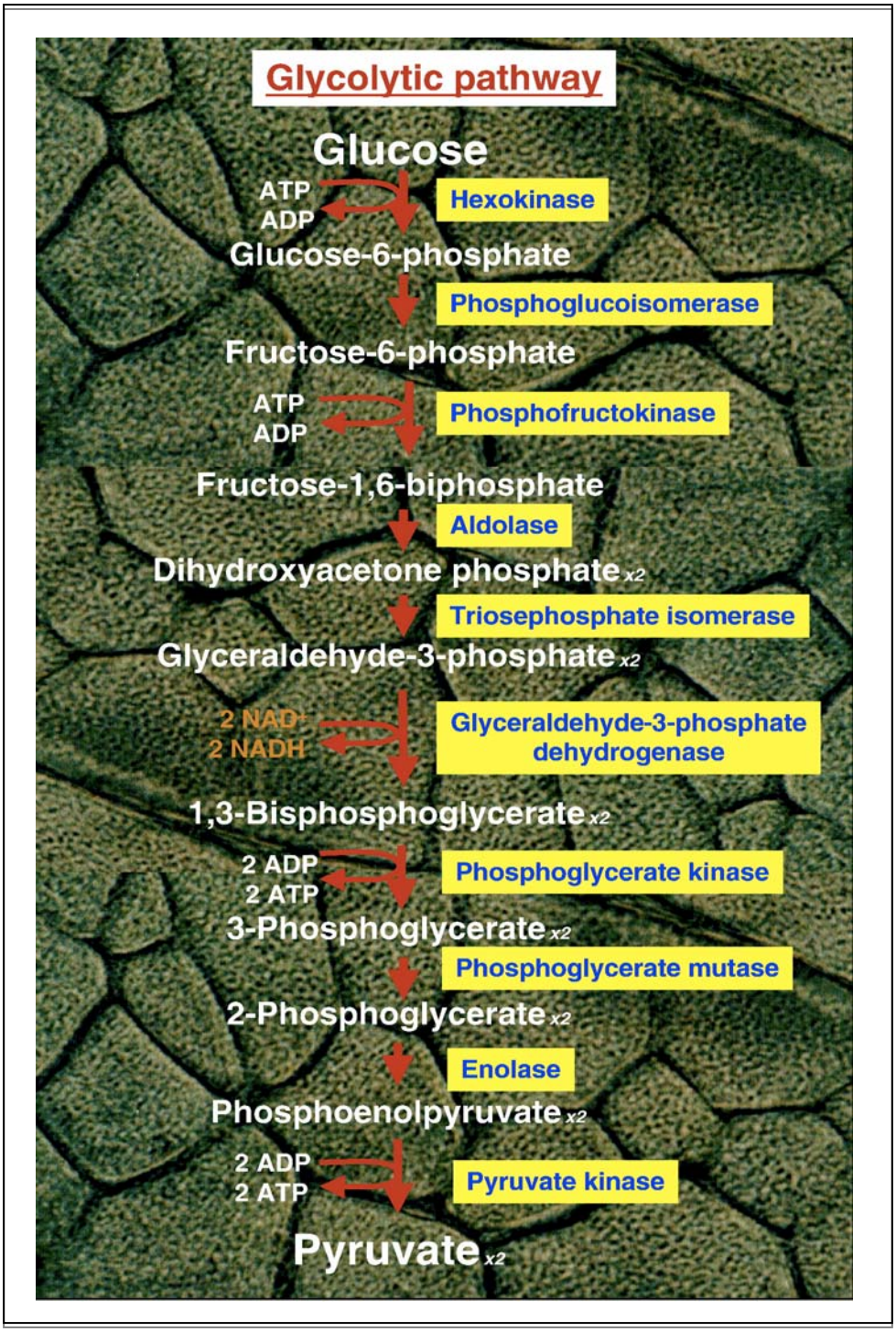

Figure 1.5: Summary of the enzymatic steps of glycolysis. The various enzymes and their biochemical reactions involved in the glycolytic pathway are listed in the flowchart (Ohlendieck, *et al*., 2010). The backround shows a bright field image of a transverse section through adult rabbit biceps femoris muscle.

1.2.3 Citric Acid Cycle

Acetyl CoA is one of the key intermediates in the interconversion of small organic acids. Acetyl CoA is formed by the oxidative decarboxylation of pyruvate with the release of CO_2. The reaction is catalyzed by the pyruvate dehydrogenase enzyme complex (3 enzymes and 5 coenzymes). During the conversion of pyruvate to Acetyl CoA NAD+ is reduced to NADH. The pathway known as the citric acid cycle, the tricarboxylic acid cycle (TCA), or the Krebs cycle (after Hans Krebs who discovered it in the 1930s), carries out the oxidation of acetyl groups from acetyl CoA to CO2 with the production of four pairs of electrons. The cycle operates in the mitochondria of eukaryotes and in the cytosol of prokaryotes. The cycle has eight stages.

I. Citrate (6C) is formed from the irreversible condensation of acetyl CoA (2C) and oxaloacetate (4C) which is catalyzed by citrate synthase.

II. Citrate is converted into isocitrate (6C) by an izomerisation catalyzed by aconitase.

III. Isocitrate is oxidized to a-ketoglutarate (5C) and CO_2 by isocitrate dehydrogenase. This is a mitochondrial enzyme that requires NAD+, which is reduced to NADH.

IV. □-Ketogluterate is oxidized to succinyl CoA (4C) and CO_2 by the □-ketogluterate dehydrogenase complex. This complex utilises 3 enzymes NAD^+ as a cofactor.

V. Succinyl CoA is converted to succinate (4C) by succinyl CoA synthase. The

reaction uses the energy from the cleavage of the succinyl-CoA bond to synthesize GTP from P_i and GDP. GTP is guanosine triphosphate one for which is equivalent to one ATP.

VI. Succinate is oxidized to fumarate (4C) by succinate dehydrogenase. The only membrane-bound enzyme in the citric acid cycle is succinate dehydrogenase and is embedded in the inner mitochondrial membrane. FAD is tightly bound to the enzyme and is reduced to produce $FADH_2$.

VII. Fumarate is converted to malate (4C) by fumarase; this reaction is a rehydration reaction involving the addition of a water molecule.

VIII. Malate is oxaloacetate (4C) by malate dehydrogenase. NAD^+ is again required by the enzyme as a cofactor to accept the free pair of electrons and produce NADH.

The NADH and $FADH_2$ produced by the citric acid cycle are re-oxidized and the energy generated is used to synthesize ATP by oxidative phosphorylation. The citric acid cycle is portrayed diagrammatically in Figure 1.6.

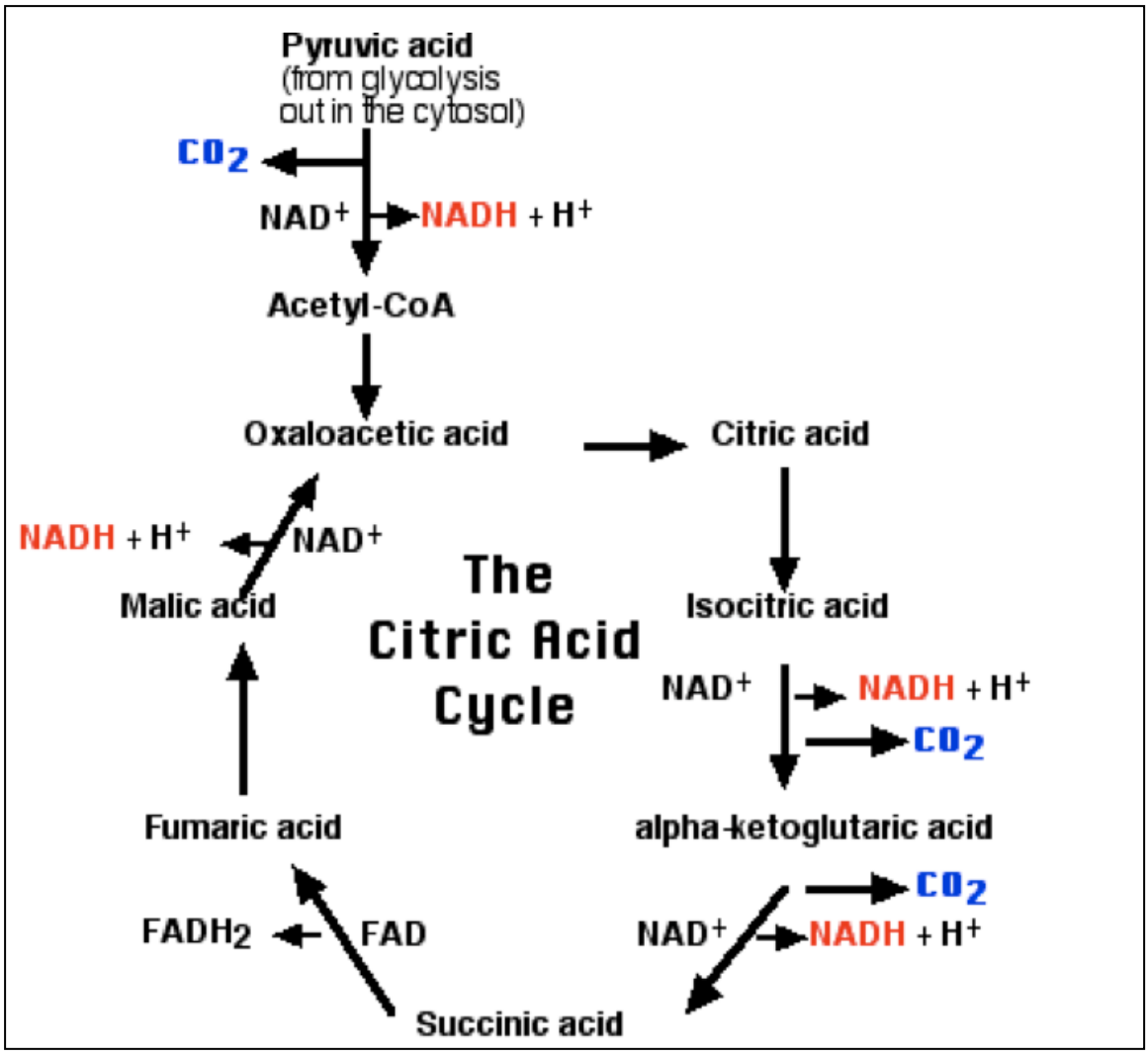

Figure 1.6: Summary of the enzymatic steps of the citric acid cycle. The various enzymes and their biochemical reactions involved in the cycle are listed in the flowchart.

http://users.rcn.com/jkimball.ma.ultranet/BiologyPages/C/CellularRespiration.html

1.2.4 Oxidative Phosphorylation and Electron Transport.

Electron transport and oxidative phosphorylation occur in the inner membrane of mitochondria. These events re-oxidize the NADH and the FADH2 that arise from the citric acid cycle and glycolysis and trap the energy released as ATP. Oxidative phosphorylation is by far the major source of ATP in the cell. The

oxidation of a molecule involves the loss of electrons and reduction involves the gain of electrons. So if one molecule is oxidized another must be reduced.

The oxidation of NADH releases sufficient energy to drive the synthesis of several molecules of ATP. Electrons are transferred from NADH to oxygen along a chain of electron carriers collectively called the electron transport chain. NADH dehydrogenase, the cytochrome bc1 complex and cytochrome oxidase are large protein complexes embedded in the inner mitochondrial membrane and constitute the main part of the electron transport chain. Electrons are carried from NADH to oxygen.

Oxidative phosphorylation does not involve phosphorylated intermediates. In 1961 Mitchell reported that energy liberated by electron transport is used to create a proton gradient across the inner membrane of the mitochondria. This gradient was suggested to couple electron transport and ATP synthesis. ATP synthase is the enzyme responsible for ATP synthesis.

H^+ ions are pumped out of the mitochondrial matrix across the inner mitochondrial membrane into the intermembrane space. NADH dehydrogenase, cytochrome bc1 complex and cytochrome oxidase are the H^+ pumps that force the H^+ ions into the intermembrane space. A higher concentration of H^+ ions in the intermembrane space and an electrical potential, with the side of the inner mitochondrial membrane facing the intermembrane space being positive is generated by the three H^+ pumps. An electrochemical proton gradient is formed. The protons flow back into the mitochondrial matrix through ATP synthase which is the driving force for ATP synthesis. Because $FADH_2$ is reoxidised via

ubiquinone, its oxidation causes H^+ ions to be pumped out only by the cytochrome *bc*1 complex and cytochrome oxidase and so the amount of ATP made from $FADH_2$ is less than from NADH. 3 ATP molecules are synthesized for every NADH oxidised and 2 ATPs are made per FADH2 oxidation.

Electron transport is normally tightly coupled to ATP synthesis. Therefore ATP is not synthesized unless electron transport is occurring to provide the proton gradient.

1.3 Insulin Signaling

Blood glucose levels are controlled in mammals by a hormone called insulin. When glucose levels in the blood are high and need to be decreased insulin is secreted from the β cells of the pancreas and stimulates glucose influx and general increase in glucose metabolism in muscle and adipocytes. Insulin also inhibits gluconeogenesis by the liver. Gluconeogenesis synthesizes glucose from non-carbohydrate predecessor and is of importance for the maintenance of blood glucose levels during times of starvation. The insulin receptor mediates all insulin signalling within the cell.

1.3.1 Insulin Receptor

The insulin receptor is a transmembrane glycoprotein with an inherent protein tyrosine kinase activity, which is reflected by the serum concentration of insulin. The insulin receptor is composed of two □-subunits that are each linked to a β-subunit. Disulfide bridges link them to each other. The □-subunits are located

entirely outside the cell and contain the insulin binding sites, whereas the intracellular portion of the β-subunit contains the insulin-regulated tyrosine protein kinase. The insulin receptor family contains two other structurally related molecules, the insulin-like growth factor (IGF-1) receptor, and the insulin receptor-related receptor, which is an orphan receptor. These receptors share approximately 80% sequence homology in the kinase domain but low homology in the extracellular domain (Shier, *et al*., 1989). The external ligand-binding domain of the insulin receptor is linked to the tyrosine kinase by a single transmembrane fragment, which can adapt well to structural changes or substitutions (Frattali, *et al*., 1991). The intracellular juxtamembrane region is one of the several functional regions established in the β-subunit. An ATP binding domain, a regulatory region and the COOH terminus have also been determined. The juxtamembrane region has been shown to be essential for signal transmission (Lee, *et al*., 1993). Insulin binds to the insulin receptor, which causes the autophosphorylation of tyrosine residues and tyrosine phosphorylation of insulin receptor substrates such as IRS1 and Shc. This is mediated by the insulin receptor tyrosine kinase. Tyrosine autophosphorylation appears to occur through a transmembrane mechanism, in which insulin binding to the α-subunit of one of the αβ-dimers stimulates the phosphorylation of the adjacent covalently linked β-subunit (Hotamisigil, *et* al., 1993). The autophosphorylation permits the interaction of IRSs with downstream molecules such as PI-3K due to its Srchomology 2 (SH2) domains leading to end point events such as GLUT 4 translocation.

Signal transduction is one of the functions of the insulin receptor. Endocytosis of the insulin-receptor complex leads to insulin degradation. Acidification of the endosomal lumen due to proton pumps, results in the dissociation of insulin from its receptor. Most unoccupied receptors recycle to the plasma membrane, but after lengthily exposure and stimulation to insulin the receptor itself is degraded (Backer *et al*., 1990).

1.4 Diabetes

Type 2 diabetes and other associated traits such as obesity; hypertension, glucotoxicity and dyslipidemias have become an epic challenge for worldwide health care systems. An estimated $132 billion dollars was spent on the management of diabetic conditions and lost productivity in the year 2002 in the United States of America alone. According to Hogan *et al* (2003) $91.8 billion was spent on direct medical expenditures alone. These encompassed $44.1 billion for the excess prevalence of general medical conditions, 24.6 billion on chronic complications attributable to diabetes and 23.2 billion on diabetes care. Clearly a greater understanding for a condition reaching endemic proportions is merit enough for both proteomic and genetic research. Unraveling the genetic causes of type 2 diabetes (T2D) will lead to the identification of new therapeutic targets, which will then affect the methods used to treat the disabling and life-threatening complications of the disease.

1.4.1 Type 2 Diabetes

Type 2 diabetes is a heterogeneous condition of polygenic beginnings. It is the most common form of diabetes and involves both defective insulin secretion and

insulin resistance. It is a metabolic disorder that is characterized by high blood glucose levels. Type 2 diabetes mellitus represents a highly complex and heterogeneous disease that is affected by both intrinsic and extrinsic factors, which affect muscle metabolism and strength making it a physical disability. Modern lifestyles are commonly believed to play an important role in the establishment of type 2 diabetes due to high fat, high sugar diets paired with little or no exercise. Obesity-associated metabolic complications play a fundamental role in the development and progression of this disease. The pathophysiology of type 2 diabetes involves defects in tissue sensitivity to insulin and decreased insulin secretion. Type 2 diabetes entails progressive deterioration in β cell function (Porte *et al*., 2001, Leahy *et al*., 2005), associated with loss of β cell mass due to apoptosis (Steil *et al*., 2001). Type 2 diabetes patients often develop type 2 diabetes related complaints such as, hyperglycemia (high blood sugar), dyslipidemia (high levels of lipids and lipoproteins in the blood, glucotoxicity (describes the effect of long-term hyperglycemia on β cell function) and lipotoxicity, which make the disease harder to treat.

1.4.1.1 Obesity

Modern sedentary lifestyle and obesity-associated metabolic complications clearly play a role in the progression of type 2 diabetes. Obesity is defined as a BMI (body mass index) greater than 30. It is estimated that 20% of adult Americans are clinically obese. Free fatty acids (FFA) are known to play crucial physiological roles in skeletal muscle, heart, liver and pancreas. FFA

concentrations are commonly elevated in obese individuals. This is believed to be due to a increased FFA release which is associated with an expansion in fat mass (Jensen *et al*., 1989). Elevated FFAs have been shown to be a good predictive marker for the transition of patients from impaired glucose tolerance (IGT) to type 2 diabetes as FFA's are commonly elevated in type 2 diabetes patients. A reduced oxidative enzyme capacity of skeletal muscle has been found in type 2 diabetes as well as in obesity that is not complicated by diabetes. Approximately 80% of people with type 2 diabetes are obese, with nearly all being insulin resistant (Boden *et al*., 2003). There is a strong relationship between increased plasma FFA, intramyocellular lipid accumulation and insulin resistance (Perseghin *et al*., 1997). High plasma FFA concentrations are associated with a number of cardiovascular risk factors linked to insulin resistance including hypertension (chronic high blood pressure) and dyslipidaemia (high levels of lipid and lipoproteins in the blood).

1.4.1.2 Animal Models of Diabetes

The Goto-Kakizaki rat inbred model was developed by Tohoku University in 1975 by selective breeding of an outbred colony of Wistar rats. Oral glucose tolerance test where performed and animals with high glucose levels were selected for further breeding. This animal model is spontaneously diabetic and experiences unabating insulin signalling (Krook *et al*., 1997) which usually transpire by 4 weeks of age. These animals have been well characterised and have been reported to experience increased blood glucose levels without adjustments in

non-fasting plasma insulin levels (Witte *et al*., 2002), a reduced employment of GLUT 4 the glucose transporter (Mulvey *et al.,* 2005), abnormal mitochondrial functioning (Shen et al., 2008), a reduced percentage of oxidative fibres (Yasuda *et al.,* 2002) and an inhibition of insulin-receptor autophosphorylation. In GK rats, the neonatal β cell-mass deficit is considered to be the primary defect leading to basal hyperglycaemia, which is detectable around 3.5 weeks of age. After 8 weeks, hyperglycaemia deteriorates and glucose-stimulated insulin release by the islets is more severely impaired (Suzuki *et al.,* 1997). Heritability of defective β-cell mass and its function in the GK model is thought to reflect the complex interactions of the following pathogenic factors: (a) three independent loci containing genes responsible for impaired insulin secretion; (b) heritable gestational metabolic (hyperglycaemic) impairment inducing deficiency in endocrine pancreas; and (c) secondary (acquired) loss of β–cell differentiation due to long-term exposure to hyperglycaemia (glucotoxicity) (Portha *et al*., 2003). Prolonged exposure to hyperglycaemia is one of Key factors in the induction of progressive diabetic nephropathy in humans. The same phenomenon was observed in GK rats.

The Leprfa mutaion was discovered in 1961 in the 13 M outbred rat stock by Lois and Zucker. The Zucker rat inherited a defective leptin recepror in the hypothalamus and does not resist feeding or weight gain. This model has since been well characterized as a model of obesity showing commonly published metabolic symptoms including insulin resistance and hyperlipidemia. This model faces diminished GLUT4 protein translocation of glucose (Dokken *et al*., 2006,

Furnsinn *et al.,* 1997), premature skeletal muscle fatigue (Frisbee *et al*., 2003) and remodeling of skeletal muscle microvasculature (Frisbee *et al*., 2006). I chose to work with GK muscle tissue because they represent a suitable model system for studying fundamental mechanisms of type 2 diabetes without the potentially complicating factors due to obesity. For the purpose of this study all animals where weight and age matched. The animals used in chapters 3 and 4 where donated from UCD, and all experienced the same living conditions and all where fed on the same diet. The animals used in the later studies (chapters 5 and 6) where bought from Taconic in Denmark. Taconic is a commercial supplier of transgenic, inbred, outbred and hybrid mice and rats and follows stringent breeding protocols.

Figure 1.8: The Goto-Kakizaki rat spontaneously presents with the diabetic condition.

1.4.2 Insulin Resistance

Insulin resistance is caused by the decreased ability of peripheral target tissues such as muscle, to respond correctly to normal circulating concentrations of insulin. Ordinarily, insulin binds to the insulin receptors on the surface of the target cells, which triggers a cascade of cellular events, which result in glucose

transport and metabolism. When glucose levels in the blood increase, the level of insulin also increases to rectify glucose levels. However when glucose levels are maintained at high levels in the blood insulin levels become exhausted. So after a period of compensatory insulin secretion, impaired glucose tolerance eventually develops, despite elevated insulin levels as insulin resistance increases. Insulin resistance in muscle and fat cells reduces glucose uptake, whereas insulin resistance in the liver results in reduced glycogen synthesis and therefore higher levels of glucose, which are released into the blood. Insulin resistance is believed to precede type 2 diabetes by up to 2 decades (Cowie, *et al*., 2009), and is often referred to as "pre-diabetes".

1.4.2.1 β cell dysfunction

β cells of the pancreas are most commonly known for the secretion of the hormone insulin. They are found in the islets of Langerhans and make up 65-80% of the cell population in these regions. β cells secrete insulin in response to an increase in blood glucose levels, and as a result play a critical role in maintaining glucose homeostasis. Normoglycemia or β cell compensation is how the body responds to increased blood glucose levels in insulin resistant states. When the pancreata of lean versus obese candidates were examined, it was seen that the obese subjects experienced an increase in β cell mass when both groups had not developed type 2 diabetes (Butler *et al*., 2003). For β cell mass expansion an increase in nutrient supply is important. It has been reported that GLP-1 enhances β cell proliferation (Jhala *et al*., 2003) and PKB prevents cell death through apoptosis via phosphorylation and inhibition of BAD which is a

proapoptotic protein (Jetton *et al*., 2005). It is important to note thatβ cell mass expansion does not necessarily result in β cell failure and type 2 diabetes. A study of β cell volume and markers for β cell proliferation and apoptosis in autopsy pancreata was conducted on unaffected patients and those with type 2 diabetes. This study showed a 63% loss of islet β cell volume in obese type 2 diabetic subjects. The study concluded that cell mass changes are not confined to late-stage type 2 diabetes.

1.5 Proteomics

The concept of the proteome was first proposed by Wilkens and Williams in 1995 (Wilkens *et al* 1995), and is defined as the PROTein expressed by a genOME and is the systematic analysis of protein profiles of a tissue or a biological fluid. Proteomics therefore is the mass screening of a system and the documentation of the proteins within.

The complexity of the proteome is caused by regulated degradation, alternative RNA splicing and post-translational modifications (Gygi *et al*., 1999). There are more than 200 possible chemical modifications that a protein can undergo. Some of these modifications affect function, location and activity within the cell. Some of the more common modifications encountered are ubiquitination, glycosylation, methylation, acetylation, palmitoylation, histone modifcation and phosphorylation. It has become very clear to researchers that knowing the genome does not predict the proteins that are expressed. In other words genetic information does not always confer a function to a gene product and the abundance of mRNA

does not always correlate to the amount of protein produced (Anderson *et al*., 1997). To overcome this, the total expression complement of the cell is studied.

Expression proteomics involves the complete denaturation of proteins, destroying the three-dimensional structure, and using further analysis to determine quantitative changes in the abundance of proteins under different conditions. Acquiring functional information about specific proteins requires the maintenance of protein structure. Functional proteomics allows researchers to identify the purpose of the protein being studied and its role within the cell.

1.5.1 Advantages of proteomics in disease analysis

Differential proteomics is a treasured technique for improving the understanding of critical cellular biochemical reactions. Two-dimensional gel electrophoresis (2DGE) and the subsequent identification of proteins via mass spectrometry has become the main technique used by many research groups. Utilising these techniques has shown to be extremely informative for many diseases.

The information obtained through these proteomic studies have lead to the uncovering of many new biomarkers for the specific disease studied as well as markers for the progression of the diseased state.

1.5.2 Analysis of the proteome

To establish the function of a protein the location, expression and structure of that protein must be determined (Pennington, 1997). Often the protein mixtures of interest are complex and intricate and require comparative proteomics. A good starting point is protein separation via 2D gel electrophoresis where complex

protein samples are sequentially separated by two unrelated physical properties to reduce sample complexity. 2DE (two-dimensional electrophoresis) is commonly paired with protein identification by means of mass spectrometry. Validation of mass spectrometry results is commonly conducted by immunological methods such as western blotting or immunohistochemistry. Over the last thirty years, two-dimensional gel electrophoresis has been at the heart of protein analysis as it can differentiate between different post-translational modified proteins, which are of significant importance to the study of disease (Gorg *et al*., 2004, Hanash, 2003), as well as discriminating between different isoforms of a protein. Complex protein mixtures are difficult to work with and require separation across two dimensions for more successful analysis of protein expression alterations and changes in function, location and structure. Separation proteins based on charge is called isoelectric focusing (IEF). IEF manipulates the fact that a molecules charge will change with the pH of its environment. Proteins migrate under electrical currents towards their isoelectric point (p*I*), which is the point at which a protein has a net charge of zero. IEF is conducted under a pH gradient and is the first-dimension of the two-dimensional separation of proteins. The second dimension separation in based on molecular mass and utilises a procedure called polyacrylamide gel electrophoresis (PAGE). Proteins are denatured and given a negative charge via treatment with sodium dodecyl sulphate (SDS). The proteins being analysed are negatively charged and migrate toward an anode when an electrical current is applied. The polyacrylamide gel acts as a sieve through which the smaller proteins pass more

quickly.

In 1975 Klose published a paper showing how an earlier method (Smithies & Poulik, 1956) utilised only for serum proteins, could be manipulated and modified for use with other more complex groups of proteins such as whole cell lysates. The method reported by Klose replaced the paper and starch protein separation method with a polyacrylamide gel. Around the same time O'Farrell reported the tandem use of IEF cylindrical gels and SDS-PAGE. This was the first description of IEF and SDS-PAGE coupled protein separation. The evolution of these two-dimensional protein separation techniques has lead to the development of more reproducible immobilne pH gradients (IPG) of different and smaller pH ranges for first dimension separation and the development of high-resolution slab gels. These improvements, along with better software for image analysis and the ever evolving field of mass spectrometry have resulted in a technique which is up to date constantly developing.

1.5.2.1 Isoelectric Focusing

Prior to separation proteins must be lysed from within the cell without inducing protein modifications which may cause fictitious spots on the gel, while still liberating as many protein species as possible. Mechanical breakdown of muscle samples through pulverisation with liquid nitrogen preceding chemical lysis is the most effective method to release proteins from tissue samples. Different samples require different buffers, based purely on the solubility of the protein to be

recovered. One of the most popular solubilisation buffers used is that documented by O'Farrell (1975). Detergents such as SDS aid in the disruption of noncovalent protein interactions but can also interfere with IEF as this detergent id anionic. A zwitterionic detergent like CHAPS for example, can resolve this problem as it carries no charge and therefore does not interfere with IEF. Urea and thiourea are also commonly used in solubilisation buffers as they are denaturing agents which also aid in solubility of proteins. Nucleic acids cause mimicked migration and streaking in the second dimension as well as increasing sample viscosity and so are often removed from the sample. DTT or □-mercaptoethanol reduces disulfide bonds within protein structures. DTT is charged and migrates out of the gel during IEF. Amino acid side chains on proteins can carry different charges, positive, negative or zero net electrical charge. The proteins can be forced to the pH, which correlates with the p*I* by an electrical field. IEF manipulates the fact that proteins net charge is determined by the pH of their local environments. Synthetic carrier ampholytes create a gradient on the IPG strip and increase the reproducibility of IEF. IPG strips (Amersham Pharmacia Biotech) employ eight acrylamide derivatives, which are attached to the polyacrylamide strip by vinyl bonds. These strips are rehydrated using a lysis buffer without any additional salts as salts interfere with IEF and protein separation. Protein samples can be applied to the IPG strips in several ways, for example in-gel rehydration (where the protein and rehydration buffer are mixed) or cup-loading (where a plastic cup is used to incorporate the protein on to the strip). IEF should be performed at 20^0C to prevent urea re-

crystalisation. Lower voltages at the beginning of IEF protocols allow the sample to be gentle introduced to the strip and higher voltages to drive the proteins to their correct p*I*. These IEF methods must be optimised for sample to sample as focusing times can lead to streaking and artificial spots being present on the resulting 2D map.

1.5.2.2 Polyacrlamide gel electrophoresis

Equilibration between the dimensions is critical as it allows the protein on the strip to interact with SDS. This ensures that the proteins will migrate appropriately during PAGE as SDS transmits a negative charge to the protein. DTT, as previously discussed, is a reducing agent and disrupts the disulfide bridges within proteins and is present in the first equilibration step. Excess or residual DTT causes point streaking and therefore should be removed before PAGE. DTT is easily removed via the second equilibration step, which contains iodoacetamide (IAA). IAA alkylates free DTT, removing it for the second dimension separation.

Commonly polyacrylamide gels are usually 12.5% acrylamide. IPG strips are placed onto a large slab gel and an electrical current is applied forcing proteins to travel through pores in the gel. As the proteins travel through the gel smaller proteins travel faster than large ones and therefore smaller proteins resolved at the bottom of the gel and larger ones at the top as larger proteins are stunted by the small pore size. The resolution experienced using 2DE is dependent on the

size of the area available for separation. Using smaller pH ranges on large 2D gels increases the number of protein spots that can be separated and visualised.

The limitations experienced during 2D can vary from the limited capacity for protein concentration of IPG strips and masking of proteins (more abundant proteins resolving at the same point as a protein of smaller abundance). Despite these limitations 2D electrophoresis is an ever-improving field and remains the method of choice for protein separation.

1.5.2.3 Protein Visualisation

The selection of the suitable protein detection and visualisation method is hugely important, as it is necessary to be able to measure changes in expression levels of proteins quantitatively. Two factors must be taken into account when choosing a stain; the sensitivity and the dynamic range of the stain (Westemeier and Marouga, 2005). Coomassie Blue is a commonly used protein stain. It works by binding to the amino groups of the proteins by electrostatic and hydrophobic interactions in acidic conditions. Coomassie Blue staining is highly reproducible, shows little to no backround and is an endpoint stain (Neuhoff et *al*., 1988). This stain however, has a limited detection range of 200-500ng/spot.

Silver staining has a very high sensitivity of 0.1ng and is a commonly used technique. Silver staining has a number of drawbacks, firstly it is a multistep procedure but the results are available relatively quickly. It also has a low dynamic range and can on occasion negatively stain proteins. Silver staining is unsuitable for mass spectrometry and the silver particles must be removed from

the protein plugs prior to protein identification.

Alternatives to these stains are fluorescent stains that are gaining in popularity due to a superior linear dynamic range and greater sensitivity. Some drawbacks of fluorescent staining include the altered mobility of pre-labelled proteins and the rapid decay of signal.

1.5.2.4 Identification of proteins

There are several methods of identifying proteins after 2D gel electrophoresis. Several of these can be both time consuming and costly when dealing with a large number of proteins, for example Western blotting or immunohistochemistry. Mass spectrometry is the current method of choice for the identification of proteins due to its high analytical sensitivity and the magnitude of protein identification achievable through protein databases. Protein mixtures from cellular lysates can be digested with trypsin into peptides (Tabb *et al*., 2003). These peptides are then separated using capillary liquid chromatography and electrospray interface of Electron Spray Ionisation (ESI) that fragments the peptides by collision induced dissociation. In ESI the analyte is in solution. From a spray of highly charged droplets the ions are ejected into the gas phase and moved into the mass analyser. A nebulising gas, usually nitrogen or helium, is used to stabilise the spray. To nebulise is to convert a liquid into a mist or fine spray.

Large ions such as peptides are easily analysed by ESI as they are typically multiply charged, which brings them into the range of mass-to-charge (m/z) ratio

of a typical mass spectrometer. Once the m/z is determined the peptide mass fingerprint (PMF) is generated. The mass accuracy and the percentage of the protein sequence covered are analysed using state of the art highly developed scoring algorithms in a bid to calculate the level of confidence for the match (Berndt., *et al* 1999). When high mass accuracy is achieved, as a rule at least two peptide sequences must be matched to the sequence of the protein suggested and 10-15% of the sequence must be covered for an unambiguous identification. When PMF is used for the identification of protein species, the organism from which the sample was generated must have its genome completely sequenced. This method of protein identification can identify 50-90% of proteins analysed when at least a few hundred femtomole of gel-separated protein is present (Mann *et al.,* 2001)

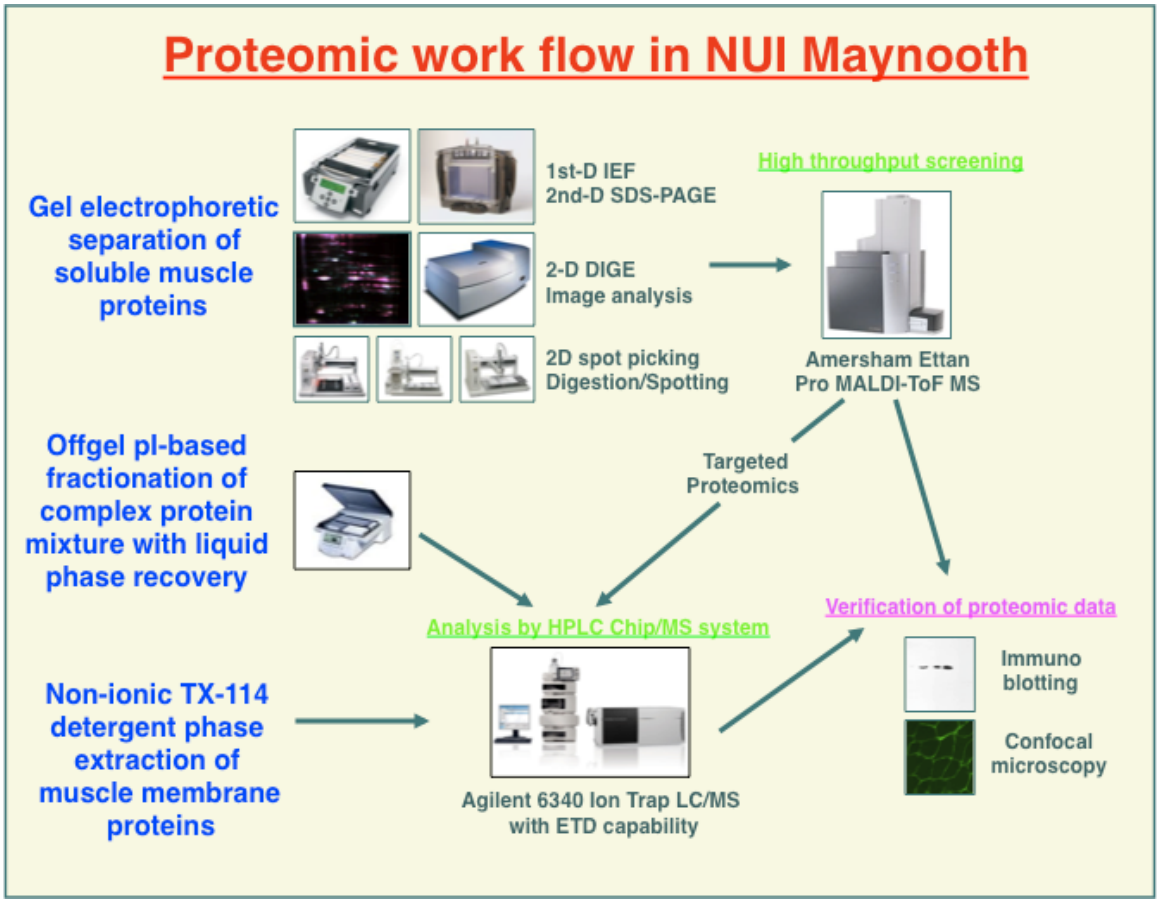

Figure 1.9: Two-dimensional electrophoresis separation of proteins. To compare the proteome of cells treated with two conditions, first the proteins must be solubilized using various chemicals designed to lyse proteins from within the cell. The protein lysate can then be separated first based on the p*I* and then based on molecular weight (MW). This creates a 2D map of the proteins. The proteins are then visualized using various staining methods and then these maps are compared using software which matches protein spot patterns between gels and then compare the abundance of the proteins. Any proteins which have changes in abundances can then be excised from the gels and enzymatically digested in order to identify the protein in question using mass spectrometry techniques.

1.5.3 Immunoblotting

It is important to validate and confirm mass spectrometry data through a different method. Some popular techniques are immunoblotting (Towbin *et al*., 1979) and immunofluorescence microscopy. Western blotting can detect the abundance of one protein within a complex protein mixture. The technique takes advantage of the specificity of antibodies to detect a protein of interest. After SDS PAGE negatively charged proteins are transferred to a nitrocellulose or polyvinylidene fluoride (PVDF) membrane via an electrical current. The membranes which now have protein bound to them, are blocked with milk proteins to limit non-specific binding of the antibody to be used. The protein of interest is detected by treating the membrane with an antibody specific for the protein and then treating the membrane with a secondary antibody which is species specific to the primary antibody. Conjugated to the secondary antibody is the enzyme horseradish peroxidise which cleaves the chemiluminescent substrate to produce light. X-ray film exposed to the light generated results in a quantifiable banding pattern that can be used to establish protein abundance.

1.5.4 Experimental Design

When studying any condition one must take into consideration the affected population. From this population many or few affected may arise. Depending on the incidence of the condition one must also devise a manageable number of test subjects. In most incidences human test subjects are not used due to large variances in lifestyle such as diet and environment. The Wistar rat has proven to

be a reliable and reproducible model for human conditions such as ageing (Doran *et al*., 2005) and as a control for many more (Mulvey *et al*., 2007). The design of an experiment is crucial to the statistical relevance of the results. Obviously cultivated rat specimen populations are much smaller than that of the human condition it mirrors and as a result smaller test groupings are used depending on the sample numbers available. At this point one must consider replicates. Replicates by definition mean to duplicate, copy, reproduce, or repeat. Biological replicates are animals which present with the same condition and have experienced similar if not the same living conditions. Biological variation occurs from animal to animal even when possible variables are reduced to a minimum and can be substantial or subtle. Depending on the number of biological replicates available for experimentation one must also consider technical replicates. When regarding experimental data a technical replicate can be either a replicate from the same animal within a population or another individual animal for which the population number is big enough for it to be statistically significant independently. As previously discussed by Karp et al (2007) depending on the available resources to the experiment, technical replicates generated from the same animal are hard to avoid and biological repeats provide more statistically sound scientific information. From this the power of an experiment can be deduced (Karp *et al*., 2007). The power can be calculated for each individual or for the entire experiment. The power of an experiment is the probability that an effect will be detected. Another common concern arises when interests do not lie with diagnostics only but biomarker studies. The issue of pooling sample has

always been controversial and yet unavoidable for some. Pooling of samples can lead to a reduced biological variance seen throughout an experiment and can also hamper the statistical relevance of the data recovered from such an experiment (Karp *et al.,* 2007).

1.5.5 Image analysis

Thousands of individual proteins can potentially be visualised on a large two-dimensional gel. The maps generated from 2D PAGE must be analysed to highlight spots and therefore proteins of interesting abundance alterations. To compare high-resolution 2D gels sensitive densitometric software had been developed like Progenesis SameSpot software (Non-Linear), Image Master (Amersham Biosciences), Impressionist (Gene Data) and DeCyder (GE Healthcare) which is specifically designed to manipulate DIGE experiments. The software maps the gel images to each other creating vectors from the correlating spots on one gel to that on another while removing noise and artefacts. Detection and quantification of the spots present on all gels ensues with the normalised volumes of all matched spots being calculated. The normalised volumes are compared to generate abundance changes across biological and technical replicates. The softwares available all require the user to establish backround threshold and statistical cut offs.

1.5.6 Aims of the project

The aim of this project was to study type 2 diabetes without the complications

associated with obesity. In an attempt to further understand the disease proteomic techniques where employed to analyse skeletal muscle tissue from a non-obese animal model, the Goto-Kakizaki rat. We proposed that proteomic analysis of skeletal tissue from the non-obese animal model would yield a greater understanding of the mechanisms by which glucose metabolism in affected in type 2 diabetes. By the use of proteomic techniques, the identity of several potential biomarkers for altered glucose, fatty acid and amino acid metabolism were uncovered as well as proteins affecting the contractile apparatus and cellular stress response.

The analysis of the mitochondria was of key importance to this primarily metabolic condition. The analysis of the mitochondrial proteome was undertaken to highlight any changes in its role in apoptosis, metabolism and free radical production. This enrichment yielded a great deal of data, some of which highlighted the fundamental role of the mitochondria in normal muscle homeostasis.

Hydrophobic protein enrichment using a detergent phase separation technique was also employed in a bid to highlight potential defects in the membrane proteins associated with glucose uptake and insulin receptor signalling.

Chapter 2

Materials and Methods

2 Materials and Methods

2.1 Materials

2.1.1 General chemicals and reagents

General chemicals and reagents were purchased from Sigma Chemical Company (Dorset, UK) and were of reagent/electrophoresis grade, unless otherwise stated. Distilled H2Owas purified using a Millipore Milli-Q apparatus to obtain milli-Q water (mQH2O). Complete Mini tablets containing Protease inhibitors were purchased from Roche Diagnostics and Bradford reagent from BioRad.

2.1.2 1-D and 2-D electrophoresis

Acrylamide stock solutions were obtained as Ultrapure Protogel (30% (w/v) Acrylamide: 0.8% (w/v) bis Acrylamide (37.5:1)) from Natural Diagnostics (Atlanta, GA, USA). Isoelectric focusing pH Gradient (IPG) drystrips for 2-d electrophoresis, ampholytes and cover fluid were purchased from Amersham Biosciences/GE Healthcare (Little Chalfont, Bucks, UK). All protein molecular weight markers were purchased from New England Biolabs (Herts, UK).

2.1.3 Protein Visualization

PhastGel Coomassie Blue R-350 tablets, Coomassie Blue G-250 and PlusOne Silver Stain Kit were purchased from Amersham Bioscience/GE Healthcare (Little Chalfont, Bucks, UK). RuBPs (Ruthenium 2 Bathophenanthroline Disulfonate Chelate 20mM stock solution) was synthesised in lab. Potassium pentachoro aquo ruthenate, bathophenanthroline disulfonate and sodium ascorbate were purchased from Sigma Chemical Company (Dorset, U.K.).

2.1.4 Mass Spectrometry

Acetonirtile was obtained from Amersham Biosciences/GE Healthcare (Little Chalfont, Bucks, UK). Sequence grade-modified trypsin was purchased from Promega (Madison, WI, USA). Formic Acid and LC/MS Chromasolv water were from Fluka (Dorset, UK)

2.1.5 Western Blotting

Nitrocellulose membrane was obtained from Millipore (Bedford, MA, USA). Chemiluminescence substrate was purchased from Pierce and Warriner (Chester, UK). X-ray film was purchased from Fuji Photo Film Co. Ltd. (Tokyo, Japan). GBX Developer/Replenisher, GBX Fixer and Replenisher and Ponceau S-Red Staining Solution were obtained from Sigma Chemical Company (Dorset,

UK). All commercially available antibodies used in this research were purchased from the companies detailed in Table 2.1. List of antibodies used for this project including the appropriate dilutions for both the primary and secondary antibodies, host species can be seen in Table 2.2.

Table 2.1: Antibody Suppliers

Company	Address
Abcam	Abcam Plc (Cambridge, Uk)
ABR	Affinity Bioreagents (Golden, CO., USA)
Abgent	San Diego, CA, USA
Calbio	Calbiochem (San Diego, CA., USA)
Chemicon	Chemicon International (Temecula, CA., USA)
Sigma	Sigma Chemical Company (Poole, Dorset, Uk)
Upstate	Upstate Biotechnology (Lake Placid, NY., USA)

Table 2.2 Antibodies

List of antibodies used for this project including the appropriate dilutions for both primary and secondary antibodies. 1^{o}= primary, 2^{o}= secondary, Species = host species.

Antibody	1^{o} Ab dilution	2^{o} Ab dilution	Species	Company
α_{1s} DHPR	1:1000	1:1000	Mus	ABR
F1 ATPase	1:1000	1:1000	Mus	Abcam
Malate dehydrogenase	1:500	1:1000	Shp	Abcam
Mitofilin	1:1000	1:1000	Rb	Abcam
Myosin fast	1:1000	1:1000	Mus	Sigma
NADH dehydrogenase	1:500	1:500	Rb	Abcam
Na+/K+ ATPase	1:1000	1:1000	Mus	Abcam
Phosphoglycerate kinase 1	1:1000	1:1000	Rb	Abgent
Prohibitin	1:500	1:500	Rb	Abcam
Pyruvate kinase 1	1:500	1:500	Gt	Abcam
SDHA	1:1000	1:1000	Gt	Abcam
SERCA 1	1:1000	1:1000	Mus	ABR
VDAC1	1:500	1:500	Mus	Abcam

2.1.6 Immunofluorescence Microscopy

OCTT™ Compound was purchased from Sakura Finetek Europe B.V (Zoeterwoude, Netherlands). DAPi and Liquid Blocker Super PAP Pen were obtained from Sigma Chemical Company (Dorset, UK). Florescent secondary antibodies (Goat Anti-Rabbit IgG, Goat anti-Rat, Goat anti-Mouse) were from Molecular Probes (Eugene, Oregon, USA). Superfrost Plus positively-charged microscope slides were from Menzel Glasser (Braunschweig, Germany). PPD-glycerol was obtained from CITIFLUOT Limited (London, UK).

2.2 Methods

2.2.1 Animals and Dissections

An out-bred strain of albino Wistar rat was used as a control model. Wistar rats are a strain of rats belonging to the species *Rattus norvegicus*. These rats are the first rat strain specifically developed for use in biological and medical research. The Wistar rat is characterised by its wide head, long ears and they also have a tail length that is less than its body length. The non-obese, spontaneous Type 2 Diabetic Goto-Kakizaki rat was used as the diseased model. The Goto-Kakizaki rat is a non-obese Wistar substrain which develops Type 2 diabetes mellitus early in life. Goto and Kakizaki at Tohoku University, Sendai,

Japan developed the model in 1975. This animal also develops mild hyperglycemia, is insulin resistant and presents with hyperinsulinemia.

The gastrocnemius muscles were dissected, snap frozen in liquid nitrogen and stored at -70^{0}C. Control and diseased animals were kept at a standard light-dark cycle fed at libidum, were obtained from the Biomedical Facility of the National University of Ireland, Dublin. Rats had been originally purchased from M & B Taconic Ltd. Animal suppliers (Ry, Denmark).

2.2.2 Extraction of total muscle protein complement for 1-D gel electrophoresis

Muscle specimens were kept frozen in liquid nitrogen while being ground into a fine powder using a mortar and pestle. Equal quantities of 250 mg wet weight of muscle were used for both diseased and control samples. The resulting powder was placed into 1 ml of homogenisation buffer (0.5 M(N-[2hydroxyethyl]piperazine-N'-[2-ethanesulfonic acid]) HEPES, 200mM ethylene glyolbis(□-aminoethyl ether)- N, N,N',N'- tetraacetic acid (EGTA), 10% (w/v) sucrose, 3mM Mg^{2+} and a 0.1%(w/v) NaN_3. To remove DNA, 2□l of DNAase-1 (200) units were added per 100□l of lysis buffer. The buffer was also supplemented with 5 complete mini tablets, which were added to every 50mls of homogenisation buffer. The complete mini tablets supplement the homogenisation buffer with a protease inhibitor cocktail containing 1 □M leupeptin, 1.4□M pepstatin, 0.15 □M aprotinin, 0.5 □M soybean trypsin inhibitor, 0.2 mM prefabloc, 0.3 □M E-65 and 1mM ethylenediaminetetraacetic acid

(EDTA). The samples were then incubated on ice with vortexing every 10 minutes for 10 seconds, for two and a half hours. The suspension was the centrifuged for 20 minutes at 20,000 g in an Eppendorf 5417 R centrifuge (Eppendorf, Hamburg, Germany), after which protein quantification was conducted as described in **Section 2.2.5.** Samples were then reduced with an equal volume of reducing buffer (0.05 M Tris, 3% (w/v) sodium-dodecyl-sulfate (SDS), 75 mM DTT 0.05% (w/v) bromophenol blue, 20% (w/v) sucrose) at 100^0C for 5 minutes. The samples were then either run on a 1-D gel or aliquoted and stored at -70^0C for future use.

2.2.3 Extraction of total muscle protein complement for 2-D electrophoresis

As described in Section 2.2.2, the specimens were ground into a fine powder but were resuspended in 1 ml of lysis buffer (7 M urea, 2M thiourea, 65 mM (3-[(3-Cholamidopropyl)-Dimethylammonio]-1-Propane sulfonate) (CHAPS), 100 mM dithiothretiol (DTT) and 5% (v/v) ampholytes, 5 tablets/50ml of buffer Mini Complete). To remove DNA, 2□l of DNAase-1 (200 units) were added per 100□l of lysis buffer. The buffer was also supplemented with 5 complete mini tablets, which were added to every 50ml of homogenisation buffer. The complete mini tablets supplement the homogenisation buffer with a protease inhibitor cocktail as described above in section 2.2.2. Samples were incubated at room temperature for two and a half hours on a shaker with vortexing for 10 seconds at regular intervals. The suspension was then spun at 20,000g for twenty minutes

using an Eppendorf 5417 R centrifuge (Eppendorf, Hamburg, Germany). The resulting pellet was discarded with only the lower layer of supernatant being retained and stored at -70^{o}C and protein concentration was ascertained by a Bradford Assay.

2.2.4 Preparation of Mitochondria-Enriched Fraction

Three grams of gastrocnemius muscle tissue was cut into small pieces and homogenised in 20 ml of homogenisation buffer (220mM mannitol, 70mM sucrose, 2mM Hepes, pH 7.4 supplemented with 1 PIC complete mini tablet per 10 ml (Roche Diagnostics). The resulting mixture was centrifuged at 1100 x g for 5 minutes at 4 ^{o}C. The supernatant was retained. The pellet was resuspended in 10 ml of homogenisation buffer (HB) and centrifuged as before. Again the supernatant was retained and the pellet resuspended in 5 ml of HB. The supernatants from all of the above steps were pooled and centrifuged at 7000 x g for 15 minutes. The resulting pellet was resuspended in HB and centrifuged at 20,000 x g for 15 minutes. This was repeated three times with the pellet retained each time. After the final spin the pellet was resuspended in either 500 ml of homogenisation buffer for western blotting or 2D lysis buffer. Samples for DIGE were pH 8.5. The protein content was of the samples was determined via Bradford Assay.

2.2.5 Preparation of Hydrophobic Protein Enriched Fraction.

Rat gastrocnemius tissue samples (250mg) were ground into a fine powder under liquid nitrogen using a pestle and mortar. The ground tissue was

immediately added to 8ml of cold PBS and 2 ml of 10% Triton X-114 and left overnight at 4^0C on a rotary shaker. The suspended sample was spun at 20,000 x g for 30 min at 4^0C to remove tissue debris. The supernatant was placed at 37^0C for 30 min followed by a 5000 x g centrifuge spin for 30 min at 25^0C to separate the detergent (DT) and aqueous phases (AQ). The AQ top later was removed to a fresh 50 ml tube to which 2 ml of 10% Triton X-114 was added. The bottom DT phase was resuspended in 8ml of cold PBS. Both samples were placed at 37^0C for 15 min followed by a 15 min centrifuge spin at 5000xg at 25^0C. This process was repeated 3 times in order to wash each phase and remove contaminants. Protein was extracted from each phase by acetone precipitation at -20^0Cfor 1 hr. Following a 30 min spin at 5000xg precipitated protein extracts were resuspended in 1ml (AQ) and 200ml (DT) of lysis buffer.

2.2.6 Acetone Precipitation

Adding three volumes of 100% ice cold acetone to the sample and vortexing briefly, the mixtue was then incubated for one hour at -70^0C first precipitated samples. The sample was spun for 15 minutes at 12,000g in an Eppendorf 5417 R centrifuge (Eppendorf, Hamburg, Germany) and the supernatant was discarderd. The pellet was then resuspended in three times the volume of the original sample of 80% ice cold acetone and left at 70^0C for ten minutes, the procedure was repeated twice before the sample was resuspended in the original volume of lysis buffer (**Section 2.2.3)** aided by vortexing or sonication with a Sonoplus HD2200, Bandelin (Berlin, Germany).

2.2.7 Protein Quantification via Bradford Assay

Quantification of sample protein concentration was ascertained according to the method of Bradford (1976). A standard curve was prepared by diluting a stock solution of 5 mg/ml BSA with sample buffer in the range 0-100 mgs. Standard were diluted with sample buffer, 80 ml milliQ water, and 10 ml 0.1 M HCl. 10 ml of sample was also diluted with 80 ml milliQ water, and 10 ml 0.1 M HCl. To both samples and standards 3.5 mls of working Bradford reagent (1 part Bradford reagent dye to 3 parts distilled water) was added, inverted and incubated for 5 minutes at room temperature in the dark. Absorbance was then read for the standards and samples at 595 nm and protein concentration were then obtained by comparing the unknown samples to the standard curve (Bradford 1976).

2.2.8 1-D gel electrophoresis

One-dimensional SDS polyacrylamide gel electrophoresis was performed according to Laemmli (1970), using a Bio-Rad Mini-Protean 3 gel system (Bio-Rad Labs., Hemel-Hempstead, Herts., UK). 5% resolving gel was made of 5% (w/v) acrylamide from a 30% acrylamide/bisacrylamide (37:5:1) mixture, 0.303 M Tris-PO_4 pH 8.8, 0.438 M SDS, 0.69 M APS and 0.1% (v/v) N,N,N',N'-tetramethylethylenediamine (TEMED). 10% resolving gels were made of 10% (w/v) acrylamide, 0.303 M Tris-PO_4 pH 8.8, 0.438 M SDS, 0.69 M APS and 0.1% (v/v) TEMED. These two mixtures were used to create a 5-10% gradient gel. The stacking gel was made of 5% (w/v) acrylamide, 0.5 M Tris-PO_4 pH 6.7, 0.438

M SDS, 0.69 M APS and 0.1 % (v/v) TEMED and was layered over the resolving gel. 15-100µg protein solution (**Solution 2.2.2)**, was loaded per well. Electrophoesis was carried out using running buffer (0.0125 M Tris, 0.96 M Glycine, 0.1% (w/v) SDS). Post electrophoresis gels were either fixed for staining or blotting.

2.2.9 2-D gel electrophoresis

For Isoelectric focusing, IPG strips were rehydrated for 12 hours with rehydration buffer (7 M urea, 2 M thiourea, 65mM CHAPS, 100 mM DTT and 5% (v/v) ampholytes; containing 0.05% (w/v) bromophenol blue as tracking dye) in a re-swelling tray from Amersham Biosciences/GE Healthcare (Little Chalfont, Bucks., UK).

Table 2.3: Volume of rehydration buffer required based on strip length for isoelectric focusing**.**

Strip Length (cm)	Volume (l)
7	125
11	200
13	250
18	350
24	450

After re-swelling, the IPGstrips were loaded gel side up in an Amersham Ettan IPGphor manifold and covered with 108 ml of cover fluid. An appropriate amount

of sample was added to the strips either by anodic cup loading or in-gel rehydration, and run on an Amersham IPGphor IEF system, employing pH range specific running conditions (Table 2.4).

Table 2.4: IEF focusing protocols

pH range 3-10	**pH range 4-7**	**pH range 6-11**
3500V 21hrs	3500V 21hrs	80V 4hrs
8000V 10min	8000V 10min	100V 2hrs
8000V 3hrs	8000V 3hrs	500V 2hrs
		1000V 1hrs
		2000V 1hrs
		4000V 1hrs
		6000V 2hrs
		8000V 2.5hrs

Following isoelectric focusing, IPG strips were equliberated twice for 20 minutes using 6 M urea, 30% (w/v) glycerol, 2% (w/v) SDS, 100mM Tris-HCl, pH 8.8, whereby the first incubation step was performed with the addition of 100mM DTT and the second incubation step with 0.25 M iodoacetamide. The strips were then briefly washed in SDS running buffer (0.0125 M Tris, 0.96 M glycine, 0.1% (w/v) SDS) and placed on top of a 12.5% (w/v) SDS resolving gels and set using a 1% (w/v) agarose sealing gel. The gel electrophoretic separation of the Type 2

Diabetic skeletal muscle proteome in the second dimension was carried out by standard SDS-PAGE using an Amersham Ettan DALT-Twelve system (Doran *et al.,* 2006). Gels were electrophoresed at 1.5 W overnight until the bromophenol blue dye front had ran off the gel.

2.2.10 Protein Staining

2.2.10.1 DIGE Labelling

Cy3 and Cy5 DIGE dyes were reconstituted as a stock solution of 1mM in fresh DMF (Dimethylformamide). The stock solution was diluted to a working solution of 0.2mM prior to labelling, and was used within two weeks. 50 mg of sample for each biological replicate was minimally labelled with 200 pmols of Cy3 working solution. A pooled sample consisting of equal quantities of protein from all replicates used in the experiment were labelled at 200 pmol of Cy5 working solution to 50 mg of protein. The pool generated was used as an internal standard. All samples at pH 8.5 were labelled with the appropriate amount of dye and after brief vortex, incubated on ice in the dark for 30 minutes. The reaction was quenched by adding an equal volume of lysine as dye and incubating the dye:protein mixture for 10 minutes on ice in the dark. Samples where loaded onto IPG strips with an equal volume of 2x sample buffer (7M urea, 2M thiourea, 65mM CHAPS, 2% ampholytes and 2% DTT) during rehydration, or where frozen at -80^{0}C for future use.

2.2.10.2 Colloidal Coomassie Staining

Colloidal Coomassie staining was carried out according to the procedure of Neuhoff (*et al.,*1988). After electrophoresis gels were washed twice with dH2O and placed into colloidal coomassie staining solution, (1 part Stock Solution A (5% (w/v) coomassie brilliant blue G-250); 40 parts Stock Solution B (10% (w/v) ammonium sulphate, 2% (v/v) phosphoric acid); 10 parts methanol), overnight. The gels were then washed with neutralisation buffer (0.1 M Tris-PO_4 adjusted to pH 6.5) for 1-3 minutes. The bakround was reduced by a one minute wash in destain (25% methanol) and the dye was fixed by an overnight wash in fixation solution (20% (w/v) ammonium sulphate). This procedure was repeated a minimium of three times or until sufficient visualisation of protein was achieved.

2.2.10.3 Hot Coomassie Staining

The staining solution (0.025% (w/v) PhastGel Coomassie Blue R-350 tablet and 10% (v/v) acetic acid) was heated to 90^0C and poured over the gels to be stained. The gel was then placed on a laboratory shaker for 10 minutes for mini gels and one hour for larger gels, at room temperature. Gels were destained in a 10% (v/v) acetic acid solution with slow agitation. Excess coomassie dye was soaked up with filter paper. Gels were processed immediately for mass spectrometric analysis or stored in a 1% (v/v) acetic acid solution. The gels were the scanned using a Umax Image scanner from Amersham Biosciences/GE Healthcare (Little Chalfont, Bucks., UK) and spots cut and processed for LC/MS

analysis.

2.2.10.4 Silver Staining

After electrophoresis, the gels were placed into fixing solution (30% ethanol, 10% acetic acid) for a minimum of 30 minutes. The gels were then rinsed in 20% ethanol twice for 10 minutes, which was followed by two 10-minute washes in milli-Q dH_2O. Sensitising solution (0.8mM sodium thiosulfate) was poured onto the gels for one minute after which the gels were once again washed in milli-Q dH_2O twice for 2 minutes. The staining solution (12 mM silver nitrate) was then left on the gels for 20 minutes to 2 hours. After the staining solution was removed and gels were washed in milli-Q dH2O for 10 seconds the developing solution (3% sodium potassium carbonate, 250 ml formalin, 125 ml 10 % sodium thiosulphate) was added to the gel. Once the protein map was visualised the gel was placed into stopping solution (40g Tris, 2% acetic acid) for storing.

2.2.10.5 RuBP's Staining

Following overnight in fix solution (30% ethanol, 10% acetic acid), slab gels were then washed 3 times with 20% ethanol for 30 minutes. The gels were stained for 6 h in 20% (v/v) ethanol containing 200 nM of the ruthenium chelate. The gels were re-equilibrated twice for 10 minutes in distilled water prior to imaging.

2.2.10.5.1 Preparation of Ruthenium 2 Bathophenathroline Disulfonate Chelate 20mM stock solution

Potassium pentachloro aquo ruthinate (0.2g) was dissolved in 20 ml boiling water and kept under reflux (deep red brown solution). Bathophenanthroline disulfonate (3M) (0.9g) was then added and the reflux was continued for 20 min (greenish-brown solution). Sodium ascorbate solution (500 mM) (5ml) was added and the reflux was continued for 20 minutes (deep orange-brown). The solution was allowed to cool and then adjusted to pH7 with sodium hydroxide. The volume was adjusted to 26 ml and was stored at 4oC (several months).

2.2.11 ESI LC/MS

2.2.11.1 Sample preparation for mass spectrometry

The gel was first washed with deionised water (2 x 10 min) and the Coomassie Blue-stained spots of interest were excised from the gels and placed into siliconised 1.5 ml Eppendorf tubes. The gel plugs were then destained, desalted and washed as follows: Gel plugs were first washed with water and then with 50mM NH4HC3/acetonitrile 1:1 (v/v) for 15 min at 37^0C. The liquid was removed and the enough acetonitrile was added to cover the gel plugs. Acetonitrile was removed and the gel plugs were rehydrated in 50mM NH_4HCO_3. After 5 min, an equal volume of acetonitrile was added. After 15 min of incubation all the liquid was removed and the gel plugs were then dehydrated in 100% acetonitrile. The acetonitrile was removed and, the gel plugs were then dried down for 30 min

using a Heto type vacuum centrifuge from Jouan Nordic A/S (Allerod Denmark). Individual gel plugs were then rehydrated in enough digestion buffer (1mg of trypsin in 20ml of 50mM NH_4HCO_3) to cover the gel plugs. More digestion buffer was added if all the initial volume had been absorbed by the gel pieces. The samples were then incubated at 37^0C 4 hr – over night. The peptides generated by tryptic digestion were recovered by removing supernatants from the digested gel plugs. Further recovery was achieved by adding 30% acetonitrile/ 0.2% trifluroacetic acid to the gel plugs for 10 min at 370C with gentle agitation. The resulting supernatants were added to the initial peptide recovery following trypsin digestion. Exhaustive peptide recovery was achieved through the addition of 60% acetonitrile/0.2% trifluotoacetic acid to each plug for 10 min at 370C with gentle agitation. Supernatants were added to the peptide pool and the sample volume was reduced until dry through vacuum centrifugation. Samples were resuspended in 15ml of ultrapure ddH2O and 0.1% formic acid for identification by ion trap LC/MS (Liquid Chromatography/ Mass Spectrometry) analysis.

2.2.11.2 Ion Trap Mass Spectrometry

The mass spectrometric analysis of peptides was carried out in the Proteomics Suite of the National University of Ireland, Maynooth with a Model 6340 Ion Trap LC/MS apparatus from Agilent Technologies (Santa Clara, CA). Excision, washing, destaining and treatment with trypsin, was performed by the above optimised method. Separation of peptides was performed with a nanoflow Agilent 1200 series system, equipped with a Zorbax 300SB C18 5mm, 4mm, 40 nl

precolumn and a Zorbax 300SB C18 5 mm, 43mm x 75mm analytical reversed phase column using HPLC-Chip technology (Staples et al., 2009). The mobile phases utilised were A: 0.1% formic acid, B: 50% acetonitrile and 0.1% formic acid. Samples (5ml) were loaded into the enrichment column st a capillary flow rate set to 4ml/min with a mix of A and B at a ratio 19:1 (v/v).Tryptic peptides were eluted with a linear gradient of 10-90% solvent B over 15 min with a constant nano pump flow rate of 0.60ml/min. A 1min post time of solvent A was used to remove sample carry over. The capillary voltage was set to 2000 V and the flow and the temperature of the drying gas was 4ml/min and 300^0C, respectively. For protein identification, database searches were carried out with Mascot MS/MS Ion search (Matrix Science, London, UK). All searches used '*Rattus norvegicus*' as taxonomic category and the following parameters: (i) two missed cleavages by trypsin, (ii) mass tolerance of precursor ion 2.5 Da and product ions 0.7 Da, (iii) carboxymethylated cystines fixed modification, and (iv) oxidation of methionine as variable modification. In addition, the percentage of coverage was set at over 10%, with at least 2 matched distinct peptides. Importantly, all p*I*-values and molecular masses of identified proteins were compared to the relative position of their corresponding two-dimensional spots on analytical slab gels.

2.2.12 Immunoblotting

Electrophoretic transfer of proteins to Immobilin NC-pure nitrocellulose membranes was carried out according to Towbin et al., (1979) using a Bio-Rad Mini-Protean II transfer system (Bio-Rad Labs., Hemel-Hempstead, Herts., U.K.).

Proteins were transferred for one hour at 100V and at 4oC. Efficiency of transfer was evaluated by Ponceau-S-Red staining of membranes, followed by de-staining in phosphate buffered saline (PBS) (50mM sodium phosphate, 0.9% (w/v) NaCl, pH 7.4). Membranes were blocked for 1 h in 5% (w/v) fat-free milk powder in PBS. Membranes were then incubated for three hours at room temperature or overnight at 4oC with primary antibody, appropriately diluted with blocking buffer (refer to Table 2.3 for primary and secondary antibody dilutions). Nitrocellulose blots were subsequently washed (2 x 10min) in blocking solution and then incubated with an appropriate dilution of the corresponding peroxidase-conjugated sondary antibody (anti-mouse and anti-rabbit secondary antibodies for monoclonal and polyclonal primary antibodies, respectively), for one hour at room temperature. The nitrocellulose membranes were then washed extensively (2x10min) in blocking solution and rinsed (2x10min) with PBS. Immunoreactive were visualized using SuperSignal® Enhanced Chemiluminesence substrate luminol/enhancer (Pierce and Warriner, Chester, Cheshire, U.K.), for the detection of horseradish peroxidase in Western blotting. Densitometric scanning of immunoblots was performed on a Molecular Dynamics 300S computing densitometer (Sunnyvale, CA, USA) with Imagequant V3.0 software. Statistical analysis of densitometry results from immunoblots was carried out using Graphpad prism statistical software (Graphpad software Inc.). $p<0.05$ is significant.

Chapter 3

Proteomic profiling of non-obese type 2 diabetic skeletal muscle

3 Proteomic profiling of non-obese type 2 diabetic skeletal muscle

3.1 Introduction

Abnormal glucose handling has emerged as a major clinical problem for millions of diabetic patients worldwide. The number of diabetic patients suffering from severe metabolic disturbances and glucotoxic complications is rapidly increasing and the incidence of diabetes is fast approaching endemic proportions (King *et al*., 1998). Type 2 diabetes mellitus represents a highly complex and heterogeneous disease that is influenced by both genetic and environmental factors (Luna *et al.* 2005). A modern inactive lifestyle coupled with obesity-associated metabolic complications play an essential role in disease development and progression. An abnormal sensitivity of peripheral tissues to insulin and decreased levels of hormone secretion are the typical and foremost characteristics of T2D. Since contractile fibres are responsible for most of the insulin-stimulated whole body glucose disposal, skeletal muscle tissues are particularly affected by insulin resistance, and as a result impaired insulin signalling and disturbed glucose metabolism in muscle tissues becomes a prominent aspect of T2D (Peterson*, et al.,*2002).

There is a limited understanding as to how abnormal tissue sensitivity to insulin causes decreased skeletal muscle strength (Andersen*, et al.,* 2004), especially in older patients (Park, 2006). Fatty acid metabolism has an overwhelming influence on diabetic side effects. As outlined by Phielix and Mensink (2008),

impaired insulin-mediated glucose uptake is not the only trait that stands out in the diabetic condition. High levels of circulating free fatty acids, diminished mitochondrial functioning and an overall weakened metabolic adaptability in the skeletal muscle tissues aid in the development of some of the more common type 2 diabetes associated conditions such as inhibited insulin signalling and insulin resistance.

In order to further our molecular understanding of diabetes-related abnormalities in skeletal muscles, mass spectrometry based proteomics nominates itself as an ideal analytical tool for performing global screening approaches to determine potential alterations in protein expression levels (Korc, *et al.,* 2003). Proteins are the biological effector molecules of the cell. Proteomics is the large-scale and high throughput biochemical approach to study entire protein complements (De Hoog and Mann, 2004), which are qualities appropriate for the global identification of complex alterations in diabetic tissues. Sundsten and Ortsaeter (2009) recently discussed how numerous proteomics projects have been instigated to disentangle complex pathobiochemical mechanisms that underlie diabetes. Many of these studies have focused on the pancreas, blood, adipose tissue and the liver for reasons such as highlighting the underlying dysfunction of b cells in the pancreas and studying protein patterns in organs involved in glucose homeostasis such as the liver and adipose tissue. Deduction of altered protein expression patterns during the aging process may lead to the discovery of new therapeutic targets as well as protein biomarkers for disease progression of the diabetic condition.

In this study, we carried out the proteomic profiling of crude skeletal muscle extracts from the Goto-Kakizaki (GK) rat model of type2 diabetes (Kitahara *et al.* 1978). The animal model has been a staple in investigating muscular disorders over the past few decades. Skeletal muscle specimens from inbred animal strains exhibit genetically much less inter-individual differences as compared to patient biopsies, and therefore considerably lower experimental repeats are required in initial proteomic profiling experiments. As a result cohorts of new biomarkers identified by animal model proteomics can then be used for an in-depth characterisation of diseased human muscle in order to improve diagnostic procedures or design better treatment strategies. GK rats are spontaneously diabetic animals that exhibit chronically impaired insulin signalling (Abdel-Halim *et al*,. 1994, Krook *et al.,* 1997), which usually occurs by 4 weeks of age (Portha *et al*., 1991). They are characterised by increased blood glucose levels without significant alterations in non-fasting plasma insulin levels (Witte *et al.,* 2002). Diabetic GK skeletal muscles are characterised by a diminished recruitment of the glucose transporter isoform GLUT4 (Mulvey *et al.,* 2005), membrane cytoskeletal defects in the dystrophin-dystroglycan complex (Mulvey *et al*, 2008), an inhibition of insulin receptor auto-phosphorylation (Dadke *et al.,* 2000), impaired activities of insulin signalling intermediates (Steiler *et al*., 2003), abnormal mitochondrial functioning (Shen *et al.,* 2008) and a reduced percentage of oxidative fibres (Yasuda *et al.,* 2002). Since diabetic GK rats are non-obese, fundamental mechanisms of type 2 diabetes can be investigated without potentially complicating obesity-related factors.

The proteomic analysis of normal versus non-obese diabetic skeletal muscles presented in this chapter has revealed a moderate differential pattern for 21 proteins, where 7 proteins where found to be reduced and 14 proteins to be increased in there abundance in GK tissue. With respect to neuromuscular disorders, the mass spectrometric cataloguing of normal muscle and the profiling of genetic and physiological animal models over the last few years have established large proteomic maps (Doran *et al*., 2007). Databanks of biomarkers that are implicated in muscular atrophy, fibre transformation, muscular dystrophy or age-related muscle wasting are now available for comparative biochemical studies (Doran *et al.,* 2007). In this respect, the proteomic findings of this study agree with the idea that diabetes mellitus is associated with a generally perturbed protein expression pattern. Insulin resistance appears to be closely related to abnormalities in glucose, fatty acid, nucleotide and amino acid metabolism, as well as changes in the contractile apparatus, the anti-oxidant defence system, detoxification mechanisms and the cellular stress response.

3.2 Methods

3.2.1 Animal Model.

As an internationally established animal model of type 2 diabetes, the spontaneous GK rat (Kitahara, 1978) was used in this study. In obesity-related diabetes, high levels of circulating free fatty acids and an extensive intramyocellular accumulation of triacylglycerol probably play a key role in causing decreased tissue sensitivity for insulin. Since the GK rat is non-obese, the analysis presented herein eliminates complicating factors due to excess lipids

in muscle fibres and focuses instead on the core defects in a spontaneous from of type 2 diabetes. Rats were purchased from M&B Taconic Ltd. Animal suppliers (Ry, Denmark). For comparative proteomic studies, the accessible protein complement was extracted from freshly dissected gastrocnemius muscles from 9-week-old normal Wistar rats and age-matched GK rats. The validation of the diabetic status of the cohort of the GK rats used in this study has been previously documented (Mulvey, et al., 2005). Non-fasting blood samples from GK rats showed a significant increase in glucose levels in comparison to Wistar rats, but plasma insulin levels were relatively comparable between both rat strains. The average body weight of the diabetic animals was found to be slightly below that of normal rats.

3.2.2 Preparation of total gastrocnemius muscle extracts.

Muscle samples with a wet weight of 200mg were quick-frozen in liquid nitrogen and ground into a fine powder using a mortar and pestle. The muscle powder was subsequently placed into 1ml lysis buffer (7M urea, 2M thiourea, 4%(w/v) CHAPS, 100 mM DTT and 2% (v/v) pH 3-10 ampholytes), which was supplemented with a protease inhibitor cocktail. Following incubation at room temperature for 3h, the suspension was centrifuged at 14,000x*g* for 20min at 4^0C. The total protein complement extracted from normal and diabetic tissues was quantified by the Bradford method.

3.2.3. Two-dimensional gel electrophoresis.

Total muscle extracts from normal and diabetic muscle tissues were separated in the first dimension by isoelectric focusing and in the second dimension by sodium dodecyl sulphate polyacrylamide gel electrophoresis, as previously described. For the comparative proteomic analysis, 4 biological repeats of normal and 4 biological repeats of diabetic samples was used. Isoelectric focusing strips were rehydrated in rehydration buffer (7M urea, 2M thiourea, 4% (w/v) CHAPS, 1.2% deStreak and 2% (v/v) pH 3-10 ampholytes) and 700 mg of muscle protein sample for 12 hours. First-dimension protein separation was carried out on an Amersham IPGphor IEF system, following the manufacturer's recommendations and the optimized protocol of our laboratory for the separation of skeletal muscle proteins. Following chemical reduction and alkylation by a standardized protocol, first-dimension strips were carefully placed on top of 12.5% (w/v) slab gels and electrophoresed in an Amersham Ettan DALT-Twelve system at 1.5W per gel until the bromophenol blue dye front had just ran off the gel. The protein separation pattern on two-dimensional gels was visualized by colloidal Coomassie Blue, silver or fluorescent RuBPs staining. High-resolution gel images where analysed with the Progensis software programme from Non Linear Dynamics (Newcastle upon Tyne, UK).

3.2.4. Mass spectrometric identification of muscle proteins.

In order to unequivocally identify proteins of interest, the peptide mass spectrometric analysis of muscle proteins with a changed abundance in diabetic

muscle tissue was carried out on a Model 6430 Ion Trap LC/MS apparatus from Agilent Technologies (Santa Clara, CA, USA). Excision, washing, destaining and treatment with trypsin were preformed by a previously optimised method. Trypsin-generated peptides were obtained by removing supernatants from digested gel plugs. Further recovery was achieved by adding 30% acetonitrile/0.2% trifluoroacetic acid to the gel plugs for 10 min at 37 ^{0}C with gentle agitation. Resulting supernatants were pooled with the initially recovered cohort of peptides following trypsin digestion. Further peptide recovery was achieved through the addition of 60% acetonitrile /0.2% t trifluoric acid to each plug for 10 min at 37^{0}C with gentle agitation. Supernatants were added to the peptide pool. The sample was dried through vacuum centrifugation and the concentrated peptide fractions were then resuspended in mass spectrometry-grade distilled water and 0.1% formic acid for identification by ion trap LC-MS analysis. Separation of peptides was performed with a nanoflow Agilent 1200 series system, equipped with a Zorbax 300SB C18 5 µm, 4mm 40nl pre-column and an Zorbax 300SB C18 5 µm, 43 mm x 75 µm analytical reversed phase column using the HPLC-Chip technology. Mobile phases utilized were A: 0.1% formic acid, B: 50% acetonitrile and 0.1% formic acid. Samples were loaded into the enrichment at a capillary flow rate set to 2µl/min with a mix of A and B at a ratio 19:1. Tryptic peptide fragments were eluted with a linear gradient of 10-90% solvent B over 2 □l/ min with a constant nano pump flow of 0.6 ml/ min. A 1 min post time of solvent A was used to remove sample carry over. The capillary voltage was set to 1700V. The flow and the temperature of the drying gas were

4l/ min and 300^{o}C, respectively. Database searches were carried out with Mascot MS/MS Ion search (Matrix Science, London, UK; MSDB database, release 20063108). All p*I* values and molecular masses of identified muscle proteins were compared to the relative position of their corresponding two-dimensional spots on analytical slab gels.

3.3 Results

3.3.1 Differential protein expression pattern in Wistar rat versus Goto-Kakizaki rat

3.3.1.1 Colloidal Coomassie

In order to determine potential differences in the skeletal muscle proteome from normal Wistar rats versus diabetic GK rats, crude total tissue extracts were separated by high-resolution two-dimensional gel electrophoresis. The gastrocnemius muscle with a mixed fibre type was chosen for the initial proteomic survey of diabetic effects on the muscle protein complement, since comparative data from numerous proteomic studies exist with respect to this muscle (Okumura *et a*l., 2005, Gelfi *et al*., 2006, Gannon *et al*., 2008). Figure. 3.1 shows representative gels of normal versus diabetic muscle preparations stained with CBB, silver or fluorescent RuBPs. The high-resolution gels contained 929, 1236 and 1561 detectable spots in CBB, silver and RuBPs-labelled gels, respectively. In general, the two-dimensional spot pattern of the normal muscle

protein complement was found to be in agreement with previously published studies on the gel electrophoretic separation of total skeletal muscle extracts (O'Connell *et al*., 2007). The protein spot distribution of normal versus diabetic preparations did not show extensive differences, but densitometric scanning revealed moderate alterations in distinct classes of muscle proteins.

3.3.1.2 Densitometric analysis of normal versus diabetic skeletal muscle.

Analytical two-dimensional gels were stained with colloidal Coomassie Blue and images from normal versus diabetic preparations compared with the help of a typhoon Trio variable imager and Progenesis samespot software. Fig. 3.2 shows a reference gel of a diabetic rat skeletal muscle used for the mass spectrometric identification of proteins with a differential expression profile. Muscle proteins with a changed abundance are marked by circles and are numbered 1-23. Protein species with a changed abundance in GK gastrocnemuis muscle ranged in molecular mass from 15.9 kDa (Cu/Zn superoxide dismutase) to 67.6 kDa (dihydrolipoamide s-acetyltransferase of the pyruvate dehydrogenase complex) and covered a p*I* –range from p*I* 4.9 (ATP synthase) to p*I* 8.9 (β-globulin). A decreased expression was found in the case of seven proteins, and 16 proteins were shown to be increased in their abundance.

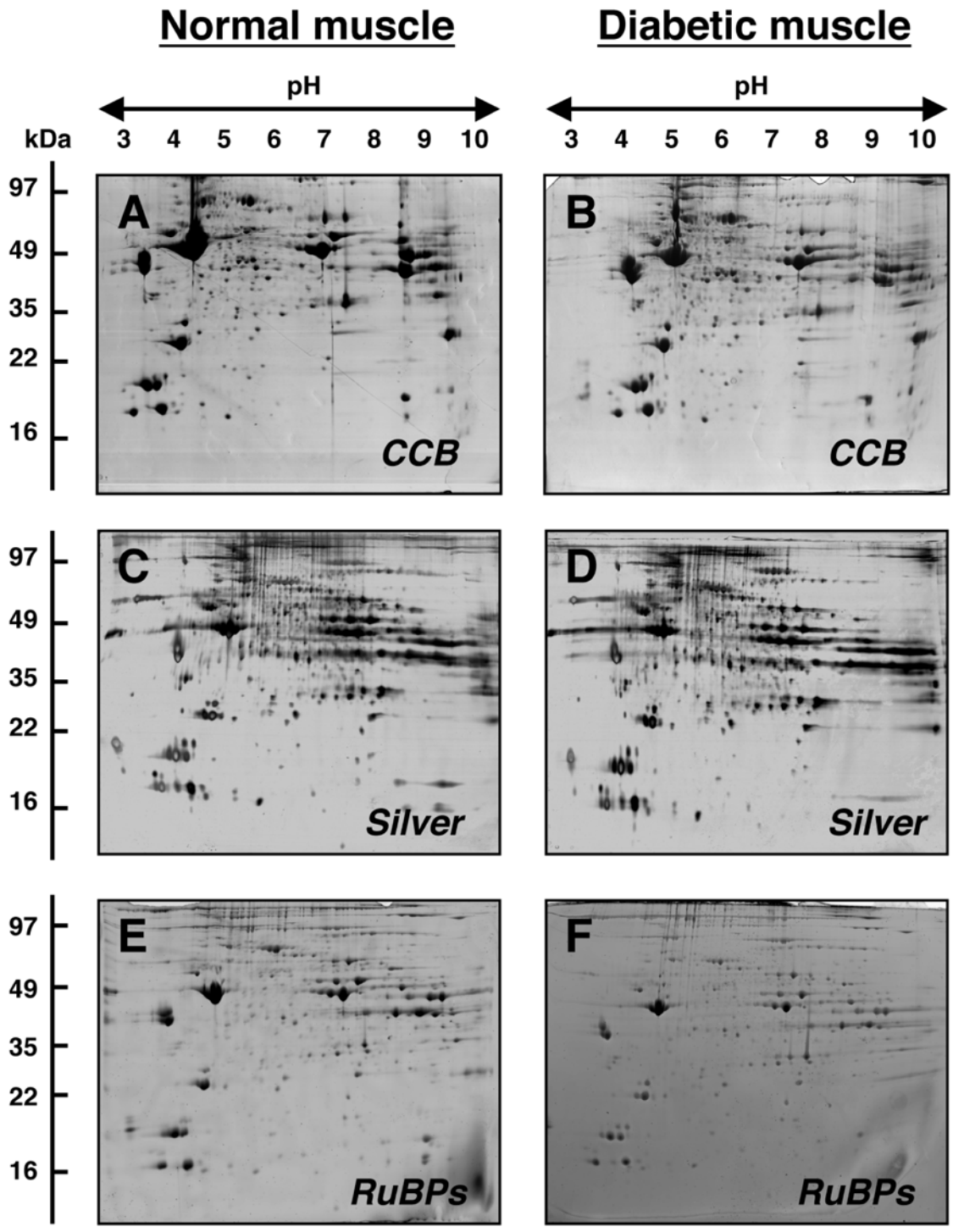

Figure 3.1: Comparative two-dimensional gel electrophoretic analysis of normal versus diabetic rat skeletal muscle. Crude total muscle extracts from normal and Goto-Kakizaki (GK) muscle tissue were separated in the first dimension by

isoelectric focusing and in the second dimension by sodium dodecyle sulfate polyacrylamide gel electrophoresis. Shown are Colloidal Coomassie Blue (CCB: A and B), silver (C and D) or fluorescent Ruthenium 2 bathophenanthroline disulfonate chelate (RuBP's E and F) stained gels of normal (A, C and E) versus diabetic GK muscle (B, D and F). The pH values of the first dimension gel system and molecular mass standards (in kDa) of he second dimension are indicated on the top and on the left of the panels, respectively.

3.3.1.3 Mass spectrometric identification of proteins with a diabetes-related change in abundance.

ESI MS analysis was used to unequivocally identify protein species contained in two-dimensional spots with an altered density in normal versus diabetic preparations. A list of the 23 muscle-associated proteins that exhibited a significantly altered expression level in GK muscle is shown in Table 1. The table summarises CCB-stained proteins separated in the pH 3-10 range and outlines matched peptide sequences, percentage sequence coverage, Mascot score, the relative molecular mass, p*I*-value, protein accession number and the fold change of individual muscle proteins affected by the diabetic phenotype.

The spot numbers of MS-identified protein species listed in Table 1 correlate with the numbering of two-dimensional spots marked in Fig. 2. The majority of identified muscle proteins were found to be constituents of various metabolic pathways. This included enzymes and transporters involved in glycolysis, the

citric acid cycle, oxidative phosphorylation, lypolytic catabolism, nucleotide metabolism, carbon dioxide removal, oxygen transportation and amino acid catabolism. In addition, components of the contractile apparatus, the cellular stress response, anti-oxidant defence mechanisms and formaldehyde detoxification appear to be affected in diabetic muscle tissue.

Table 1: **List of protein species that exhibit a differential expression pattern in normal versus diabetic skeletal muscle extracts.** The normal versus the diabetic rat skeletal muscle was stained with colloidal Coomassie Blue and differentially expressed proteins were identified by ESI-LCMS

Spot No.	Protein Name	Peptide Sequences	Acession No.	pI	M.W	No. of pep	Macot Score	%Coverage	Fold Change
1	3-hyroyisobutrate dehydrogenase	K.DLGLAQDSATSTK.T K.TPILLGSVAHQIYR.M K.EAGEQVASSPADVAEK.A K.MGAVFMDAPVSGGVGAAR.S K.KGSLLIDSSTIDPSVSK.E K.EAGEQVASSPADVAEKADR.I R.IITMLPSSMNSIEVYSGANGILK.K K.DLGLAQDSATSTKTPILLGSVAHQIYR.M	gi|556389	8.58	36748	11	240	30	-2.2
2	carbonic anhydrase 3	R.GGPLSGPYR.L R.VVFDDTFDR.S K.TILNNGKTCR.V K.GDNQSPIELHTK.D K.EPMTVSSDQMAK.L R.SMLRGGPLSGPYR.L R.VVFDDTFDRSMLR.G K.GDNQSPIELHTKDIR.H K.DIRHDPSLQPWSVSYDPGSAK.T	gi|31377484	6.89	29703	10	45	29	-2.2

3	dihydrolipoamide s-acetyltransferase E2 component of 2-oxo-gluterate complex	R.GLVVPVIR.N R.TINELGEK. A K.LGFMSAFVK.A K.VEGGTPLFTLR.K K.AKPAEAPATAHK.A R.NVETMNYADIER.T K.ASAFALQEQPVVNAVIDDATK.E	gi|195927000	8.9	49216	8	142	17	-1.8
4	ATP synthase beta subunit	K.ILQDYK.S K.IGLFGGAGVGK.T K.VVDLLAPYAK.G R.GQKVLDSGAPIK.I R.TIAMDGTEGLVR.G R.IMNVIGEPIDER.G K.AHGGYSVFAGVGER.T R.VALTGLTVAEYFR.D K.TVLIMELINNVAK.A K.VALVYGQMNEPPGAR.A R.LVLEVAQHLGESTVR.T R.IMNVIGEPIDERGPIK.T R.IMDPNIVGSEHYDVAR.G K.VLDSGAPIKIPVGPETLGR.I R.AIAELGIYPAVDPLDSTSR.I R.FLSQPFQVAEVFTGHMGK.L K.SLQDIIAILGMDELSEEDK.L R.IPSAVGYQPTLATDMGTMQER.I	gi|1374715	4.92	51171	22	341	55	-1.8

5	enolase 3, beta	K.LGELYK.S K.YNQLMR.I R.IEEALGDK.A R.YLGKGVLK.A K.LSVVDQEK.V K.TLGPALLEK.K K.KLSVVDQEK.V K.TAIQAAGYPDK.V R.LAKYNQLMR.I R.IGAEVYHHLK.G K.FMIELDGTENK.S R.GNPTVEVDLHTAK.G R.GNPTVEVDLHTAK.G R.IEEALGDKAVFAGR.K K.FGANAILGVSLAVCK.A K.VVIGMDVAASEFYR.N R.GNPTVEVDLHTAKGR.F K.VNQIGSVTESIQACK.L K.VDKFMIELDGTENK.S K.AVEHINKTLGPALLEK.K R.AAVPSGASTGIYEALELR.D K.LAMQEFMILPVGASSFK.E K.LAMQEFMILPVGASSFK.E K.LAMQEFMILPVGASSFK.E R.EILDSRGNPTVEVDLHTAK.G R.FRAAVPSGASTGIYEALELR.D R.SGETEDTFIADLVVGLCTGQIK.T K.LAMQEFMILPVGASSFKEAMR.I K.TAIQAAGYPDKVVIGMDVAASEFYR.N K.DATNVGDEGGFAPNILENNEALELLK.T R.HIADLAGNPDLVLPVPAFNVINGGSHAGNK.L K.YGKDATNVGDEGGFAPNILENNEALELLK.T	gi|126723393	7.08	47326	40	817	65	-1.5

6	esterase D/formylglutathione hydrolase	K.KAFNGYLGPDQSK.W K.SGCQQAASEHGLVVIAPDTSPR.G	gi|157823267	6.44	31981	2	46	12	-1.5
7	enolase 1 (alpha)	K.YNQILR.I R.IEEELGSK.A K.LNVVEQEK.I R.IGAEVYHNLK.N R.GNPTVEVDLYTAK.G R.YITPDQLADLYK.S K.VNQIGSVTESLQACK.L R.AAVPSGASTGIYEALELR.D K.LAMQEFMILPVGASSFR.E K.DATNVGDEGGFAPNILENK.E K.YGKDATNVGDEGGFAPNILENK.E R.HIADLAGNPEVILPVPAFNVINGGSHAGNK.L	gi|59808815	6.16	47476	14	225	35	-1.5
8	ATP synthase beta subunit	R.TIAMDGTEGLVR.G K.AHGGYSVFAGVGER.T R.TIAMDGTEGLVRGQK.V R.LVLEVAQHLGESTVR.T R.IMNVIGEPIDERGPIK.T K.VLDSGAPIKIPVGPETLGR.I R.FLSQPFQVAEVFTGHMGK.L R.EGNDLYHEMIESGVINLK.D	gi|1374715	4.92	51171	8	157	21	1.6
9	adenylate kinase isozyme 1	K.IIFVVGGPGSGK.G K.ATEPVISFYDKR.G K.YGYTHLSTGDLLR.A K.VDSSNGFLIDGYPR.E K.GELVPLETVLDMLR.D K.IAQPTLLLYVDAGPETMTQR.L R.KIAQPTLLLYVDAGPETMTQR.L	gi|8918488	7.71	21646	12	184	50	1.6

10	Cu-Zn soperoxide dismutase	R.HVGDLGNVAAGK.D K.DGVANVSIEDR.V R.VISLSGEHSIIGR.T K.GDGPVQGVIHFEQK.A	gi|203658	5.88	15874	6	155	32	1.6
11	immunoglobulin light chain	K.DSTYSLSSTLTLSK.A R.TVAAPSVFIFPPSDEQLK.S K.VDNALQSGNSQESVTEQDSK.D K.VDNALQSGNSQESVTEQDSK.D	gi|243868	8.47	25892	4	114	22	1.6
12	phoshoglucomutase 1	M.VKIVTVK.T K.VDLSVLGK.Q R.IAAANGIGR.L R.LIFADGSR.I R.SMPTSGALDR.V R.LSGTGSAGATIR.L K.DLEALMLDR.S K.FFGNLMDASK.L K.IALYETPTGWK.F K.TIEEYAICPDLK.V R.YDYEEVEAEGANK.M K.QFSANDKVYTVEK.A K.TQAYPDQKPGTSGLR.K K.ADNFEYSDPVDGSISK.N K.LSLCGEESFGTGSDHIR.E R.YDYEEVEAEGANKMMK.D K.INQDPQVMLAPLISIALK.V	gi|77627971	6.14	61642	25	362	42	1.7
13	Coq 9 protein	K.LVQLGQAEK.R R.MLIPYIEHWPR.A K.STGEALVQGLMGAAVTLK.N R.YTDQSGEEEEDYESEEQIQHR.I	gi|51259441	5.5	35095	4	76	19	1.7

14	dihydrolipoamide s-acetyltransferase	R.VFVSPLAK.K K.ILVPEGTR.D K.LIPADNEK.G K.DIDSFVPTK.A K.GRVFVSPLAK.K K.ELNKMLEGK.G K.AAPAAAAAAPPGPR.V K.YLEKPVTMLL.- K.GIDLTQVKGTGPEGR.I R.DVPLGTPLCIIVEK.Q K.VPLPSLSPTMQAGTIAR.W R.VAPTPAGVFIDIPISNIR.R R.VAPTPAGVFIDIPISNIRR.V K.DIDSFVPTKAAPAAAAAAPPGPR.V	gi|78365255	8.76	67637	14	121	21	1.8
15	isocitrate dehydrogenase 3 (NAD+) alpha	K.APIQWEER.N R.NVTAIQGPGGK.W K.IEAACFATIK.D R.HMGLFDHAAK.I K.CSDFTEEICRR.V K.TPIAAGHPSMNLLLR.K K.DMANPTALLLSAVMMLR.H R.NVTAIQGPGGKWMIPPEAK.E	gi|16758446	6.47	40052	8	94	24	1.9
16	cytochrome c oxidase, subunit Va	R.LNDFASAVR.I R.RLNDFASAVR.I K.GMNTLVGYDLVPEPK.I K.GMNTLVGYDLVPEPK.I R.KGMNTLVGYDLVPEPK.I	gi|24233541	6.08	16354	5	85	17	1.9

17	capping protein (actin filament) muscle z-line, apha 2	R.LLLNNDNLLR.E K.EHYPNGVCTVYGK.K K.FTVTPSTTQVVGILK.I K.DIQDSLTVSNEVQTAK.E K.IQVHYYEDGNVQLVSHK.D K.FIIHAPPGEFNEVFNDVR.L R.EGAAHAFAQYNLDQFTPVK.I K.EATDPRPYEAENAIESWR.T K.IVEAAENEYQTAISENYQTMSDTTFK.A	gi|6671672	5.57	33121	9	162	53	2
18	Actin a isoform CRA_α	K.IIAPPER.K K.AGFAGDDAPR.A R.DLTDYLMK.I R.DLTDYLMK.I R.GYSFVTTAER.E K.EITALAPSTMK.I R.AVFPSIVGRPR.H	gi|149043182	5.23	42372	7	279	16	2.1
19	heat shock protein 27 HspB1	R.QLSSGVSEIR.Q R.LFDQAFGVPR.F R.VSLDVNHFAPEELTVK.T K.AVTQSAEITIPVTFEAR.A K.YTLPPGVDPTLVSSSLSPEGTLTVEAPLPK.A R.KYTLPPGVDPTLVSSSLSPEGTLTVEAPLPK.A	gi|6978487	6.12	22937	2	122	40	2.3

20	fructose-bisphosphate aldolase A	R.QLLLTADDR.V K.GILAADESTGSIAK.R K.ADDGRPFPQVIK.S M.PHPYPALTPEQK.K K.CPLLKPWALTFSYGR.A K.IGEHTPSSLAIMENANVLAR.Y K.IGEHTPSSLAIMENANVLAR.Y K.GVVPLAGTNGETTTQGLDGLSER.C K.VDKGVVPLAGTNGETTTQGLDGLSER.C	gi|6978487	8.31	39791	11	166	37	2.3
21	beta globulin minor	M.VHLTDAEK.A K.ATVSGLWGK.V R.LLVVYPWTQR.Y K.VNADNVGAEALGR.L K.EFTPCAQAAFQK.V K.VVAGVASALAHKYH.- K.FGDLSSASAIMGNPQVK.A K.ATVSGLWGKVNADNVGAEALGR.L R.YFSKFGDLSSASAIMGNPQVK.A	gi|164448680	8.91	16088	10	159	59	2.4
22	3 mercaptopyruvate sulfertransferase	R.FQVVDAR.A R.RFQVVDAR.A R.FQGTQPEPR.D K.LLDASWYLPK.L R.AQPEHVISQGR.G R.ALVSAQWVAEALK.S K.THEDILENLDAR.R K.THEDILENLDARR.F K.SPSEPAEFCAQLDPSFIK.T R.DGIEPGHIPGSVNIPFTEFLTSEGLEK.S	gi|20304123	5.88	33209	12	199	36	2.5

23	monoglyceride lipase	R.IDSSVLSR.N R.MVVSDFQVFVR.D K.GAYLLMESSPSQDK.T R.LTLPFLLLQGSADR.L	gi|19923092	6.92	33826	3	110	10	2.8

3.3.1.4 Skeletal muscle proteins with diabetes-associated expression changes.

The two muscle protein species with the highest fold decrease were identified as carbonic anhydrase isoform CA3 (spot 1) and 3-hydroxyisobutyrate dehydrogenase (spot2). Other proteins with reduced expression level were found to be the E2 component of the 2-oxo-glutarate dehydrogenase complex (spot 3) enolase (spots 5 and 7) and esterase D formylglutathione hydrolase (spot 6). Spots 4 and 8, which were both identified as mitochondrial ATP synthase, exhibited decreased and increased levels, respectively. These findings are difficult to interpret, but may be due to differential pathological effects on post-translational modifications in ATP synthase molecules. This might explain the opposite alterations in expression levels of two ATP synthase isoforms with differing isoelectric points and molecular masses. Muscle-associated proteins with an increased abundance in GK muscle preparations were identified as adenylate kinase isoform AK1 (spot 9), Cu/Zn superoxide dismutase (spot 10), immunoglobulin light chain (spot 11), phosphoglucomutase 9spot 12), Coq 9 protein (spot 13), the E2 component of the pyruvate dehydrogenase complex (spot 14), isocitrate dehydrogenase (spot 15), cytochrome c oxidase (spot 16), capping protein of the actin filament (spot 17), alpha-actin (spot 18), stress protein Hsp27/B1 (spot 19), fructose-biphosphate aldolase (spot 20), beta-globulin (spot 21), and 3-mercaptopyruvate sulfurtransferase (spot 22). Interestingly, the muscle protein species with the highest fold increase was identified as the enzyme monoglyceride lipase (spot 23).

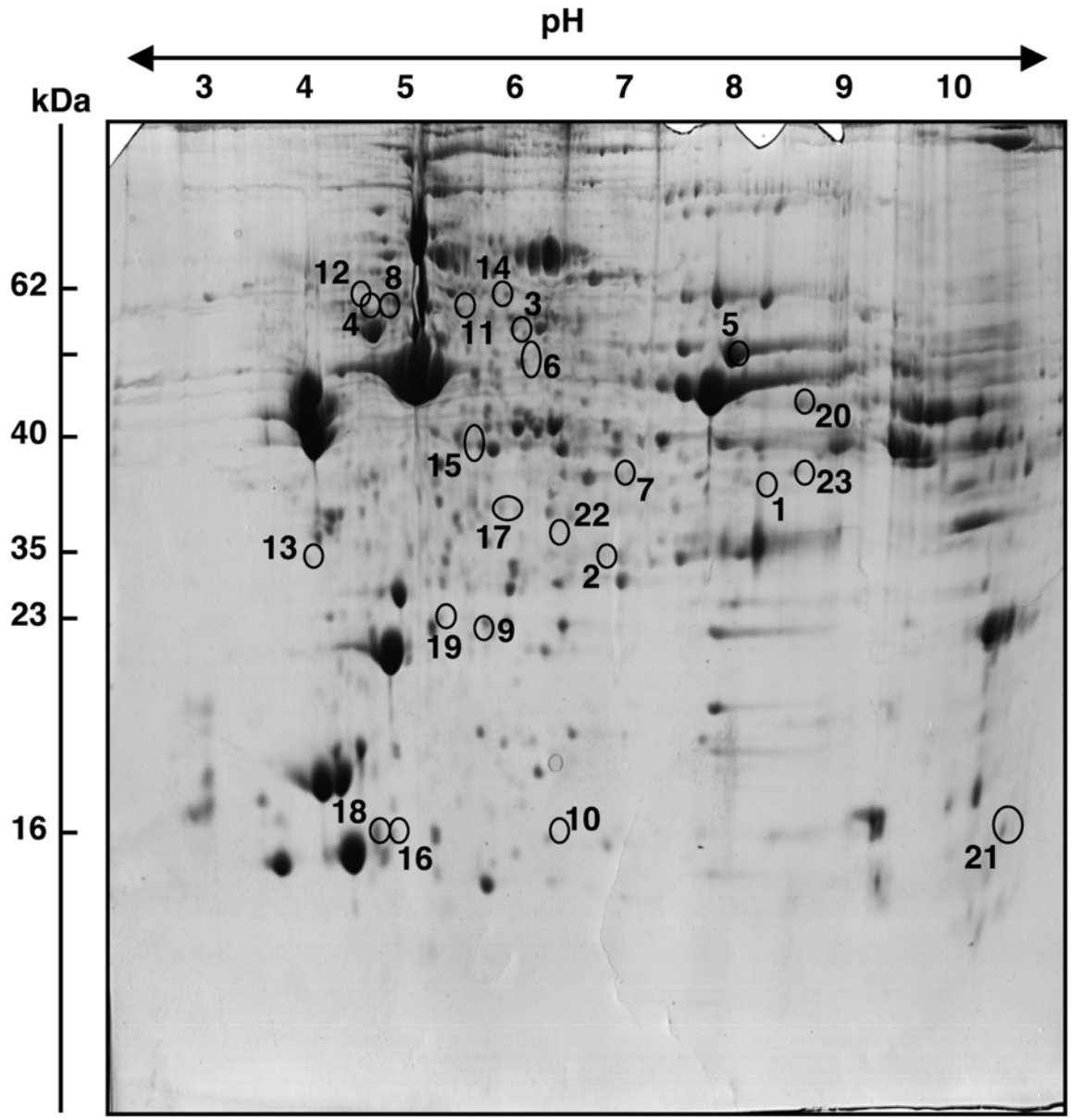

Figure 3.2: Two-dimensional reference gel of diabetic rat skeletal muscle. Shown is a colloidal Coomassie Blue stained reference gel of diabetic rat skeletal muscle, used for mass spectrometric identification of proteins with a differential expression profile. The pH-values of the first dimension gel system and molecular mass standards (in kDa) of the second dimension are indicated on the top and left of the panel, respectively. Identified muscle proteins are marked by circles

and are numbered 1 to 23. See Table 1 for a detailed listing of proteins that exhibit a diabetes-associated change in their abundance.

3.3.1.5 Silver- and RuBP's-stained protein candidates with diabetes-associated expression changes.

Following the detailed MS-based identification of CBB-stained proteins, diabetes-related changes in the expression of silver- or fluorescent RuBPs-labelled proteins was carried out. Although larger numbers of total protein spots were visualized by these two methods, surprisingly no additional components with a markedly higher fold changes were identified. Interesting silver-stained proteins with a lower abundance in GK muscle were found to be acyl-CoA dehygrogenase (gi|56541110|; p*I* 8.9; 70.8 kDa) and pyruvate kinase (gi|1675994|; p*I* 6.6; 57.8 kDa). Fluorescent RuBPs staining revealed a reduced expression of malate dehydrogenase isoform MDH-1 (gi|37590235|; p*I* 6.1; 36.5 kDa) in diabetic tissue preparations.

3.4 Discussion

Diabetes mellitus and its associated complications affect millions of patients worldwide, causing blindness, cardiomyopathy, kidney failure, stroke and skeletal muscular weakness (Zimmet *et al*., 2001). Older adults with type 2 diabetes exhibit significantly decreased muscle strength (Park *et al.,* 2006), which is thought to be a major contributor to the development of physical disability in the senescent population (Gregg *et al*., 2000). These clinical facts clearly warrant

detailed biochemical investigations into the molecular and cellular mechanisms that underlie abnormal hormone signalling in diabetic muscle tissue. Insulin resistance in peripheral organ systems, representing one of the main features of diabetes-related dysregulation, is believed to be already present at a very early stage of the pre-diabetic state (Korc *et al* 2003). In early type 2 diabetes, low levels of insulin resistance can probably be partially compensated by increased secretion levels via enhanced pancreatic β-cell activity. However, at more advanced stages of diabetes, β-cell failure occurs leading to inadequate amounts of circulating insulin to overcome defects in tissue sensitivity (Phielix *et al*., 2003). Since type 2 diabetes is an extremely complex and heterogeneous disorder, and probably involves both genetic and environmental factors, an unbiased global analysis of diabetic tissues by proteomics should be useful to identify novel indicators of its molecular pathogenesis. In this respect, the mass spectrometry-based proteomic survey of diabetic skeletal muscle tissue presented here has successfully revealed a variety of expression changes in key muscle proteins. However, as compared to more severe muscular defects, the diabetes-related expression changes of metabolic enzymes are relatively moderate.

The proteomic analysis of GK muscles indicates that abundant enzymes, transporters and structural components are affected in the non-obese diabetic phenotype. This includes muscle-associated proteins involved in glycolysis, the citric acid cycle, oxidative phosphorylation, lipolytic catabolism, nucleotide metabolism, carbon dioxide removal, oxygen transportation, amino acid catabolism, the contractile apparatus, cellular detoxification mechanisms and the

stress response. The muscle protein species with the highest fold decrease were identified as 3-hydroxy-isobutyrate dehydrogenase and carbonic anhydrase CA3. Hydroxy-isobutyrate dehydrogenase is involved in a rate-limiting step of the degradation of valine, leucine and isoleucine (Murin *et al.,* 2008). The resulting carbon skeleton can be utilized as a metabolic substrate for the generation of energy, and this mechanism appears to be weakened in diabetic muscle tissues. Interestingly, the CO_2-removal mechanism and a specific detoxification mechanism seem to be affected in GK muscles. Since the muscle-specific isoform CA3 of carbonic anhydrase catalyses the vital conversion of CO_2 into carbonic acid (Geers *et al*., 2000), its reduced expression suggests an impaired removal of CO_2 in diabetic fibres. In addition, a decreased concentration of esterase D formylglutathione hydrolase might cause toxic side effects. The reduced expression of dihydrolipoamide succinyltransferase, the core enzyme of the 2-oxoglutarate dehydrogenase complex in muscle mitochondria that participates in succinyl-CoA production (Matuda *et al*., 1997), agrees with the idea of abnormal mitochondrial functioning in diabetes (Mogensen *et al*., 2007). However, other mitochondrial markers such as isocitrate dehydrogenase, cytochrome c oxidase and Coq 9 protein (Sohal *et al*., 2007) were shown to be increased in GK muscle, possibly representing a compensatory mechanism to improve the oxidative capacity. This would agree with the increased level of beta-globulin.

Diabetes seems to have a differential effect on key enzymes of the glycolytic pathway. While enolase levels were shown to be decreased,

phosphoglucomutase and aldolase exhibited an elevated concentration in GK muscles. Since many glycolytic enzymes are multi-functional, it is difficult to interpret how insulin resistance triggers these altered expression patterns. However, changed abundances in these enzymes will certainly alter the glycolytic flux in diabetic muscle. Interestingly, pyruvate dehydrogenase, the key linker enzyme that connects glycolysis with the citric acid cycle, is elevated. This might be a compensatory mechanism in glucose-starved diabetic muscle tissues and might help to maximise the transformation of glycolysis-derived pyruvate into acetyl-CoA. In analogy to a recent proteomic survey of obese muscle (Hittle *et al*., 2005), the AK1 isoform of adenylate kinase is increased in diabetes, suggesting alterations in nucleotide metabolism. Higher concentrations of the contractile elements alpha-actin and the capping protein of the actin filament indicate diabetes-dependent repair mechanisms of the thin filament. This would agree with increased levels of stress proteins and anti-oxidant markers, such as the small heat shock protein Hsp27/B1, 3-mercaptopyruvate sulfurtransferase and Cu/Zn superoxide dismutase. Their up-regulation demonstrates a considerable need to counter-act cellular damage due to diabetes.

The protein species with the highest fold increase in GK muscle was identified as monoglyceride lipase. This enzyme mediates a critical step in the hydrolysis of stored triglycerides (Zechner *et al*., 2009) and its up-regulation might represent increased energy utilization by the lipolytic pathway in glucose-starved muscle tissues. More detailed biochemical studies have to be carried out to determine the general suitability of monoglyceride lipase as a muscle marker of non-obese

diabetes. However, it is clear that insulin resistance results in a lack of glucose uptake by muscle cells, which in turn has an effect on other metabolic pathways such as gluconeogenesis, triacylglycerol hydrolysis, fatty acid oxidation and ketone body formation.

3.5 Conclusion

In conclusion, this initial study of changes in the protein expression pattern of GK muscle has identified interesting new candidates for the establishment of a biomarker signature of diabetic skeletal muscle. It will now be critical to correlate these findings to investigations on human skeletal muscle (Hojlund *et al*., 2003, Stentz *et al*., 2007) and to conduct more detailed studies with other protein dyes that exhibit a different dynamic labelling range, such as fluorescent methodologies (Viswanathan et *al.,* 2006). In the future, new signature molecules will hopefully be useful for the improvement of diagnostic methods and the identification of superior therapeutic targets to eliminate diabetes-associated muscle weakness

Chapter 4

Skeletal muscle from the Goto-Kakizaki rat model of type 2 diabetes exhibit increased levels of the small heat shock protein Hsp27

4 Skeletal muscle from the Goto-Kakizaki rat model of type 2 diabetes exhibit increased levels of the small heat shock protein Hsp27

4.1 Introduction

The application of gel electrophoresis-based proteomics in diabetes research is a fast growing field (Sundsten, 2009), especially in the area of the proteomic analysis of diabetic skeletal muscle tissues (Hojlund, e*t al.,* 2003, Stentz, *et al.,* 2007 and Hwang, *et al*., 2010). Since diabetes appears to be reaching endemic proportions, research into the complex pathophysiological mechanisms that underlie abnormal signaling in crucial target organs, such as skeletal muscle, is of central importance (Petersen *et al*., 2002, Phielix *et al*., 2008, Abdul-Ghani e*t al*., 2010) . It is now clear that type-2 diabetes mellitus represents a group of heterogeneous disorders with abnormal expression patterns in various genes and protein products (Scheen *et al*., 2003, Sander *et al*., 2003, Tusie-Luna *et al*., 2003). Peripheral insulin resistance in the liver, adipose tissue and muscles, as well as impaired pancreatic β-cell functioning, are the principal features of type-2 diabetes (Sander *et al.,* 2003). The worldwide incidence of type-2 diabetes is dramatically increasing (King *et al.,* 1998) and the prevalence of diabetes has been estimated to rise to a staggering 4.4% by the year 2030 with 366 million

affected patients (Wild *et al.,* 2004). Importantly, type-2 diabetes is associated with a loss of skeletal muscle mass and contractile strength (Gregg *et al.,* 2000, Andersen *et al*., 2004, Park *et al.,* 2006) warranting detailed investigations into diabetes-related muscle weakness (Mulvey *et al.,* 2008). In this respect, large-scale biochemical approaches, such as gel electrophoresis-based proteomics, are ideal analytical tools for an unbiased identification of novel protein factors that are associated with abnormal functioning in diabetic fibres.

High-resolution two-dimensional gel electrophoresis has long been established as one of the most powerful biochemical techniques for the comparative analysis of large protein complements (Issaq *et al*., 2008, Weiss *et al*., 2009 Westermeier *et al*., 2009). The more recent combination of advanced gel electrophoretic methods with mass spectrometry has further reinforced the central importance of gel electrophoretic techniques for analytical protein chemistry (Gorg *et al.,* 2004, Wittmann-Liebold *et al*., 2006, Rabilloud *et al*., 2009). The unprecedented advancements of mass spectrometric methods for the swift identification of minute amounts of protein (Domon *et al.,* 2006) and the emergence of high-throughput proteomics as a major new field in modern biochemistry (Canas et al., 2006) have opened unparalleled opportunities for the in-depth analysis of complex pathological processes. However, a major obstacle for the inclusive cataloging of large and diverse protein complements is the dynamic concentration range of protein species within a given class of cells or tissues. Since different staining techniques used in two-dimensional gel electrophoresis visualize varied dynamic expression ranges, protein labeling may considerably

influence proteomic identification protocols. Here, we have used fluorescence difference in-gel electrophoresis (DIGE) for the determination of potential expression changes in the soluble proteome from normal Wistar rat muscle versus type-2 diabetic Goto-Kakizaki (GK) rat muscle. The GK rat is an established animal model of non-obese type-2 diabetes (Kitahara *et al.,* 1978) that exhibits peripheral insulin resistance (Abdel-Halim *et al*., 1994) and numerous molecular and cellular abnormalities due to its diabetic status (Portha *et al*., 1991, Witte *et al*., 2002), including abnormal skeletal muscle functions (Krook *et al*., 1997, Dadke *et al*., 2000, Mulvey *et al.,* 2005, Shen *et al*., 2008).

Our comparative mass spectrometry-based proteomic analysis revealed a moderately disturbed protein expression pattern in diabetic muscle fibres. Mass spectrometry identified 15 distinct 2-D protein spots with an altered abundance in diabetic muscle tissue preparations, using analytical DIGE gels with a pH 3-10 range. Besides altered expression patterns in various contractile and metabolic muscle proteins, a striking increase in two heat shock proteins (Hsp), αB-crystallin and Hsp27, was established by densitometric scanning and mass spectrometry. Muscle-associated Hsps protect contractile fibres during hyperthermia, hypoxic insult, ischemic damage, extensive periods of exercise, traumatic injury and in numerous neuromuscular diseases (Nishimura *et al.,* 2005). Hsps of low molecular mass are specifically induced during muscle injury (Golenhofen *et al*., 2004), whereby their main cytoprotective functions include the prevention of deleterious protein aggregation and the modulation of intermediate filament assembly (Nicholl *et al.,* 1994). Small Hsps are characterized by a

conserved 90-residue carboxy-terminal sequence, the α-crystallin domain (van Montfort *et al.,* 2001). These small cytoprotective chaperones appear to be up-regulated in GK muscle tissue. Hence, diabetes-related changes in the cellular stress response, the contractile machinery, metabolic pathways and various regulatory mechanisms are possibly linked to peripheral insulin resistance in skeletal muscles. In the future, these novel signature molecules might be helpful for the establishment of a comprehensive biomarker signature of type-2 diabetes mellitus.

4.2 Methods

4.2.1 Diabetic animal model.

For the comparative proteomic analysis of normal versus diabetic muscle tissue, normal Wistar rats and the spontaneous diabetic Goto-Kakazaki (GK) rat were used in this study. The GK rat is an established model of non-obese type-2 diabetes. Rats were purchased from M & B Taconic Ltd. Animal Suppliers (Ry, Denmark). The total soluble proteome was extracted from gastrocnemius muscles from 9-week old normal rats and age-matched GK rats. The diabetic status of the cohort of GK rats employed in this study has previously been described in detail.

4.2.2. Preparation of muscle extract.

Gastrocnemius muscle samples from normal and GK rats with a wet weight of 200 mg were quick-frozen in liquid nitrogen and then ground into a fine powder using a mortar and pestle. The muscle powder was transferred into 1ml lysis

buffer containing 2% (v/v) pH 3-10 ampholytes, 7M urea, 2M thiourea, 4%(w/v) CHAPS and 100 mM dithiothreitol. A freshly prepared protease inhibitor cocktail was added to the buffer to prevent proteolytic degradation of sensitive muscle proteins. The suspension was incubated for 3 hours at room temperature and then centrifuged at 14,000x*g* for 20min at 4^0C. The Bradford dye-binding method was used to determine the protein concentration of the final extracts from normal versus GK muscle tissue.

4.2.3. Gel electrophoretic analysis.

Total crude skeletal muscle extracts of normal (n=4) and diabetic (n=4) muscle tissues were separated in the first dimension by isoelectric focusing and in the second dimensional by standard sodium dodecyl sulphate polyacrylamide gel electrophoresis, as previously described by our laboratory. IPG strips were rehydrated for 12 hours in a buffer consisting of 7M urea, 2M thiourea, 4% (w/v) CHAPS, 1.2% deStreak and 2% (v/v) pH 3-10 ampholytes. The buffer system contained 400 µg of muscle protein. The first-dimension protein separation was conducted using IPG strips on an Amersham IPGphor IEF system (Amersham Bioscience/GE Healthcare, Little Chalfont, Bucks, UK) following the protocol previously described in detail. The first dimension strips were further subjected to reduction and alkylation before separation in the second-dimension on 12.5% (w/v) slab gels using an Amersham Ettan DALT-Twelve system.

4.2.4. Protein Visualisation.

For DIGE analysis, Cy3 and Cy5 dyes were reconstituted as a stock solution of 1mM in fresh dimethylformamide. The stock solution was diluted to a working solution of 0.2 mM prior to protein labelling. Individual samples (50 µg protein) were minimally labelled with 200 pmols of Cy3 working solution. A pooled sample consisting of equal quantities of protein from all replicates used in the experiment were labelled at a ratio of 200 pmol of Cy5 working solution to 50 µg of muscle protein. All samples were labelled with the appropriate amount of dye at pH 8.5 and then incubated on ice in the dark for 30 minutes. The reaction was quenched by 10 mM lysine for 10 minutes on ice in the dark. During the subsequent rehydration step, samples were loaded onto IPG strips with an equal volume of 2x sample buffer (7M urea, 2M thiourea, 65mM CHAPS, 2% ampholytes and 2% dithiothreitol). Slab gels were stained for total protein with Coomassie Brillinat Blue or ruthenium bathophenanthroline disulfonate (RuBPs). A stock solution of RuBPs dye was prepared as described by Rabilloud et al. Two-dimensional gels were fixed overnight in 30% (v/v) ethanol and 10% (v/v) acetic acid and subsequently washed 4 times for 30 min in 20% (v/v) ethanol to remove traces of acetic acid. The ruthenium fluorophore was then applied to the gels by adding 10 ml of the freshly synthesized dye to 1 litre of 20% (v/v) ethanol in the dark. Gels were incubated for 6 hours in the staining solution. Labelled gels were then destained in 40% (v/v) ethanol and 10% (v/v) acetic acid. Reference gels for spot picking were stained with Commasie Brillinat Blue. Gel images were analysed

using Progenesis SameSpots software version 3.2.3 from NonLinear Dynamics (Newcastle upon Tyne, UK)

4.2.5. Mass spectrometric identification of skeletal muscle proteins.

The mass spectrometric analysis of peptide mixtures derived from distinct two-dimensional spots was carried out on a Model 6430 Ion Trap LC/MS apparatus from Agilent Technologies (Santa Clara, CA, USA). The excision of protein spots and subsequent washing, destaining and digestion steps were preformed by a previously optimised method. Trypsination-generated peptides were recovered from supernatants of digested gel plugs and samples dried through vacuum centrifugation. The resulting peptides were resuspended in 10 □l of MS-grade ddH_2O and 0.1% (w/v) formic acid for identification by ion trap LC-MS analysis. Separation of peptides was performed with a nano flow Agilent 1200 series system, equipped with a Zorbax 300SB C 185 mm, 4 mm 40nl pre-column and a Zorbax 300S B C 185 mm, 43mm x 75μm analytical reversed- phase column using HPLC-Chip technology. Mobile phases utilized were A: 0.1% formic acid, B: 50% acetonitrile and 0.1% formic acid. Samples (5 □l) were loaded into the enrichment at capillary flow rate set to 2 □l/min with a mix of A and B at a ratio 19:1. Tryptic peptides were eluted with a linear gradient of 10-90% solvent B over 2 □l/ min with a constant nano pump flow of 0.6 ml/ min. A 1 min post time of solvent A was used to remove sample carry over. The capillary voltage was set to 1700 V. The flow and the temperature of the drying gas were 4 □l/ min and

300^{o}C, respectively. Database searches were carried out with Spectrum Mill Work Bench or Mascot MS/MS Ion search (Matrix Science, London, UK).

4.2.6. Immunoblot analysis.

To verify changes in the abundance of select proteins in GK muscle preparations, immunoblotting was carried as previously described in detail. Gels were transferred to nitrocellulose and blocked with a milk protein solution consisting of 5% (w/v) fat-free milk powder in 0.9 % (w/v) NaCl, 50 mM sodium phosphate, pH 7.4 for 1h. Subsequently, membranes were incubated overnight with sufficiently diluted primary antibody, washed and then incubated for 1h with secondary peroxidase-conjugated antibodies, diluted in blocking solution. The visualization of immuno-decorated bands was carried out by the enhanced chemiluminescence method using blotting substrate from Roche Diagnostics (Mannheim, Germany). Densitometric scanning of immunoblots was performed on a Molecular Dynamics 300S computing densitometer (Sunnyvale, CA, USA) with ImageJ (NIH, USA) and GraphPad Prism (San Diego, CA, USA) software.

4.3 Results

4.3.1 Proteomic analysis of diabetic GK muscle extracts.

Difference in-gel electrophoresis (DIGE) represents an excellent analytical tool for large-scale proteomic surveys (Tonge et al., 2001, Marouga et al., 2005, Viswanathan et al., 2006) and this method was applied here for the comparative

analysis of normal versus diabetic muscle extracts. With the help of a Typhoon Trio variable imager and Progenesis 2-D analysis software, 15 protein species out of 1734 detectable 2-D spots were found to be differentially expressed. Representative Cy3 and Cy5 gels with electrophoretically separated proteins from normal versus diabetic muscle tissue are shown for the pH 3-10 range in Fig. 4.1a-d. The protein spot patterns of normal versus pathological preparations were relatively comparable. However, the detailed densitometric analysis of Wistar rat versus GK rat muscle tissue identified distinct changes in a variety of protein species. A representative DIGE master gel of GK rat skeletal muscle preparations employed for the mass spectrometric identification of proteins with a diabetes-related differential expression pattern is shown in Figure. 4.1e. Skeletal muscle proteins that exhibited a more than 2-fold change in expression levels are marked by circles and are numbered 1 to 15. Proteins species with a changed concentration in GK gastrocnemius muscle ranged in molecular mass from 16 kDa (hemoglobin) to 223 kDa (myosin heavy chain) and covered a p*I*-range from p*I* 4.1 (troponin) to p*I* 8.9 (bisphosphoglycerate mutase). An increased abundance was found in the case of 10 skeletal muscle-associated proteins, and 5 proteins were shown to be decreased in their concentration.

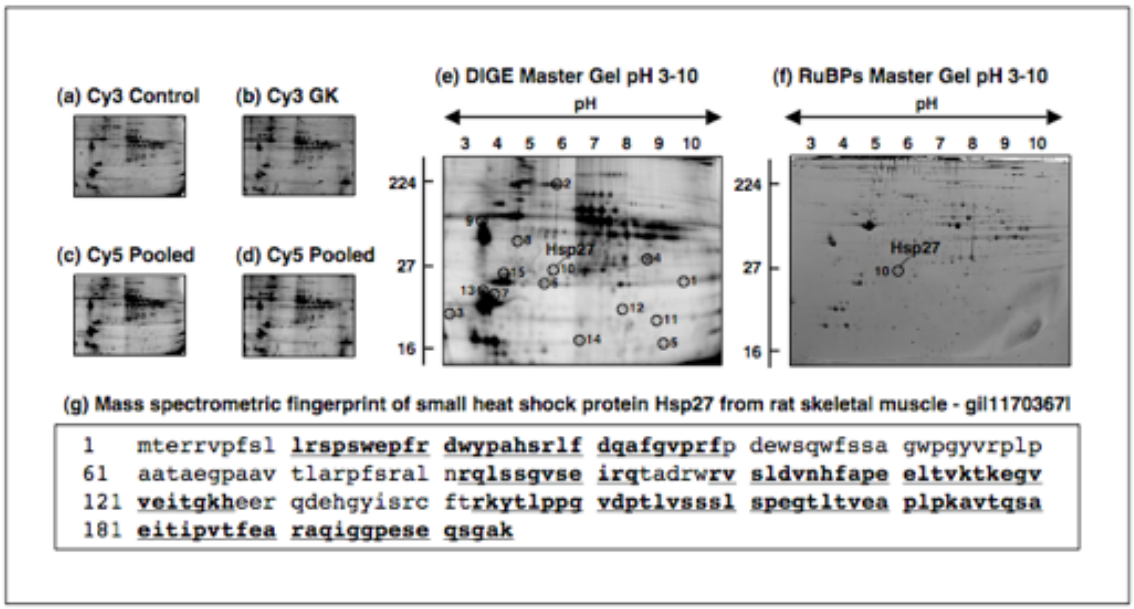

Figure 4.1. Proteomic profiling of diabetic rat GK skeletal muscle using fluorescent DIGE analysis and RuBPs staining. Crude total muscle extracts from normal and Goto-Kakizaki (GK) gastrocnemius muscle tissue were separated in the first dimension by isolelectric focusing and in the second dimension by sodium dodecyl sulfate polyacrylamide gel electrophoresis. Shown are Cy3-labeled control samples (a), Cy3-labeled diabetic GK samples (b) and Cy5-labeled pooled standards (c, d). A DIGE master gel with a pH 3-10 range is shown in panel (e). Identified muscle proteins are marked by circles and are numbered 1 to 15. See Table 1 for a detailed listing of protein species that exhibited a diabetes-related alteration in their expression levels. To verify the changed abundance in the molecular chaperone Hsp27 (spot no. 10), fluorescent ruthenium bathophenanthroline disulfonate (RuBPs) staining was used (f). The 2D-spot representing Hsp27 is marked by a circle. The pH-values of the first dimension gel system and molecular mass standards (in kDa) of the second dimension are indicated on the top and on the left of panels (e, f), respectively. The mass spectrometric fingerprint of Hsp27 is shown in panel (g).

4.3.2 Proteomic profile of diabetic skeletal muscle tissue.

A list of the 15 DIGE-identified muscle proteins, which exhibited a drastically

altered expression level in the non-obese diabetic GK rat, is shown in Table 4.1. Listed are the names of the identified proteins, their international protein accession number, pI-values, their relative molecular masses, number of matched peptide sequences, percentage sequence coverage, Mascot scores, and fold-change of individual proteins affected in diabetic muscle tissue. The identified muscle proteins were found to be mostly associated with the contractile apparatus, muscle metabolism, metabolite transportation and the cellular stress response. The numbering of spots in the DIGE-labeled master gel of Fig. 4.1e correlates with the listing of mass spectrometry-identified protein species in Table 4.1. The protein with the highest decrease in concentration was identified as bisphosphoglycerate mutase and that with the highest increase in abundance shown to be the fast 1f-isoform of myosin light chain. Muscle proteins with a drastic decrease were found to be bisphosphoglycerate mutase (spot 1), myosin heavy chain 4 (spot 2), troponin C (spot 3), Tip1 protein (spot 4) and hemoglobin (spot 5). In contrast, muscle proteins with an increased expression in diabetic muscle tissue were identified as fast troponin T (spots 6 and 11), tropomyosin (spot 7), slow myosin light chain 3 (spot 8), fast myosin light chain 1f (spots 9 and 15), Hsp27 (spot 10), αB-crystallin (spot 12), myozenin (spot 13) and myoglobin (spot 14).

Table 4.1 **DIGE-identified proteins with a changed abundance in diabetic GK muscle extracts**

Spot No.	Protein Name	Accession No.	pI	M.W	No. of pep	Macot Score	%Coverage	Fold Change
1	bisphosphoglycerate mutase 2	gi8393948	8.85	28911	16	185	43	-3.3
2	myosin heavey chain 4, skeletal muscle	gi|106879208	5.58	223669	17	181	7	-2.4
3	troponin C, type 2	gi|82654194	4.06	18142	19	482	65	-2.2
4	Tip1 protein	gi|38512111	7.07	27228	26	459	81	-2.1
5	major beta-hemoglobin	gi|204570	7.88	16099	3	141	28	-2
6	troponin T, fast skeletal muscle	gi|136385	6.19	30732	2	78	11	2
7	Tropomyosin 2, beta	gi|11875203	4.66	32933	16	361	33	2.1
8	myosin, light chain 3, alkali; ventricular, skeletal, slow	gi|6981240	5.03	22258	16	288	75	2.1
9	fast myosin alkali light chain 1f	gi|117676401	4.99	20782	9	113	51	2.1
10	heat shock protein 27	gi|1170367	6.12	22937	11	119	60	2.4
11	troponin T, fast skeletal muscle	gi|136385	6.19	30732	4	86	15	2.4
12	alpha B-crystallin	gi|57580	8.84	19945	13	204	55	2.5
13	myozenin 1	gi|157819165	8.57	31379	2	109	11	2.6
14	myoglobin	gi|11024650	7.83	17204	2	98	21	3.2
15	fast myosin alkali light chain 1f	gi|117676401	4.99	20782	6	125	31	3.4

4.3.3 RuBPs analysis of Hsp27 in GK muscle extracts.

To verify the increased levels of the low-molecular-mass molecular chaperone Hsp27 in GK muscle, as revealed by DIGE analysis, the fluorescent dye ruthenium bathophenanthroline disulfonate (RuBPs) was employed for labeling electrophoretically separated muscle proteins. As illustrated in Fig. 4.1f, a protein spot with an approximate p*I* value of 6 and a relative molecular mass of 27 kDa was identified as Hsp27/HspB1. The mass spectrometric fingerprint of the RuBPs-stained Hsp27 protein spot is shown in Fig. 1g and illustrates 60% coverage of matched peptides. Thus, the densitometric analyses of two independent fluorescent labeling approaches agreed and clearly demonstrated a drastic increase in the small stress protein Hsp27.

4.3.4. Immunoblot analysis of GK muscle extracts.

In order to correlate the findings of the DIGE-based study described here and a previously published proteomic survey of GK muscle using Coomassie Brillinat Blue, an immunoblot analysis was carried out with normal versus GK preparations. Both, the drastic diabetes-related increase in Hsp27 and the actin binding-protein myozenin were clearly confirmed by immunoblotting (Fig. 4.2a, b, g). The previously established drastic decrease in carbonic anhydrase isoform CA3 and moderate increase in isocitrate dehydrogenase, Cu/Zn superoxide dismutase and actin capping-protein were also confirmed (Fig. 4.2c-f, h). Hence, immunoblotting verified the increased abundance of Hsp27 in diabetic GK muscle tissue and the differential expression pattern of other novel muscle-associated marker proteins of type 2 diabetes.

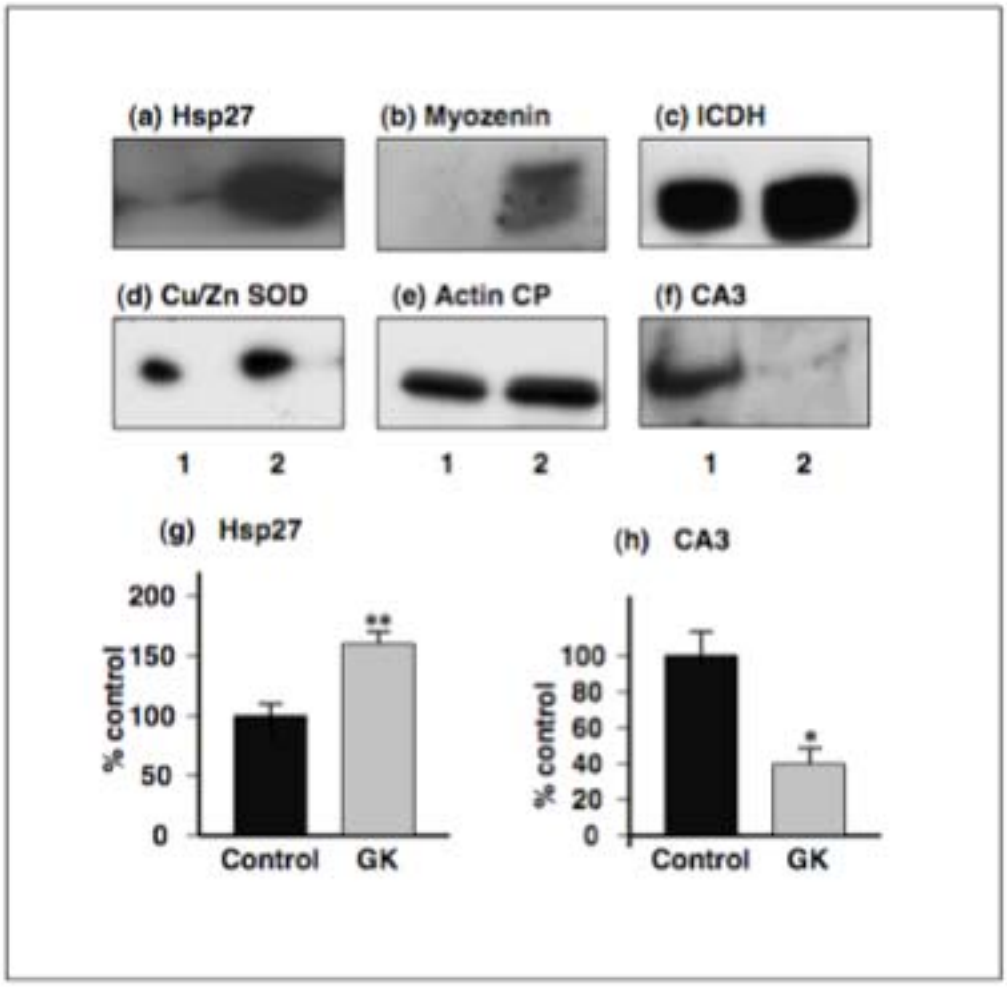

Figure 4.2. **Immunoblot analysis of diabetic rat GK skeletal muscle**. Shown are representative immunoblots with expanded views of immuno-decorated bands. Immunoblotting was performed with antibodies to the molecular chaperone Hsp27 (a), the actin binding protein myozenin (b), the enzyme isocitrate dehydrogenase (c; ICDH), the enzyme Cu/Zn superoxide dismutase (d; SOD), actin capping-protein (e; CP) and the enzyme carbonic anhydrase isoform CA3 (f). Shown is the graphical presentation of the statistical evaluation of immuno-decoration using antibodies to Hsp27 (g) and carbonic anhydrase CA3 (h). The comparative blotting was statistically evaluated using an unpaired

Student's *t*-test (n=5; *p<0.05; **p<0.01). Lanes 1 and 2 represent normal and diabetic muscle extracts from control and GK rats, respectively.

4.4 Discussion

The GK rat is an established animal model of non-obese type-2 diabetes. Importantly, these animals are spontaneously diabetic (Kitahara *et al.,* 1978) and clearly exhibit increased blood glucose levels without significant alterations in non-fasting plasma insulin levels and body weight (Abdel-Halim *et al*., 1994, Portha *et al*., 1991, Witte et al., 2002, Krook, *et al*., 1997) . We chose GK muscle tissues because they represent a suitable model system for studying fundamental mechanisms of type 2 diabetes without potentially complicating factors due to obesity. It is important to stress that no animal model represents a perfect replica of all pathobiochemical aspects seen in a highly complex human pathology. However, if one keeps in mind species-specific differences, findings from animal model proteomics can be extrapolated to the human situation (Doran *et al*., 2007). Ideally, a diabetic animal model should closely resemble the etiology of the human disease in onset, progression, complexity and severity, as well as develop all or most of the multi-factorial aspects usually observed in end-stage human pathology. A good model system should also mimic the basic mechanisms of human physiology and metabolism that are important for the development of diabetic side effects. It is therefore critical to choose the right age range of pathological GK tissues to study diabetic dysfunctions at a prominent stage of disease progression. It was previously reported that cellular defects in insulin secretion and peripheral insulin resistance occur by 4 weeks of age in the

GK rat (Abdel-Halim *et al*., 1994, Portha *et al.,* 1991). The proteomic profiling of diabetic muscle described here was therefore performed with 9-week old animals that clearly exhibited elevated levels of glucose (Mulvey *et al*., 2005).

Diabetic GK skeletal muscles are characterized by an inhibition of insulin receptor auto-phosphorylation (Krook *et al.,* 1997), impaired activities of numerous key insulin signaling intermediates (Witte *et al.,* 2002, Dadke *et al*., 2000), a diminished recruitment of glucose transporter GLUT4 molecules possibly linked to membrane cytoskeletal defects in the dystrophin-dystroglycan complex (Mulvey *et al.,* 2005, Mulvey *et al* 2008), drastically lowered mitochondrial enzyme activities (Shen *et al*., 2008) and a reduced percentage of oxidative fibres (Yasuda *et al*., 2002). These findings demonstrate chronically impaired insulin signaling in GK skeletal muscles making them a suitable model system to determine global changes in the protein expression pattern due to diabetic complications. The proteomic analysis presented here has clearly shown increased levels of the small chaperone Hsp27, also termed HspB1 (van Montfort *et al*., 2001), in GK muscle preparations. Importantly, results of our DIGE analysis were confirmed by fluorescence RuBPs labeling and immunoblotting. This report therefore confirms the findings of a previous proteomic characterization of GK muscle using Coomassie Brilliant Blue staining (Mullen *et al.,* 2010) and suggests a considerable up-regulation of specific low-molecular-mass chaperones in diabetic muscle tissue. The main cytoprotective functions of small Hsps include the modulation of intermediate filament assembly and the prevention of deleterious protein aggregation (Nicholl *et al.,* 1994). In addition,

increased levels of Cu-Zn superoxide dismutase (Miao *et al.,* 2009) suggest a critical need of diabetic muscles for an up-regulation of the anti-oxidant defense system. Thus, in analogy to dystrophic and aged skeletal muscles (Doran et al., 2006, Doran et al., 2007), contractile tissue seems to be associated with considerable levels of cellular stress due to type-2 diabetes.

In addition, the proteomic screening of GK muscle tissue also revealed protein alterations in the contractile apparatus and metabolic elements, suggesting a generally perturbed protein expression patterns due to diabetic side effects. These diabetes-related changes might be directly or indirectly associated with peripheral insulin resistance. The status of these the newly identified markers of type 2 diabetes has now to be verified by detailed biochemical, physiological and cell biological characterizations in order to establish a reliable biomarker signature of diabetes mellitus. Differential expression patterns of crucial contractile proteins agree with the concept of impaired muscle strength in diabetes (Gregg *et al.,* 2000, Park *et al.,* 2006, Park *et al.,* 2009). The pattern of altered abundance in contractile and regulatory elements does not indicate a fibre type-specific shift. On the one hand, protein spots representing myosin heavy chain 4 and troponin C were decreased in GK muscle. On the other hand, crucial contractile elements such as slow and fast isoforms of myosin light chain, myozenin and fast troponin T were found to be increased in diabetic preparations. Thus, in agreement with previous studies that have shown marked pathophysiological alterations in GK rat tissues (Steiler *et al.,* 2003, Shen *et al.,* 2008) and diabetic specimens from patients (Hojlund *et al*., 2003 Stentz *et al*.,

2003), the results presented here confirm the drastic effects of type 2 diabetes on voluntary contractile fibres.

In the field of neuromuscular pathology, there is an urgent need for the establishment of disease-specific biomarker signatures that can be used to differentiate between common changes due to general fibre degeneration versus pathobiochemical mechanisms that are unique to a particular muscular disorder. Various proteomic profiling programmes have been initiated to identify novel signature molecules of muscular atrophy, muscular dystrophy, muscle transformation and age-related muscle wasting (Ohlendieck *et al.,* 2010). In our experience, it is advisable to initially carry out small-scale pilot experiments to determine the general suitability of different protein dyes for specific proteomic applications. Thus, besides taking into account differing electrophoretic mobilities of soluble versus integral proteins, it is also important to keep in mind the affinity of diverse classes of proteins for different dye staining protocols. Here, we have shown that the DIGE method and the fluorescent dye RuBPs are highly suitable to determine protein alterations in the non-obese diabetic GK gastrocnemius muscle. In conclusion, the proteomic identification of the biomarker signature of diabetic effects on skeletal muscle may be useful for complementing future physiological and biochemical investigations into the molecular mechanisms of peripheral insulin resistance (Korc *et al*., 2003). The newly established tissue-specific combination of disease markers might also be exploitable in the evaluation of the effects of novel drug regimes, gene therapy approaches or cell-based therapies for counter-acting serious side effects of type 2 diabetes in

peripheral tissues.

Chapter 5

Enrichment and Analysis of the Mitochondrial Proteome

5 Enrichment and Analysis of the Mitochondrial Proteome

5.1 Introduction

5.1.1 Mitochondria

Depending on the function of the cell in question, hundreds to thousands of mitochondria may be present. For example muscle cells have more mitochondria than other cells due to the high energy demands of these cells. Mitochondria are organelles consisting of a double membrane, and the space between them is the inter membrane space. Cristae are projections formed from the many invaginations of the inner membrane. The cristea greatly increases the surface area of the inner membrane, which is the site of ATP generation, a process of great importance in muscle due to its high energy demands.

The citric acid cycle is responsible for the breakdown of acetyl CoA, as well as the synthesis of ATP. Acetyl CoA is produced via the breakdown of pyruvate, the final product of glycolosis. The conversion of acetyl CoA and oxaloacetate to citrate signifies the initial step of the citric acid cycle. The pyruvate dehydrogenase converts pyruvate to acetyl CoA by importing pyruvate into the mitochondrial matrix. Over a cascade of several reactions, one triggering the start of another, oxaloacetate is reformed (Krebs *et al.* 1980). These reactions result in the production of NADH which is used during oxidative phosphorylation.

Oxidative phosphorylation occurs by the transfer of energy stored within the

carbon bonds of glucose to the third phosphate bond of ATP. In this complex reaction energy is transferred as electrons, manipulating the dinucleotide electron carriers NADH and flavin adenine dinucleotide ($FADH_2$), across a series of protein complexes bound to the inner mitochondrial membrane. This transfer of electrons is coupled with the transportation of protons from the matrix to the intermembrane space, creating a proton gradient between the two compartments. After the transfer of electrons between four complexes, (Complex 1 NADH dehydrogenase, Complex 2 Succinate dehydrogenase, Complex 3 cytochrome C reductase, Complex 4 cytochrome C oxidase), a fifth complex (ATP synthase) is responsible for the re-entry of protons to the matrix from the intermembrane space. Complexes 1, 3 and 4 are reduction- and oxidation-driven proton pumps that use energy carried by electrons to pump protons out of the matrix, creating the proton electrochemical gradient. ATP synthase utilises the available energy within the electrochemical gradient to drive the synthesis of ATP from ADP and P*i* (Saraste 1999). Other processes such as haeme biosynthesis, apoptosis and fatty acid metabolism (Mannaerts *et al*. 1979; Antonsson et al. 2000; Sano *et al.* 1959) require mitochondrial involvement. For these cellular functions and for general normal cell function, it is critical that mitochondria remain intact and fully functional.

It is well established that mitochondrial function is required for normal glucose-stimulated insulin secretion from pancreatic b cells. Insulin resistant conditions resembling Type 1 Diabetes caused by maternal inheritance of defected mitochondrial DNA that perturbs mitochondrial function have also been

well documented. On this note, recent studies utilising magnetic resonance spectroscopy (MRS) have shown that more understated defects in mitochondrial function might also play a role in the pathogenesis of insulin resistance in T2D (K, F, Petersen *et al*. 2002). In the same study it was also shown that in young insulin-resistant offspring of parents with T2D, the insulin resistant subjects were found to have a lower ratio of type 1 to type 2 muscle fibres. Type 1 fibres are mostly oxidative and contain more mitochondria than type 2 muscle fibres, which are more glycolytic.

Glucose detection requires oxidative mitochondrial metabolism, which leads to the generation of ATP. The increased concentration of ATP to ADP initiates the deactivation of the ATP/ADP-regulated potassium channel (K_{ATP}) which causes the depolarisation of the plasma membrane. An influx of calcium ions is experienced due to the opening of voltage sensitive calcium channels which open when the plasma membrane becomes depolarised. The influx of calcium ions triggers the secretion of insulin. β cell dysfunction in T2D is believed to be secondary to increased exposure of β cells to glucose (glucotoxicity) and/or lipids (lipotoxicity) (R. H. Unger *et al*., 1995; M. Prentki *et al.,* 2002). However it is possible, due to the central role of mitochondria in glucose sensing, that reduced mitochondrial activity in β cells may prompt individuals to eventually develop β cell dysfunction and T2D.

5.1.2 Mitochondria and Type 2 Diabetes

Mitochondrial dysfunction in muscle has been implicated to play a causative role or being an indirect consequence of insulin resistance in type 2 diabetes. Besides

involvement in intermediary metabolism, protein transport, cell cycle progression, calcium signalling and regulation of apoptosis, mitochondria represent the primary site for energy generation via oxidative phosphorylation. Cellular dysfunction of muscle mitochondria is believed to play a crucial part in triggering insulin resistance (Lowell *et al*., 2005). It is not clear whether mitochondrial abnormalities are secondary consequence of impaired hormonal signalling or the actual primary cause for a diminished glucose uptake into peripheral tissues (Pagel-Langenickel *et al*., 2010).

For many obese individuals frank diabetes never develops and the pancreatic □cells adapt to meet the bodies requirements for insulin. This adaption develops via the expansion of the □ cell mass. For individuals who develop type 2 diabetes the b cells of the pancreas do not produce enough insulin to compensate for the demand for the hormone. Often the lack of insulin is due to the b cells not expanding or to meet the new requirements or failure of the b cells to respond or sense glucose. Several studies have reported that for individuals with type 2 diabetes glucose sensing is impaired and therefore the required amounts of insulin are not secreted (Liu *et al*., 2002).

5.1.3 Subcellular Proteomics

The separation of protein cell extracts via 2-D gel electrophoresis is a powerful technique which presents the possibility to separate as many as 2,000 proteins on one large slab gel. However, there are limitations to how much protein can be

visualised in the second dimension of a slab gel as well as the issue of masking, where larger, more abundant proteins can hide less abundant proteins because they migrate to similar points on the gel due to similar p*I*'s and molecular masses, and therefore limit the scope of the analysis. Another limiting factor is the volume of protein, which can be applied to the first dimension separation by isoelectric focusing (IEF), here again more abundant proteins can often enter the gel with the exclusion of others.

Overcoming these limitations has given rise to many different techniques such as preferential staining, as well as to separate cellular components into less complex mixtures, allowing an enrichment of a particular cell component or organelle. In other words, to reduce the complexity of the analyte. Sub cellular fractionation is a useful technique for isolating proteins associated with organelles such as mitochondria. There are many examples of researchers manipulating differential centrifugation and other fractionation techniques (charge fractionation, affinity fractionation, immunoprecipitation and size fractionation) to enrich for specific cellular compartments such as lysosomes, endosomes, rough endoplasmic reticulum (ER), golgi apparatus and centrosomes. Combined with narrow pH gradients in the first dimension, a less complex analyte will allow for greater separation and visualisation of a larger number of proteins (Westbrook et al. 2001). In every subcellular proteomic investigation, a pertinent question is a discussion of the purity of the fraction. Mitochondrial preparations are often found to be contaminated with cytosolic, microsomal and ER proteins. In this study the enrichment of mitochondria from the non-obese Goto-Kakizaki rat was conducted

to consider changes in the mitochondrial proteome and to highlight any possible mitochondrial biomarkers of Type 2 Diabetes.

5.1.4 DIGE analysis

Two dimensional polyacrylamide gel electrophoresis (2D-PAGE) has been the workhorse of proteomics allowing for the resolution of several thousand proteins in a single sample. Often a lack of reproducibility between conventional 2D-PAGE gels leads to significant system variation and induced biological change, which means that real differences between protein abundances attributed to, for example, a diseased state can rarely be predicted with confidence. 2D fluorescent Difference in Gel Electrophoresis (DIGE) can dramatically simplify the process by enabling up to three different samples to be run on the same 2D gel.DIGE is a 2-D gel electrophoresis technique that utilises ester cyanine dyes. The technique involves labelling proteins with cyanine dyes before 2-D gel electrophoresis. The method was first described by Unlu et al., 1997. As previously described in chapter 4, only two dyes were synthesised first which were Cy3 and Cy5. These dyes label proteins by forming covalent bonds with the primary amine of the amino acid lysine resulting in an amide linkage between the dye and the protein. Cy3 and Cy5 have the same reactive group and the same molecular mass. These two factors ensure equal labelling but with a separate emission spectra and excitation. Cy2 is another cyanine dye but it differs to Cy3 and Cy5 in that it is not as diverse as they are. Cy2 is not ideally mass matched and also it experiences an overlap in excitation spectra with Cy3. Recent DIGE studies have shown that the use of only Cy3 and Cy5 reaps a much lower

variance and therefore diminishing the need for higher number of replicates (Karp *et al*. 2005).

A unique feature of DIGE experiments is the inclusion of a pooled internal standard. This concept was first introduced by Alban et al 2003. In this publication the internal standard was prepared by pooling equal amounts from all biological samples and labeling them with one of the Cy dyes, usually Cy2. The internal standard was then run on the same gel as the other labeled protein samples, allowing every protein from all samples to be represented on the gel, therefore every protein within the samples can be linked to a common internal standard. The significance of the internal standard lies with the ability to normalise each sample to the internal standard on the same gel. This in turn allows for the abundance of each protein sample in a biological sample to be expressed as a ratio to the corresponding spot in the internal standard. This normalisation grants accurate quantitation and accurate spot statistics as discussed in chapter 4.

For this experiment a minimal labelling technique was used. This method involves labelling protein at a low ratio of dye to protein, which means that at least one lysine is labelled per protein and approximately 2-5% of lysines are labelled (Unlu *et al*. 1997).

5.2 Methods

5.2.1. Preparation of mitochondria-enriched fraction from skeletal muscle.

Gastrocnemius muscle tissue (3g wet weight) from 9-week old normal versus age-matched diabetic GK rats was cut into small pieces and homogenised in 20 ml of buffer (220mM mannitol, 70mM sucrose, 20mM Hepes, pH 7.4), supplemented with 1 Roche PIC complete mini tablet per 10 ml of solution. The resulting mixture was centrifuged at 1,100*g* for 5 min at 4^{o}C to remove cellular debris. The supernatant was retained. The pellet was re-suspended in 10 ml of homogenisation buffer and re-centrifuged as described above. Supernatants from the above separation steps were pooled and centrifuged at 7,000*g* for 15 min. The mitochondrial fraction was obtained as a pellet after repeated centrifugation steps at 20,000*g* for 15 min. The final mitochondria-enriched pellet was re-suspended in 2D lysis buffer for DIGE analysis. Samples were adjusted to a pH-value of 8.5. The protein content of individual samples was determined by the Bradford assay system.

5.2.2 Fluorescent labelling of proteins

Potential differences in the protein expression patterns of normal versus diabetic mitochondria were determined by difference in-gel electrophoresis (DIGE) using the CyDye DIGE fluor minimal dyes Cy3 and Cy5. DIGE dyes were reconstituted as a stock solution of 1mM in fresh dimethylformamide. The stock solution was diluted to a working solution of 0.2mM prior to fluorescent labelling. Samples of 50 mg protein, representing each biological replicate, were minimally labelled

with 200 pmols of Cy3 working solution. A pooled sample consisting of equal quantities of protein from all replicates used in the experiment were labelled at 200 pmol of Cy5 working solution to 50 mg of protein. The pooled fraction served as an internal standard. All samples were labelled at pH 8.5 with the appropriate amount of CyDye and after brief vortexing incubated on ice in the dark for 30 min. The labeling reaction was terminated by the addition of 1µl of 10 mM lysine per 25 µg of muscle protein. Suspensions were briefly vortexed and then centrifuged at 12,000*g* for 10s and incubated on ice in the dark for 10 min. For gel electrophoretic separation, samples where loaded onto IPG strips with an equal volume of 2x sample buffer (7M urea, 2M thiourea, 65mM CHAPS, 2% ampholytes and 2% DTT) during rehydration.

5.2.3. Two-dimensional gel electrophoresis

The fluorescently labelled subproteomes from the mitochondria-enriched fraction of normal (n=4) versus diabetic (n=4) skeletal muscle tissues were separated in the first dimension by isoelectric focusing and in the second dimension by sodium dodecyl sulphate polyacrylamide gel electrophoresis, as previously optimized by our laboratory. IPG strips were rehydrated in rehydration buffer (7M urea, 2M thiourea, 4% (w/v) CHAPS, 1.2% Destreak agent and 2% (v/v) pH 3-10 ampholytes) and 700 mg of protein sample for 12 hours. The first-dimension protein separation was conducted using the IPG strips on an Amersham IPGphor IEF system following the protocol previously described in detail [28]. First dimension strips were subjected to reduction and alkylation prior to second-

dimension separation on 12.5% (w/v) slab gels. Gels were electrophoresed in an Amersham Ettan DALT-Twelve system.

5.2.4 Mass spectrometric identification of muscle proteins

In order to identify individual muscle-associated protein species, peptide mixtures were analysed by mass spectrometry on a Model 6430 Ion Trap LC/MS apparatus from Agilent Technologies (Santa Clara, CA, USA). Excision, washing, destaining and treatment with trypsin were preformed by a previously optimised method. Following tryptic digestion, generated peptides were obtained by removing supernatants from digested gel plugs. Further recovery was achieved by adding 30% acetonitrile/0.2% trifluoricacid to the gel plugs for 10 min at 37 ^{0}C with gentle agitation. Peptide-containing supernatants were pooled and samples dried through vacuum centrifugation. Peptide mixtures were then re-suspended in 10□l mass spectrometry-grade water and 0.1% formic acid for identification by ion trap LC-MS analysis. Separation of peptides was performed with a nano flow Agilent 1200 series system, equipped with a Zorbax 300SB C18 5□m, 4 mm 40nl pre-column and a Zorbax 300SB C18 5□m, 43mm x 75□m analytical reversed-phase column using the HPLC-Chip technology. Mobile phases utilized were A: 0.1% formic acid, B: 50% acetonitrile and 0.1% formic acid. Samples (5□l) were loaded into the enrichment at a capillary flow rate set to 2 □l/min with a mix of A and B at a ratio 19:1. Tryptic peptides were eluted with a linear gradient of 10-90% solvent B over 2 □l/ min with a constant nano pump flow of 0.6 ml/min. A 1 min post time of solvent A was used to remove sample carry over. The capillary

voltage was set to 1700 V. The flow and the temperature of the drying gas were 4□l/ min and 300^{o}C, respectively. Database searches were carried out with Spectrum Mill Work Bench or Mascot MS/MS Ion search (Matrix Science, London, UK).

5.3 Results

In order to determine potential diabetes related changes in the mitochondrial subproteome from skeletal muscle, we have performed here a mass spectrometry-based proteomic analysis of the gastrocnemius muscle from normal versus diabetic Goto-Kakizaki (GK) rats. The non-obese GK animal model of type 2 diabetes is a spontaneously diabetic rat, which shows clear signs of faulty insulin signalling within 4 weeks after birth (Portha *et al*., 1991). As previously discussed in chapter 1,GK rats exhibit increased levels of blood glucose with no major changes in the concentration of non-fasting plasma insulin (Witte *et al*., 2002). The proteomic analysis of the mitochondria-enriched fraction from normal versus diabetic skeletal muscles presented here has revealed a reduced expression of several mitochondrial enzymes, including NADH dehydrogenase, cytochrome b-c1 complex and isocitrate dehydrogenase. The altered abundance of these metabolic proteins might play a central role in the well-established decrease of mitochondrial oxidative phosphorylation in diabetic fibres. The proteomic results herein, shown in this report have demonstrated that the mitochondrial enzymes might aid in the pathological development of insulin

resistance.

5.3.1 Isolation of Mitochondria and Validation of Enrichment

Gastrocnemius muscle from the well characterised control model, Wistar rat (W) and the diabetic Goto-Kakizaki (Gk) rat was used to enrich for mitochondrial muscle skeletal extracts. Two grams of muscle was homogenised from each animal (n=4 W, n=4 Gk) and mitochondria were obtained by differential centrifugation described in chapter 2.

In this study undigested tissue was used to minimise the possibility of variation between samples. Common practice for the recovery of mitochondria from muscle tissues involves the exposure of the tissue to proteases in an attempt to break down the contractile apparatus. These methods often result in unequal digestion of tissues and therefore different amounts of mitochondria recovered as well as damage to the mitochondria.

Purity of the mitochondria obtained was investigated by immunoblotting with markers for contractile apparatus (Myosin Fast), outer mitochondrial membrane (VDAC1), and inner mitochondrial membrane (Mitofilin). The western blot results show a decrease in the abundance of myosin fast, whereas the mitochondrial markers probed for show a significant increase in protein abundance in mitochondria-enriched fractions. These results give sufficient confidence that the enrichment procedure was successful and procedure for further analysis to occur.

5.3.2 DIGE Analysis of Mitochondria – Enriched Muscle Extracts

We have applied here the DIGE method for the comparative analysis of the soluble mitochondrial subproteome from normal versus diabetic skeletal muscle tissue. A period of optimisation of running conditions led to the conclusion that the pH gradient to be used would be one of pH 4-7. The pH 4-7 gradients were run on 24 cm IPG strips, which allowed for a greater degree of separation of proteins over a smaller pH range. Previous studies showed that few changes in protein abundance were observed across the more basic 6-11 pH range due to mitochondria being a notoriously acid organelle. Taking this into consideration resulted in the abandonment of the more basic range and the in depth analysis of the acid 4-7 pH range. Proteins were visualised with the highly sensitive cyanine dyes by difference gel electrophoresis. 25 mg of pooled internal standard and 25 mg of individual samples were run on each gel. A total of 8 gels were run (n=4 W and n=4 Gk). From Figure 5.2 we can see a similar spot pattern between the individual samples and the pooled samples. The pooled samples are labelled with Cy5 dye and the individual samples with Cy3. The Cy dyes could be exchanged but it is important that all pooled samples are labelled with the same dye, and all individual samples are labelled likewise with the same dye.

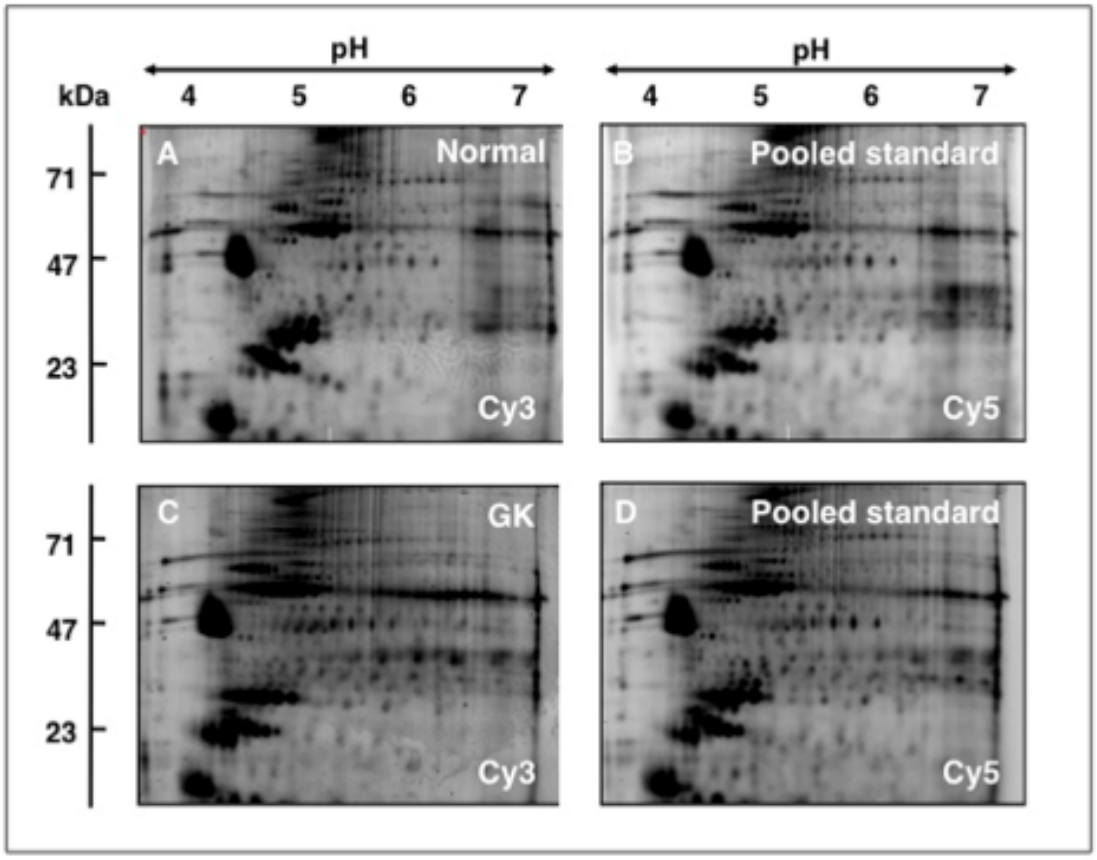

Figure 5.1: Comparative two-dimensional gel electrophoresis analysis of normal versus diabetic rat skeletal muscle. Shown is the 2-D DIGE analysis of the mitochondria-enriched fraction, using a pH 4-7 range in the first dimension. Individual panels represent Cy3-labelled gels of mitochondrial protein fractions from normal (A) and diabetic GK (C) skeletal muscle, as well as Cy5-labelled gels containing polled standards (B, D). The pH-values of the first dimension gel system and molecular mass standards (in kDa) of the second dimension are indicated on the top and on the left of the panels, respectively.

This consistency will prevent any bias in dyes from sample to sample. From each gel two images are obtained, one from Cy3/samples and the other from

Cy5/pooled internal standard, using the Typhoon Trio variable image scanner. Analysis with Progensis samespot software revealed that 1374 spots where recognised across all gels. Following fluorescent labelling with CyDyes and high resolution two-dimensional gel electrophoretic separation of the mitochondria-enriched fraction, densitometric scanning revealed a changed abundance in 24 distinct protein spots. A reduced expression was found for 18 muscle associated protiens and an increased density for 6 proteins in the mitochondria-enriched fraction.

5.3.3 Protein Identification

The DIGE master gel shown, in Figure 5.3 outlines the position of the 24 2D-spots with a changed abundance in diabetic preparations. Mass spectrometry identified the proteins with a decreased abundance as the glycolytic enzyme enolase (spots 1 and 7), the molecular chaperones Hsp60 (spot 3) and Hsp72 (spot 8), muscle glycogen phosphorylase (spot 4), the mitochondrial enzyme NADH dehydrogenase (spots 5 and 12), subunit-1 of the cytrochrome b-c1 complex (spot 6), phosphoglycerate kinase (spot 9), muscle creatine kinase (spot 10), diacylglycerol kinase (spot 11), isocitrate dehydrogenase (spot 13), myosin binding protein H (spot 14), the mitochondrial Tu translational elongation factor (spot 16), the 78kDa glucose-regulated protein (spot 17) and the fast MLC1-f isoform of myosin light chain (spot 18). Interestingly, differential changes of individual 2d spots representing pyruvate dehydrogenase (spots 15 and 22) and ATP synthase (spots 2, 19 and 24) were obsereved. Increased proteins were

identified as triose phosphate isomerase (spot 20), phosphofructokinase (spot 21) and pyruvate kinase (spot 23).

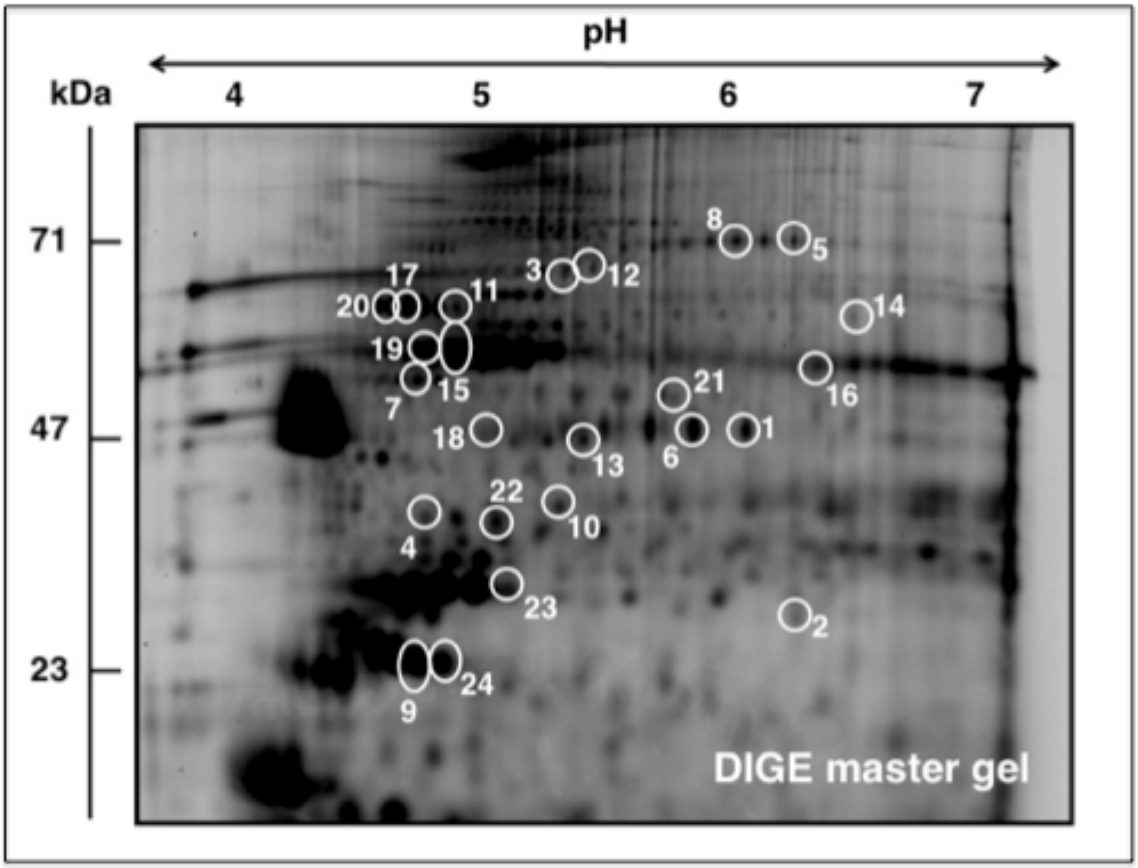

Figure 5.2. **Two-dimensional DIGE reference gel of diabetic rat skeletal muscle**. Shown is a DIGE reference gel of the mitochondria-enriched fraction from rat skeletal muscle, used for the mass spectrometric identification of proteins with a differential expression profile. The pH-values of the first dimension gel system and molecular mass standards (in kDa) of the second dimension are indicated on the top and on the left of the panel, respectively. Identified muscle proteins are marked by circles and are numbered 1 to 24. See Table 1 for a

detailed listing of proteins that exhibited a diabetes-associated change in their abundance.

The 24 spots shown to have a fold change in protein abundance of greater than +/- 1.4 were identified by liquid chromatography mass spectrometry. Table 5.1 correlates spot numbers on the DIGE master gel with the proteomic information on individual protein species as determined by mass spectrometry. The table lists the protein name, accession number, predicted isoelectric point, predicted molecular mass, number of matched peptides, mascot score, percent sequence coverage and fold change.

Table 5.1: **List of identified proteins that exhibit a changed abundance in mitochondria-enriched fraction from diabetic skeletal muscle**

Spot No.	Protein Name	Acession No.	p*I*	M.W	No. of pep	Macot Score	%Coverage	Fold Change
1	enolase 3	gi|126723393	7.08	47332	17	314	44	-4.5
2	subunit d of mitochondrial H-ATP synathase	gi|220904	5.78	18828	3	74	16	-3.3
3	Heat shock protein (Hsp60) precursor	gi|56383	5.11	61101	5	100	12	-3.2
4	glycogen phosphorylase, muscle form	gi|158138498	6.65	97749	10	112	13	-3.1
5	NADH dehydrogenase [ubiquinone] iron-sulfur protein 8, mitochondrial	gi|157821497	5.87	24419	6	56	25	-2.9
6	cytochrome b-c1 complex subunit 1 mitochondrial precursor		5.57	53511	9	241	19	-2.7
7	beta-enolase	gi|126723393	7.08	47332	17	206	44	-2.6
8	dna-k-type molecular chaperone Hsp 72-psf-rat	gi|347019	5.43	71116	12	113	17	-2.6
9	phosphoglycerate kinase 1	gi|40254752	8.02	44916	9	96	29	-2.5
10	creatine kinase M-type	gi|6978661	6.57	43224	7	111	17	-2.4
11	similar to diacylglycerol kinase, delta 130kDa isoform 1 (predicted), isoform CRA_d	gi|149037714	8.09	126993	2	50	1	-2.3
12	NADH- ubiquinone oxidoreductase 75 kDa subunit, mitochondrial precursor	gi|53850628	5.65	80348	2	44	4	-2.2

13	isocitrate dehydrogenase [NAD] subunit alpha, mitochondrial precursor	gi|16758446	6.47	40052	7	198	22	-2.2
14	myosin binding protein H	gi|38303941	6	53044	7	177	23	-2.1
15	pyruvate dehydrogenase E1 component subunit beta, mitochondrial precursor	gi|56090293	6.2	39305	11	294	34	-2.1
16	Tu translation elongation factor, mitochondrial, isoform CRA_d	gi|149067905	7.65	44023	2	74	10	-2
17	78kDa glucose-regulated protein precursor	gi|25742763	5.07	72476	2	60	4	-2
18	myosin light chain MLC1-f	gi|205485	4.99	20795	15	200	67	-2
19	F1-ATPase beta subunit	gi|203033	5.07	38747	4	187	12	2
20	Tpi1 protein	gi|38512111	7.07	27223	10	152	59	2.1
21	phosphofructokinase, muscle	gi|62825891	8.07	86159	5	89	7	2.2
22	pyruvate dehydrogenase E1 component subunit beta, mitochondrial precursor	gi|56090293	6.2	39305	3	37	10	2.6
23	pyruvate kinase isozymes M1/M2	gi|16757994	6.63	58303	13	283	30	2.7
24	ATP synthase , H^+ transporting, mitochondrial F1 complex, beta polypeptide, isoform CRA_b	gi|149029719	6.43	23434	8	94	53	3.1

5.4 Discussion

Abnormal mitochondrial functioning has been implicated to play a central role in the molecular pathogenesis of insulin resistance and contractile weakness in

diabetic skeletal muscle tissues (Dumas *et al*., 2009). The proteomic DIGE analysis of the mitochondria-enriched fraction presented here confirms a disturbed protein expression pattern in the mitochondrial subproteome from GK gastrocnemius muscle. Our previous proteomic survey of crude total extracts from diabetic GK muscle had identified moderate differential expression patterns in 21 protein species. The diabetic phenotype seems to be associated with a generally altered composition of the muscle protein complement, affecting especially glucose, fatty acid, nucleotide and amino acid metabolism, as well as the detoxification mechanisms (Mullen *et al*., 2010). With respect to changes in mitochondria, a reduction in NADH dehydrogenase, cytochrome b-c1 complex, and isocitrate dehydrogenase agrees with previously reported decreased phophorylation in type 2 diabetes (Lowell *et al*., 2005, Zorzano *et al*., 2009).

The lower concentration of the molecular chaperones Hsp60 and Hsp72 indicates an impaired cellular stress response in GK muscle tissue, which might weaken the defense mechanisms of metabolically challenged skeletal muscles. Reduced levels of muscle glycogen phosphorylase could have a negative effect on the proper utilisation of stored glycogen and a lower concentration of creatine kinase may negatively affect the creatine kinase shuttle. Both reductions in key metabolic components probably worsen the bioenergetic status of diabetic fibres and explain the contractile weakness in certain skeletal muscles from patients with type 2 diabetes (Andersen *et al.,* 2004, Park *et al*., 2006). Interestingly, glycolytic marker enzymes were differentially affected in GK muscle. The increased density of triose phosphate isomerase, phosphofructokinase and

pyruvate kinase would suggest a higher glycolytic flux rate in tissues with a reduced mitochondrial content. Phosphofructokinase and pyruvate kinase represent the rate-limiting steps of glycolysis, this alteration might be interpreted as a glycolytic shift that has previously been described in obese skeletal muscle (Hittel *et al*., 2005). On the other hand, the enzymes enolase and phosphoglycerate kinase are reduced in GK tissue, which might be associated with the multi-functionality of many glycolytic elements (Ohlendieck *et al*., 2010).

The enzyme diacylglycerol kinase catalyses the conversion of diacylglycerol to phosphatidic acid and uses ATP as a source of the phosphate. Thus reduced ATP levels in diabetic muscle tissues due to reduced content of functional mitochondria could affect this enzyme. Altered levels of the fast MLC1-f isoform of myosin light chain and myosin binding protein H indicate a certain degree of remodeling of the contractile apparatus. However, since this subproteomic analysis was carried out with a mitochondria-enriched fraction it is difficult to interpret changes in regulatory elements acto-myosin filaments. Compensatory mechanisms to counter-act the loss of mitochondrial functioning appear to be an increase in certain isoforms of pyruvate dehydrogenase and ATP synthase (Dumas *et al*., 2009).

5.4.1 Conclusions

In conclusion, DIGE analysis of mitochondria-enriched muscle extracts from normal versus diabetic show increased abundance of several key mitochondrial proteins. Alterations in the mitochondrial proteome include proteins from different metabolic pathways. The novel candidate proteins with a changed expression

level in the mitochondria-enriched fraction, as shown in this proteomic survey of the GK rat model of non-obese type 2 diabetes, should be helpful for complementing the biomarker signature of diabetes mellitus (Korc *et al*., 2003., Sundsten *et al.,* 2009). Changes in the functioning and/or density of mitochondrial enzymes may be useful for the identification of new therapeutic targets, the development of better diagnostic criteria, the improved monitoring of disease progression and biomedical evaluation of experimental regimes.

Chapter 6

Analysis of Diabetic skeletal muscle proteins using non-ionic detergent phase extraction of gastrocnemius tissue.

6 Analysis of Diabetic skeletal muscle proteins using non-ionic detergent phase extraction of gastrocnemius tissue.

6.1 Introduction

Abnormal glucose handling has emerged as a major clinical problem in millions of diabetic patients world wide (King *et al.,* 1998). Insulin resistance impinges especially on contractile fibres, making abnormal glucose handling in skeletal muscle tissues a key issue for treating side effects of type 2 diabetes (Phielix *et al.*, 2008). High levels of circulating free fatty acids, an increased intramyocellular lipid content, impaired insulin-mediated glucose uptake, diminished mitochondrial functioning and an overall weakened metabolic flexibility are pathobiochemical hallmarks of diabetic skeletal muscles.

As membrane proteins are reliable drug targets and biomarkers their successful enrichment was the aim of this study. Nonionic detergent phase extraction was carried out with Triton X-114. This detergent is ideal for the phase partitioning of soluble and membrane-associated proteins into aqueous and detergent phases, respectively.

6.1.1 Membrane proteins

Biological membranes form an essential barrier between living cells and their external environments. Intracellular organelles are compartmentalized via biological membranes. For example the inner and outer membranes of the

mitochondria, the membranes that envelope the nucleus, lysosomes and secretory vesicles. These membranes and the proteins embedded within have different and highly specialized functions, depending on their organ and tissue specific localizations.

A different set of proteins within each membrane enables it to carry out the distinctive role of the membrane in question. Biological membranes are typically composed of 50% proteins by mass (Guidotti *et al*., 1972). The importance of membrane proteins is reinforced by the fact that they carry out the essential functions of the membrane.

Membrane proteins are critical components of cellular structure and function, and constitute a particular sub-proteome that merits in-depth analysis. These proteins constitute over 30% of all cellular proteins and are predicted to be important pharmacological an therefore (replacement) biomarker targets for drug development (MacCoss *et al*., 2003). Due to their relatively high hydrophobicity and low abundance membrane proteins are infamously difficult to analyse on conventional 2D PAGE proteomic techniques (Gorg *et al*., 2004). 2D PAGE is an excellent method for the separation of soluble and less hydrophobic membrane-associated proteins. It is however, clear that hydrophobic integral membrane proteins, especially those with multiple transmembrane domains, are under-represented on 2D gels. This is due to several factors, including their poor solubility and tendency to aggregate and precipitate in aqueous media that are compatible with the first dimension separation, their generally basic p*I* values and their often relatively low abundance in whole cell and tissue extracts.

6.1.2 Detergent phase extraction

Nonionic detergents are commonly used for the solubilization and characterization of integral membrane proteins. Most of the lipid molecules in contact with the hydrophobic domains of these proteins are replaced with the nonionic detergent which leads to the formation of a soluble protein detergent micelle mix (Tanford *et al.,* 1976, Helenius *et al.,* 1975). Several properties of this mixed micelle such as size and hydrophobicity will depend on the properties of the protein solubilized as well as the properties of the detergent used.

Bordier et al. first described the detergent Triton X-114, in 1980. In this study he compared the ability of the Triton X-100 to enrich for membrane proteins with that for Triton X-114. Triton X-100 forms clear micellar solutions at room temperature. As the cloud point is approached (64^0C) the solution turns turbid and a microscopic phase separation occurs in the solution (Maclay *et al*., 1956). Over a gradient of increasing temperature, with 64^0C being the max, phase separation proceeds until two clear phases, one enriched and one depleted, are formed. Triton X-114 was shown to have a lower cloud point of 30^0C, which is a desirable trait as it promotes protein integrity post phase separation. It has also been reported that it forms micellar solutions n the same manor as its counterpart Triton X-100.

6.1.3 Visualization and Identification.

In this study 2D PAGE fluorescent RuBPs analysis was used to compare the diabetic versus the normal rat gastrocnemius muscle. Following the gel electrophoretic separation of the aqueous and the detergent-extracted fraction

from skeletal muscle homogenates, proteins of interest with a changed abundance were identified by ESI LC/MS technology. Several new potential markers of the diabetic condition were identified which might be useful for the future establishment of a comprehensive biomarker signature for the diabetic state.

6.2 Methods

6.2.1. Nonionic detergent phase extraction of muscle proteins.

Fractionation of crude skeletal muscle tissue preparations into an aqueous phase and a detergent-extracted phase was carried out as previously described for cardiac muscle (Donoghue, et al., 2008). Freshly dissected gastrocnemius muscle tissue (250 mg) from 3 Wistar and 3 GK rats were ground into a fine powder under liquid nitrogen using a pestle and mortar.Groound tissue was immediately added to 8ml of ice-cold phosphate buffered saline (PBS;0.9% (w/v) NaCl, 50mM sodium phosphate, pH 7.4) and 2 ml of 10% (v/v)

Triton X-114 and left overnight at 4^0C on a rotary shaker. The suspended samples were centrifuged at 20,000 g for 30 min at 4^0C to remove tissue debris. The supernatant was incubated for 30 min at 37^0C and then centrifuged for 5000 g at 25^0C to separate the detergent and aqueous phases. The aqueous top layer was removed to a fresh 50 ml tube to which 2 ml of 10% Triton X-114 was added. The lower detergent-extracted phase was resuspended in 8 ml of ice-cold PBS. Both samples were placed for 15 min at 37^0C, followd by a 15 min cebtrifuge spin at 5000 g and 25^0C. This process was repeated 3 times in order to wash each fraction and remove potential cross-contaminants. Differently separated proteins

were extracted from each phase by acetone precipitation at -20^{0}C for 1h. Following a centrifugation step at 5000 g for 30 min, precipitated proteins were resuspended in 1ml buffer and 200 □l of DIGE-compatible lysis buffer. The total protein yield from starting material of 250 mg of skeletal muscle tissue was 5.16± 0.38 mg in the Wistar AQ phase (n=4), 4.78±0.62 mg in the GK AQ phase (n=5), 0.45± 0.10 mg in the Wistar DT phase (n=5), and 0.40 ± 0.09 mg in the GK DT phase (n=5). Protein concentration was determined by Bradford assay.

6.2.2 Gel electrophoretic analysis

For the comparative proteomic analysis of proteins fractionated into AQ phase and DT phase, ruthenium bathophenanthroline disulfonate (RuBPs). A stock solution of RuBPs dye was prepared as described by Rabilloud et al. Following overnight in fix solution (30% ethanol, 10% acetic acid), slab gels were then washed 3 times with 20% ethanol for 30 minutes. The gels were stained for 6 h in 20% (v/v) ethanol containing 200 nM of the ruthenium chelate. The gels were re-equilibrated twice for 10 minutes in distilled water prior to imaging.

6.2.3 Expression analysis

Following nonionic detergent phase extraction of muscle proteins, 2DE separation, protein expression changes between Wistar and GK gastrocnemius samples from the AQ and DT fraction were analysed using Progenesis SameSpots analysis (SSA) software from Non Linear Dynamics (Newcastle upon Tyne, UK). Prior to analysis, individual gels were warped to a single master gel and further matched and normalized with non-gel spots manually filtered out on the basis of spot volume. SSA was used to identify proteins of interest using the

following parameters: n=4; ANOVA $p<0.05$: and a power value of >0.8. Proteins with a significantly changed abundance were picked for tyrptic digestion from coomassie-stained preparative gels.

6.2.4 Protein digestion

Excised protein spots from 2-DE gels were added to 200 mM ammonium bicarbonate solution and incubated at 37^0C for 10 min with gentle agitation. Following a brief spin, a solution of 200 mM ammonium bicarbonate/ acetonitrile 2:3 was added to each gel plug and left at 37^0C for 10 min with gentle agitation. Samples were spun again briefly and resuspended in 50 mM ammonium bicarbonate and left at 37^0C for 10 min with gentle agitation. Gel plugs were shrunk using 100% acetonitrile for 10 min at 37^0C. Proteins were digested over night at 37^0C with gentle agitation using 0.2 ng/μg of sequence grade-modified trypsin (Promega, Madison, WI, USA). Peptides were recovered by removing supernatants from digested gel plugs. Further peptide recovery was achieved by adding 30% acetonitrile/ 0.2% trifluoric acid to the gel plugs for 10 min at 37^0C with gentle agitation. Following a brief spin, supernatants were added to the initial peptide recovery following digestion. Exhaustive peptide recovery was achieved through the addition of 60% acetonitrile/0.2% tirfuoric acid to each plug for 10 min at 37^0C with gentle agitation. Supernatants were added to the peptide pool. Sample volume was reduced until dry through vacuum centrifugation. Samples were resuspended in 30μl od ultra-pure ddH_2O and 0.1% formic acid for identification by mass spectrometry.

6.2.5 ESI LC-MS/MS analysis

Nanoflow LC separation of tryptic peptides was preformed with a nanoflow 1200 series system from Agilent Technologies (Santa Clara, CA, USA), equipped with a Zorbax 300SB C18 5μm , 4mm 4o nl pre-column and a Zorbax 300SB C18 5μm, 43mm x 75μm analytical reversed phase column using HPLC-Chip technology. Samples were initially transferred with an aqueous 0.1% formic acid solution to a pre-column with a flow rate of 4ml/min for 3 min. Mobile phase A was 0.1% formic acid and mobile phase B 0.1% formic acid in acetonitrile. Peptides were separated with a gradient of 3-40% mobile phase B over 9 min at a flow rate of 400 μl/min followed by a 3 min wash with 90% of mobile phase B. Analysis of tryptic peptides was performed using and Agilent 6300 series ion trap LC mass spectrometer. All analyses were performed using positive nano-electrospray ion mode. The MS survey scan was set between 100 and 2200 m/z with a duration of 0.5s/scan and the 3 most intense peptides further selected for MS analysis. Collision energy was ramped between 1500 and 4500 V based on the observed precursor mass over charge value and charge state. Spectra were processed and anlaysed by Spectrum Mill database search software (Agilent Technologies, Santa Barbara, CA).

6.3. Results

6.2.1 Nonionic detergent phase extraction for the proteomic analysis of diabetic skeletal muscle.

The sub-proteomic investigation described here is based on the principle of nonionic detergent phase extraction (Bordier *et al*., 1980). A comparison of the

aqueous versus the detergent-extracted fraction from the GK rat versus Wistar rat gastrocnemius muscle tissue was carried out. Figure 6.1 outlines the experimental protocol used for the separation of skeletal muscle proteins by treatment with Triton X-114. Since phase separation with Triton X-114 occurs at temperatures above 22^0C, skeletal muscle protein fractionation was carried out at 37^0C (Donoghue *et al*, 2008). The separation step resulted in an aqueous AQ phase enriched in hydrophilic proteins and a detergent DT phase with predominantly hydrophobic proteins. Despite repeated washing steps, phase transition approaches always result in a certain degree of cross-contamination between soluble and membrane-associated proteins. Extracted proteins were separated by standard 2DE and proteins of interest identified by LC/MS technology.

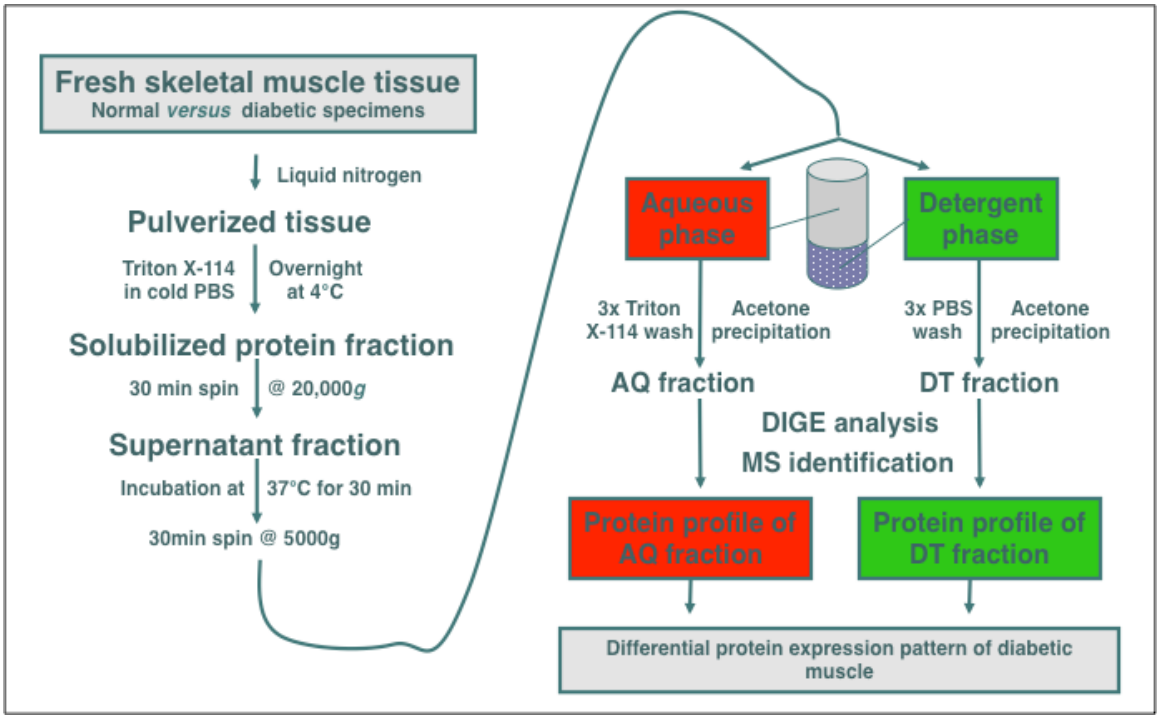

Figure 6.1: Nonionic detergent phase extraction of normal versus diabetic muscle tissue. The subcellular fractionation approach used in this subproteomic investigation is based on the principle of nonionic detergent phase extraction. The flow chart in panel (A) outlines the experimental protocol employed for the separation of skeletal muscle proteins by treatment with Triton X-114. The temperature-dependent separation step resulted in an aqueous (AQ) phase-enriched in hydrophilic proteins and a detergent (DT) phase with predominantly hydrophobic proteins.

6.2.2 Gel electrophoretic analysis of nonionic detergent phase extraction of muscle proteins

Figure 6.2 illustrates the successful enrichment of typical membrane-associated skeletal muscle proteins in the detergent-extraction fraction and a soluble enzyme in the aqueous phase-extracted fraction. The 1-DE analysis of crude preparations versus the aqueous phase and detergent-extracted phase demonstrated the differing protein band pattern between the two main fractions following phase separation. Importantly, immunoblotting revealed a clear enrichment of the fast-twitch sarcoplasmic reticulum Ca2+-ATPase isoform SERCA 1 and the inner mitochondrial membrane-associated enzyme ATP synthase in the detergent-extracted fraction from both diabetic and normal gastrocnemius muscle tissue. In stark contrast, the soluble isoform of cytosolic malate dehydrogenase was found to be enriched in the aqueous phase from both diabetic and normal tissues. Following the initial evaluation of the nonionic detergent phase extraction method by 1DE, the aqueous and detergent fractions

were electrophoretically separated on large high-resolution 2D gels covering the 3-10 pH range. Since silver staining exhibits a relatively limited dynamic range, the more discriminatory RuBPs method was employed for detailed determination of changes in protein abundance.

6.2.3 RuBPs analysis of the diabetic muscle proteome

Fluorescent staining is one of the most powerful techniques for conducting comparative expression studies of complex proteomes, making it an ideal route for sophisticated analysis of the detergent-enriched fraction from the gastrocnemius from diabetic and normal animal models. The staining protocol reported by Rabilloud (*et al*., 2001) was followed, and following scanning with an Amersham Typhoon Trio variable imager and with the help of Progenesis 2-D analysis software, 32 protein species out of 873 spots from the detergent enriched sample and 1328 on the aqueous enriched sample, detectable 2D spots were found to be differentially expressed. Master gels representing electrophoretically separated proteins from diabetic versus normal muscle fibres are shown in Figures 6.3 and 6.4. Proteins of interest were identified by ESI mass spectrometry.

6.2.4 Proteomic profile of diabetic skeletal muscle

A list of identified protein species with an altered abundance in the detergent-extracted and aqueous fraction from diabetic versus normal rat gastrocnemius muscle is shown in Tables 6.1 (AQ) and 6.2 (DT). The tables summarizes the

results with respect to protein name, the protein accession number, mascot score, the number of matched peptide sequences, the percentage sequence coverage, the molecular mass, the p*I* value and the fold change of individual proteins affected during the weakening of muscle due to the diabetic state. Overall a decreased expression level was shown for 8 protein spots in the aqueous fraction and 7 protein spots in the detergent-enriched fraction. An increased concentration was found for 10 distinct protein species in the aqueous fraction and for 9 protein spots in the detergent-enriched fraction.

In the DT fraction, protein species with an increased expression level were identified as ATP synthase alpha precursor, adenylate kinase isozyme 1, tropomyosin alpha-4 chain, glutathione-dependent dehydroascorbate reductase, 3-mercaptopyruvate sulfertransferase, apolipoprotein A1, glyoxalase, cofilin 2 and adenylate kinase. Differential effects on dissimilar 2D spots representing the same protein or protein complex were observed for pyruvate kinase, alpha-b crystallin, phosphoglucomutase-1, glyceraldehyse 3-phosphate dehydrogenase and rhoGDP-dissociation inhibitor 1.

In the AQ fraction, proteins with an increased concentration were identified as heat shock protein 1, secernin 3, isoform CRA_a, Hsp 60 mitochondrial precursor, Parkinson disease protein 7, Coq 9, Peroxiredoxin 2, Hsp 5, NADH dehydrogenase (ubiquinone) Fe-S protein 1, Pyruvate dehydrogenase (lipoamide) beta and transferrin. Differential effects on dissimilar 2D spots representing the same protein or protein complex were observed for adenylate kinase isozyme 1, fructose-bisphosphate aldose A, NADH dehydrogenase,

ubiquinol-cytochrome c reductase core protein and dihydrolipoamide S-acetyltransferase. The majority of identified proteins were found to be involved in mitochondrial metabolism, glycolysis, metabolic transportation and the cellular stress response.

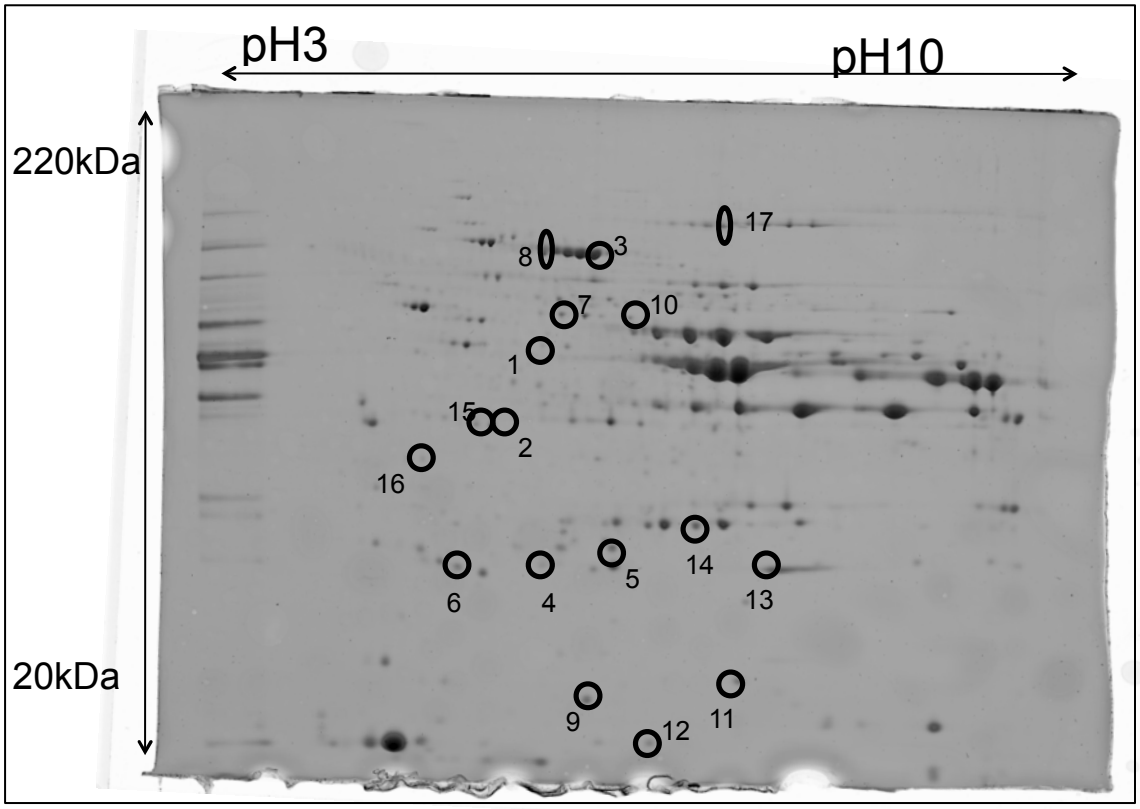

Figure 6.3: RuPB's analysis of the aqueous fraction from normal versus diabetic rat skeletal muscle. Proteins with different expression levels are numbered 1-17 and are marked by circles. See Table 6.1 for a detailed listing of aqueous phase-extracted proteins with a changed abundance in diabetic fibres. The pH values of

the IEF system and molecular mass standards (in kDa) of the 2D gels are indicated on the top and on the left of the panels, respectively.

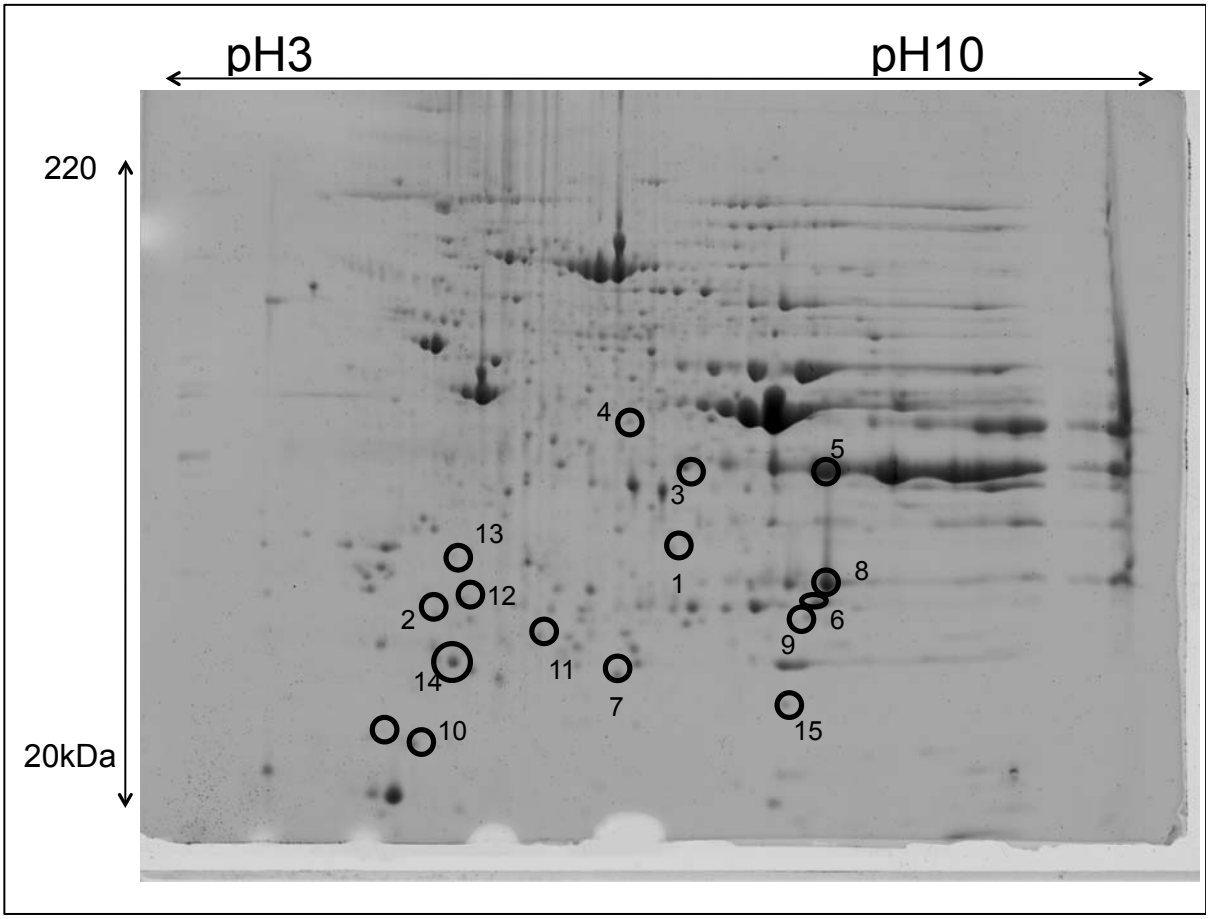

Figure 6.4: RuPB's analysis of the detergent-extracted fraction from normal versus diabetic rat skeletal muscle. Proteins with different expression levels are numbered 1-17 and are marked by circles. See Table 6.2 for a detailed listing of detergent phase-extracted proteins with a changed abundance in diabetic fibres. The pH values of the IEF system and molecular mass standards (in kDa) of the 2D gels are indicated on the top and on the left of the panels, respectively.

Table 6.1: **RuBPs identified proteins with a changed abundance in the aqueous-extracted fraction from normal versus rat gastrocnemius muscle**

Spot No.	Protein Name	Acession No.	pI	M.W	No. of pep	Macot Score	%Coverage	Fold Change
1	heat shock protein 1	gi|183396771	5.91	61091	22	388	39	3.5
2	secernin 3, isoform CRA_a	gi|149022245	5.72	48087	4	82	10	3.3
3	hsp 60 mitochondrial precursor	gi|109506917	6.36	94075	17	277	22	3
4	Parkinson disease protein 7	gi|16924002	6.32	20193	11	166	46	2.8
5	Coq 9 protein	gi|51259441	5.5	35095	6	145	20	2.6
6	peroxiredoxin 2	gi|8394432	5.34	21944	3	83	17	2.2
7	heat shock protein 5	gi|25742763	5.07	72476	17	180	29	2.2
8	NADH dehydrogenase (ubiquinone) Fe-S protein 1, 75 kDa	gi|53850628	5.65	80348	23	432	32	2.4
9	pyruvate dehydrogenase (lipoamide) beta	gi|56090293	6.2	39305	20	338	38	2.1
10	transferrin	gi|61556986	7.14	78550	18	216	24	1.5
11	adenylate kinase isozyme1	gi|8918488	7.71	21446	9	120	39	-1.5
12	NADH dehydrogenase	gi|53850628		80348	25	392	32	-1.6
12	adenylate kinase isozyme1	gi|8918488	7.71	21646	9	128	35	-1.8
13	fructose-bisphosphate aldose A	gi|6978487	8.31	39791	29	499	57	-1.8
14	pyruvate dehydrogenase (lipoamide) beta	gi|56090293	6.2	39305	9	193	30	-2.1
15	similar to alpha-enolase (2-phospho-D-glycerate hydrolase)	gi|109468300	5.81	54354	17	318	41	-2.2
16	ubiquinol-cytochrome c reductase core protein 1	gi|51948476	5.57	53511	23	313	33	-2.2

17	dihydrolipoamide S-acetyltransferase	gi|78365255	6.76	67645	15	236	28	-2.4

Table 6.2 **RuBPs identified proteins with a changed abundance in the detergent-extracted fraction from normal versus diabetic rat gastrocnemius muscle**

Spot Number	Protein Name	Acession No.	Mascot Score	pI	M.W	No. of pep	%Coverage	Fold Change
1	pyruvte kinase	gi|16757994	103	6.63	58303	2	10	-6.2
2	alpha-B crystallin	gi|6981420	71	4.71	26639	2	8	-5.4
3	phosphoglucomutase-1	gi|77627971	148	6.14	61642	8	13	-4
4	pyruvte kinase	gi|16757994	237	6.63	58303	16	32	-3.8
5	NADH dehydrogenase (ubiquinone) Fe-S protein 2 precursor	gi|58865384	116	6.52	52934	2	4	-3
6	glyceraldehyde 3-phosphate-dehydrogenase	gi|56188	208	8.43	36103	12	38	-2.5
7	rhoGDP-dissociation inhibitor 1	gi|31982030	208	5.12	23451	4	23	-2.1
8	ATP synthase alpha precursor	gi|203055	236	9.22	58906	12	27	1.5
9	adenylate kinase isozyme 1	gi|8918488	218	7.71	21646	13	60	1.8
10	tropomyosin alpha-4 chain	gi|6981672	63	4.66	28550	7	20	1.9

11	glutathione-dependent dehydroascorbate reductase	gi|12585231	55	6.25	27941	2	10	2.4
12	3-mercaptopyruvate sulfurtransferase	gi|20304123	95	5.88	33209	4	20	2.6
13	apolipoprotein A1	gi|6978515	98	5.52	30101	10	38	3.1
14	glyoxalase	gi|46485429	79	5.52	20980	3	14	3.4
15	cofilin 2	gi|6671746	98	7.66	18814	6	41	4
16	adenylate kinase	gi|8918488	95	7.71	21646	4	20	6.4

6.3 Discussion

It is estimated that 30% of the human genome encodes for membrane-associated proteins (Stevens *et al*., 2000). Proteins embedded in membranes represent crucial therapeutic targets (Hopkins *et al*., 2002) and as a result are of great importance. Subpreoteomics is the study of distinct subsets of proteins with usually results in a reduction in sample complexity (Cordwell, *et al.,* 2000). This can be beneficial for the identification of low abundance signature molecules. Crude protein extracts is often unable to reveal the complete proteome complexity of the proteome in question and recently advances have been made in the proteomic profiling of large cellular structures, organelles and membrane domains from diverse systems (Tan *et al.,* 2008, Sadowski 2008).

Here we have successfully applied a nonionic detergent phase extraction method for the analysis of the aqueous versus the membrane-associated fraction from

skeletal muscle homogenates. Immunoblotting verified the enrichment of integral membrane proteins in the detergent-extracted fraction. A variety of muscle proteins in both phases showed varying degrees of alterations which lead to difficult interpretation of their role. The increase in Hsp1 and Hsp5 could be useful for future biomarker establishment. Identified muscle proteins with a change in abundance were shown to be involved in the stress response, glycolysis and metabolic transportation. These finding show that the condition experienced by the Goto-Kakizaki rat is of a weak pathology and of a generally mild protein expression disturbance. The proteomic findings presented here suggest that a generally mildly perturbed protein expression pattern which affects mainly metabolic pathways is of key importance to the pathology of diabetic skeletal muscle tissue.

Chapter 7

General Disscussion

7 General Discussion

Type 2 diabetes is a metabolic state in which glucose is not retrieved from the blood efficiently. Insulin resistance is common in patients who experience high blood glucose levels. Often, the cells in the pancreas attempt to meet the increasing glucose levels of prediabetics. However these demands eventually exhaust the expanded cells and results in cell apoptosis and high blood glucose levels. Without Insulin production, blood glucose levels remain high and complications such as glucotoxicity ensue.

Normally insulin binds to insulin receptors on the surface of the target organ cells resulting in a series of cellular events that promote intracellular glucose transport and therefore metabolism. After a period of compensated insulin resistance impaired glucose tolerance develops despite an increase in in insulin concentration as insulin resistance increases. It is poorly understood how abnormal tissue sensitivity to insulin causes decreased skeletal muscle strength, particularly in older patients with type 2 diabetes. Fatty acid metabolism has a profound influence on diabetic side effects. Type 2 diabetes is associated with high levels of circulating free fatty acids, increased intramyocellular lipid content, diminished mitochondrial functioning and a weakened metabolic flexibility in skeletal muscle. This thesis has attempted to further understand the mechanisms of the diabetic state and to identify potential biomarkers of the condition, in context with the current understanding of the disease. This has been done by the use of rodent models to study human muscle degeneration, which is common

practice, as the Goto-Kakizaki rat model has been well established as a viable model of the type 2 diabetic diseases.

Proteins are the biological effector molecules of the cell. Proteomics is the large-scale and high throughput biochemical approach to study entire protein complements (de Hoog*, et al*., 2004). The principle technique used for protein separation and identification is 2D PAGE coupled with mass spectrometry. There are numerous constraints to the 2D technology. For example the main limitation encountered during this project was the under-representation of hydrophobic proteins on 2D gels. Also restrictions due to the pH ranges and masking of proteins have been an issue throughout this study.

Skeletal muscle is responsible for approximately 80% of all insulin mediated glucose disposal. As a result of this fact skeletal muscle was used throughout this project as the tissue of choice in a bid to better understand the mechanisms behind the disease and disease progression.

2D gel electrophoresis is a powerful tool of separation that aids in the development of a greater understanding of protein expression. When teamed with mass spectrometric techniques the two can result in the total analysis of whole proteomes. It is important to mention that significant periods of optimization (ranging from 1-3 months) are required to perfect techniques with large amounts of variables. Running conditions of both first and second dimensions, optimum LCMS gradients and sample digestions, sample preparations and sub-cellular enrichments, all require considerable stages of development. Many elements such as hydrophobicity of a sample (LCMS), salt

content (IEF), and lipid content (sample preparation), play noteworthy roles in the evolution of such methods.

7.1 Conclusion

Type 2 diabetes is a complex and difficult to understand metabolic state with a large number of underlying factors. Of these, several were identified by proteomics to be important in the pathology of skeletal muscle. The most significant changes where to muscle-associated proteins involved in glycolysis, the citric acid cycle, oxidative phosphorylation, lipolytic catabolism, oxygen transportation, the contractile apparatus and the stress response. The work reported in this thesis resulted in the identification of several potential biomarkers of diabetes associated muscle weakness, which with further study could provide means of tracking progression and therefore possible markers for early diagnosis, as well as therapeutic targets for type 2 diabetes. The sub-proteomic analysis herein, suggests a mainly metabolic alteration in diabetic skeletal muscle tissue. This is evident from the data in chapter 5 which shows an altered abundance of such proteins as triose phosphate isomerase, phosphofructokinase and pyruvate kinase, all of which presented at a higher abundance than in the control animal model. The increased abundance insinuates a higher glycolytic flux rate in tissues with reduced mitochondrial content, which is indicative of a compensatory mechanism for the drop in the number of the organelle in question. Proteins involved in metabolism were found to have an altered expression in both whole cell lysate analysis of skeletal muscle as well as sub-proteomic analysis. This is suggestive to a mild but significant change in muscle metabolism through

glycolysis. In chapter 3, the protein with the greatest fold change was identified as monoglyceride lipase. This enzyme converts monoacylglycerides to free fatty acids and glycerol. It does so by mediating a critical step in the hydrolysis of stored triglycerides (Zechner *et al*., 2009) and its up-regulation might represent increased energy utilization by the lipolytic pathway in glucose-starved muscle tissues. More detailed biochemical studies have to be carried out to determine the general suitability of monoglyceride lipase as a muscle marker of non-obese diabetes. However, it is clear that insulin resistance results in a lack of glucose uptake by muscle cells, which in turn has an effect on other metabolic pathways such as gluconeogenesis, triacylglycerol hydrolysis, fatty acid oxidation and ketone body formation.

The data presented in chapter 4 showed a significant increase in αβ-crystallin and Hsp27. Hsps of low molecular mass have specific cytoprotective functions which include the prevention of deleterious protein aggregation and the modulation of intermediate filament assembly. These findings are particularly informative as Hsp 27 associates with alpha- and beta-tubulin, and so is therefore involved in the assembly of the contractile apparatus. These small chaperone proteins were shown to be up-regulated in diabetic muscle tissue. The results presented here confirm the drastic effects of type 2 diabetes on voluntary contractile fibres.

7.2 Future Prospects

The most important long-term goal of proteomic research is not simply to catalogue protein components and define their molecular interaction but to understand how changes in protein expression and function alter and contribute to biological homeostasis, disease states and cellular pathways. The proteome is a complex and highly dynamic body, which experiences changes in expression due to both environmental and internal cues, such as growth, development, and cell division. For example the human genome constitutes of approximately 25,000 genes, but it is believed that over one million functionally distinct protein components are encoded for by these genes. This is thought to be due to post-translational modifications and alternative splicing (Zuo and Speicher 2002).

There are many potential directions type 2 diabetic studies could take. A 2D PAGE study of cardiac tissue from both the normal Wistar rat and the GK diabetic rat would provide a in depth look at the cardiac conditions experienced by type 2 diabetes sufferers.

Another avenue to explore would be to compare the non-obese GK animal model with that of the obese Zucker rat, which experiences obesity which influences the progression of the metabolic condition.

Bibliography

Bibliography

Abdel-Halim, S., Guenifi, A., Luthman, H., Grill, V., Efendic, S., Ostenson, CG. (1994). "Impact of diabetic inheritance on glucose tolerance and insulin secretion in spontaneously diabetic GK-Wistar rats." Diabetes(43): 281-288.

Abdul-Ghani, M., DeFronzo, RA. (2010). "Pathogenesis of insulin resistance in skeletal muscle." Journal of Biomedicine and Biotechnology 2010(47): 62-79.

Alban, A., S. O. David., L. Bjorkenten., C. Andersson., E. Sloge., S. Lewis., I. Currie. (2003). "A novel experimental design for comparative two-dimensional gel analysis: Two-dimensional gel electrophoresis incorporating a pooled internal standard." Proteomics 3(1): 36-44.

Andersen H, N. S., Mogensen C.E, Jakobsen J (2004). "Muscle strength in type 2 diabetes." Diabetes 53: 1543-1548.

Anderson, L., and Seilhamer (1997). "A comparison of selected mRNA and protein abundances in human liver. ." Electrophoresis 18(3-4): 533-537.

Antonsson, B., S. Montessuit, S. Lauper, R. Eskes, and J. C. Martinou. (2000). "Bax olgiomerization is required for channel-forming activity in liposomes and to

trigger cytochrome c release from mitochondria." Journal of Biochemistry 345(Pt 2): 271-8.

Asakura, S. (1961). "F-actin adenosine triphosphate activated under sonic vibration." Biochem Biophys Acta(52): 65-75.

Backer, J., Kahn, CR., White, MF. (1990). "Tyrosine phosphorylation of the insuilin receptor during insulin-stimulated internalization in rat hepatoma cells." Journal of Biological Chemistry 264(3): 1694-1701.

Berndt, P., Hobohm, U., Langen, H. (1999). “Reliable automatic protein identification from matrix-assisted laser desorption/ionization mass spectrometric peptide fingerprints.” Electrophoresis 20(18) 3521-3526.

Boden, G. (2003). "Effects of free fatty acids (FFA) on glucose metabolism: significance for insulin resistance and type 2 diabetes." Exp Clin Endocrinol Diabetes 111(3): 121-124.

Bordier., C. (1981). "Phase separation of integral membrane proteins in Triton X-114 solution." Journal of Biological Chemistry 256(4): 1604-1607.

Bradford, M. (1976). "A rapid and sensitive method for the quantitation of microgram quantities of prtein utilizing the principle of protein-dye binding." Analytical Biochemistry(72): 248-254.

Butler, A. (2004). "Diabetes due to a progressive defect in beta-cell mass in rats transgenic for human islet amyloid polypeptide (HIP rat): a new model for type 2 diabetes." Diabetes 53: 1509-1516.

Canas, B., Lopez-Ferrer, D., Ramos-Fernandez, A., Camafeita, E., Calvo, E. (2006). "Mass spectrometry technologies for proteomics." Briefings in Functional Genomics and Proteomics 4(4): 295-320.

Chan, D. (2006). "Mitochondria: Dynamic organelles in disease, aging and development." Cell 125: 1241-1252.

Cordwell, S., Nouwens, AS., Verrills, NM., Basseal, DJ., Walsh, BJ. (2000). "Subproteomics based upon protein cellular location and relative solubilities in conjunction with composite two-dimensional electrophoresis gels." Electrophoresis 21(6): 1094-103.

Cowie, C., Rust, KF., Ford, ES., Eberhardt, MS., Byrd-Holt, DD., Li, C. Williams, DE., Gregg, EW., Bainbridge, KE., Saydah, SH., Geiss, LS. (2009). "Full

accounting of diabetes and pre-diabetes in the U.S. poulation in 1988-1994 and 2005-2006." diabetes Care 32(2).

Dadke, S. L., HC., Kusari, AB., Begum, N., Kusari, J. (2000). "Elevated expression and activity of protein-tyrosine phosphatase 1B in skeletal muscle of insulin-resistant type 2 diabetic Goto-Kakizaki rats. ." Biochem Biophys Res Commun(274): 583-589.

de Hoog, C., Mann, M. (2004). "Proteomics." Annual Review of Genomics and Human Genetics 5: 267-293.

Distler, A., Kerner, J., Hoppel, CL. (2008). "Proteomics of mitochondrial inner and outer membranes." Proteomics 8(19): 4066-4082.

Dokken, B., Henriksen, EJ. (2006). "Chronic selective glucogen synthase kinase-3 inhibition enhances glucosedisposal and muscle insulin action in prediabetic obese Zucker rats. ." American journal of Physiology and Endocrinology Metabolism 291: 207-213.

Domon, B., Aebersold, R. (2006). "Mass spectrometry and protein analysis." Science 312(5771): 212-217.

Donoghue, P., Doran, P., Wynne, K., Pedersen, K., Dunn, MJ., Ohlendieck, K. (2007). "Proteomic profiling of chronic low-frequency stimulated fast muscle. ." Proteomics(7): 3417-3430.

Donoghue, P., Hughes, C., Vissers, JPC., Langridge,JI, Dun, MJ. (2008). "Non-ionic detergent phase extraction for the proteomic analysis of heart membrane proteins using label-free LC-MS." Proteomic 8: 3895-3905.

Doran, P., Martin, G., Dowling, P., Jockusch, H., Ohlendieck, K. (2006). "Proteome anlaysis of the dystrophin-deficient MDX diaphragm reveals a drastic increase in the heat shxok protein cvHSP." Proteomics(6): 4610-4621.

Doran, P., Gannon, J., O'Connell, K., Ohlendieck, K. (2007). "Aging skeletal muscle shows a dastic increase in the small heat shock proteins ab-crystallin/HspB5 and cvHsp/HspB7." European Journal of Cellular Biology(86): 629-640.

Doran, P., Gannon, J., O'Connell, K., Ohlendieck, K. (2007). "Proteomic profiling of animal models mimicking skeletal muscle disorders." Proteomics Clinical Applications(1): 1169-1184.

Doran, P., Donoghue, P., O'Connell, K., Gannon, J., Ohlendieck, K. (2007). "Proteomic profiling of pathological and aged skeletal muscle fibres in peptide mass fingerprinting (Review).
." International Journal of Molecular Medicine(19): 547-564.

Doran, P., O'Connell, K., Gannon, J., Kavanagh, M., Ohlendieck, K. (2008). "Opposite pathobiochemical fate of pyruvate kinase and adenylate kinase in aged rat skeletal muscle as revealed by proteomic DIGE analysis." Proteomics(8): 364-377.

Doran, P., Donoghue, P., O'Connell, K., Gannon, J., Ohlendieck, K. (2009). "Proteomics of skeletal muscle aging." Proteomics(9): 989-1003.

Dumas, J., Simard, G., Flamment, M., Ducluzeau, PH., Ritz, P. (2009). "Is skeletal muscle mitochondrial dysfunction a cause or an indirect consequence of insulin resistance in humans." Diabetes Metabolism(35): 159-167.

Elstner, M., Andreoli, C., Klopstock, T., Meitinger, T., Prokisch, H. (2009). "The Mitochondrial Proteome Database: MitoP2."

Engle, A., Franzini-Armstrong, C. (2005). “Mycology”.

Farley, J., Miles, PR. (1977). "Role of depolarization in acetylcholine-induced contractions of dog trachealis muscle." J Pharmacol Exp Ther 201: 199-205.

Foster, L., de hoog, Cl., Zhang, Y., Xle, X., Mootha, VK., Mann, M. (2006). "A mammalian organelle map by protein correlation profiling." Cell 125(1): 187-199.

Frattali, A., Treadway, JL., Pessin, JE. (1990). "Evidence supporting a passive role or the insulin receptor transmembrane domain in insulin-dependent signal transduction." Journal of Biological Chemistry 266: 9829-9834.

Frisbee, J. (2003). "Impaired skeletal muscleperfusion in obese Zucker rats." American Journal of Regulatory, Integrative and Comparitive Physiology. 285: 1124-1134.

Frisbee, J., Samora, JB., Peterson, J., Bryner, R. (2006). "Exercise training blunts microvascular rarefaction in the metabolic syndrome." American Journal of Heart and Circulatory Physiology 291: 2483-2492.

Furnsinn, C., Noe, C., Herdilicka, R., Roden, M., Nowotry, P., Leighton, B. (!997). "More marked stimulation by lithium than insulin of the glucogenic pathway in rat skeletal muscle." American Journal of Endocrinology and Metabolism 273: 514-520.

Gannon, J., Staunton, L., O'Connell, K., Ohlendieck, K. (2008). "Phosphoproteomic analysis of aged skeletal muscle." International Journal of Molecular Medicine(22): 33-42.

Gannon, J., Doran, P., Kirwan, A., Ohlendieck, K. (2009). "Drastic increase of myosin light chain MLC-2 in senescent skeletal muscle indicates fast-to-slow fibre transition in sarcopenia of old age.
." European Journal of Cellular Biology(88): 685-700.

Gauthier, D., Lazure, C. (2008). "Complementary methods to assist subcelular fractionation in organellar proteomics." Proteomics 5: 603-617.

Geers, C., Gros, G. (2000). "Carbon dioxide transport and carbonic anhydrase in blood and muscle." Physiology Review(80): 681-715.

Gelfi, C., Vigano, A., De Palma, S., Ripamonti, M., Begum, S., Cerretelli, P., Wait, R. (2006). "2-D protein maps of rat gastrocnemius and soleus muscles:a tool for muscle plasticity assesment. ." Proteomics(6): 321-340.

Golenhofen, N., Perng, MD., Quinlan, RA., Drenckhahn, D. (2004). "Comparison of the small heat shock proteins alphab-crystallin, MKBP, HSP25, HSP20, and cvHSP in heart and skeletal muscle
" Histochemistry and Cel Biology 122(5): 415-425.

Gordon, A., Homsher, E., Regnier, M. (2000). "Regulation of contraction in striated muscle." Physiol 80(2): 853-924.

Gorg, A., Weiss, W., Dunn, MJ. (2004). "Current two-dimensional electrophoresis technology for proteomics." Proteomics 4(12): 3665-3685.

Gregg, E., Beckles, GL., Williamson, DF., Leveille, SG., Langlois, JA., Engelgau, MM., Narayan, KM. (2000). "Diabetes and physical disability amoung US adults." Diabetes Care(23): 61-67.

Guidotti, G. (1972). "Membrane Proteins." Annual Review of Biochemistry 41: 731-752.

Gygi, S. P., Rochon, Y., Franza, B.R., Aebersold, R. (1999). "Correlation between protein and mRNA abundance in yeast." Plant Physiol 19: 1720-1730.

Hanash, S. (2003). "Disease Proteomics." Nature 422(6928): 226-232.

Heegaard, C., le Marie, M., Gulik-Krzywicki, T., Moller, JV. (1990). "Monomeric state and Ca2+ transport by sarcoplasmic reticulum Ca2(+)-ATPase, reconstituted with an excess of phospholipid." Journal of Biological Chemistry 265(20): 12020-12028.

Helenius, A., Simons, K. (1972). "The Binding of Detergents to Lipophilic and Hydrophilic Proteins." Journal of Biological Chemistry 27(11): 3656-3661.

Heukeshoven, J., Dernick, R. (1985). "Simplfied method for silver staining of proteins in polyacrylamide gels and the mechanism of silver staining " Electrophoresis(6): 103-112.

Hirano M, D. M., DiMauro S. (2001). "Mitochondria and the heart." Current opinion in Cardiology 16(3): 10.

Hittel, D., Hathout, Y., Hoffman, EP., Houmard, JA. (2005). "Proteome analysis of skeletal muscle from obese and morbidity obese women." Diabetes(54): 1283-1288.

Hodgkin, A., Horowicz, P. (1960). "Potassium contractures in single muscle fibres." Journal of Physiology(153): 386-403.

Hogan, P., Dall, T., Nikolov, P; (2003). "Economic cost of diabetes in the U.S. in 2002." Diabetes Care 26: 917-932.

Hojlund, K., Wrzesinki, K., Larsen, PM., Fey, SJ., Roepstorff, P., Handberg, A., Dela, F., Vinten, J., McCormack, JC., Reynet, C., Beck-Nielsen, H. (2003).

"Proteome analysis reveals phosphorylation and ATP synthase beta-subunit in human skeletal muscle and proteins with potential roles in type 2 diabetes." Journal of Biological Chemistry(278): 10436-10442.

Hopkins, A., Groom, CR. (2002). "The drugable genome." Nature Review Drug Discovery 1: 727-730.

Hotamisligil, G., Shargill, NS., Spiegelman, BM. (1993). "Adipose expression of tumor necrosis factor-alpha: direct role in obesity-linked insulin resistance." Science 295: 87-91.

Huxley, A., Niedergerke, R. (1954). "Interference microscopy of living muscle fibres." Nature Protocols 4412: 971-973.

Huxley, H. (2004). "Fifty years of muscle and the sliding filament hypothesis." European Journal of Biochemistry 271(8): 1403-1415.

Hwang, H., Bowen, BP., Lefort, N., Flynn, CR., De Filippis, EA., Roberts, C., Smoke, CC., Meyer, C., Hojlund, K., Yi, Z., Mandarino, LJ. (2009). "Proteomics analysis of human skeletal muscle reveals novel abnormalities in obesity and type 2 diabetes mellitus." Diabetes 59(1): 33-42

Issaq, H., Veenstra, T., (2008). "Two-dimensional polyacrylamide gel electrophoresis (2D-PAGE): advances and perspectives." Biotechniques 44(5): 697-700.

Jensen, M., Haymond, MW., Rizza, RA., Cryer, PE., Miles, JM. (1989). "Influence of body fat distribution on free fatty acid metabolism in obesity." Journal of Clinical Investigation 83: 1168-1173.

Jetton, T. (2005). "Mechanisms of compensatory beta-cell growth in insulin-resistant rats: roles of Akt kinase." Diabetes 54: 2294-2304.

Jhala, U. (2003). "cAMP promotes pancreatic beta-cell survival via CREB-mediated induction of IRS2." Genes Dev 17: 1575-1580.

Johannsen, D., Ravussin, E. (2009). "The role of mitochondrial in health and disease. ." Current Opinion in Pharmacology 9: 780-786.

Karp, N. A., and K. S. Lilley. (2005). "Maximising sensitivity for detecting changes in protein expression: experimental design using minimal CyDyes." Proteomics 5(12): 3105-3115.

Karp, N. A., and K. S. Lilley. (2007). "Design and analysis in quantitative proteomics studies." Proteomics 7(S1): 42-50.

King H., A. R. E., Herman W.H. (1998). "Global burden of diabetes, 1995-2025:prevalence, numerical estimates, and projections." Diabetes Care 21: 1414-1431.

Kitahara, A., Toyota, T., Kakizaki, M., Goto, Y. (1978). "Activities of hepatic enzymes in spontaneous diabetes rats produced by selective breeding of notmal Wistar rats." Tohoku J Exp Med(126): 7-11.

Klose, J. (1975). "Protein mapping by combined isoelectric focusin and electrophoresis of mouse tissues." Humangenetik 26: 231-243.

Korc, M. (2003). "Diabetes mellitus in the era of proteomics." Molecular Cell Proteomics 2: 399-404.

Kraegen, E., Cooney, GJ. (2008). "Free fatty acids and skeletal muscle insulin resistance." Current opinion in Lipidology(19): 235-241.

Krebs, H. A., and W. A. Johnson. (1980). "The role of citric acid in intermediate metabolism in animal tissues." FEBS Lett 117(Suppl:K1-10).

Krook, A., Kawano, Y., Song, XM., Efendic, S., Roth, RA., Wallberg-Henriksson, H., Zierath, JR. (1997). "Improved glucose tolerance restores insulin-stimulated

Akt kinase activity and glucose transport in skeletal muscle from diabetic Goto-Kakizaki rats." Diabetes(46): 2110-2114.

Leahy, J. (2005). "Pathogenesis of type 2 diabetes mellitus." Archives of Medical Research 36: 197-209.

Lowell, B., Shulman, GI. (2005). "Mitochondrial dyafunction and type 2 diabetes." Science(307): 384-387.

Lui, Y., Jeton, TL., Leahy, JL. (2002). "Beta-cel adaptation to insulin resistance. Increased pyruvate carboxylase and malate-pyruvate shutle activity in islets of nondiabetic Zucker faty rats." Journal of Biological Chemistry 277: 39163-39168.

Luna, M. (2005). "Genes and type 2 diabetes mellitus." Arch Med Res 36: 210-222.

MacCoss, M., Wu, CC., Lui, H., Sadygov, R., Yeats, JR. (2003). "A Correlation Algorythm for the Automated Quantitative Analysis of Shotgun Proteomics Data." Analytical Chemistry 75: 6912-6921.

Maclay, W. (1956). "Factors afecting the solubility of nonionic emulsifiers." Journal of Colloid Science 11(3): 272-285.

Mann, M., Hendrickson, RC., Pandey, A. (2001). "Analysis of proteins and proteomes by mass spectrometry." Annual Review of Biochemistry 70: 437-473.

Mannaerts, G. P., L. J. Debeer, J. Thomas, and P. J. De Schepper (1979). "Mitochondrial and peroxisomal fatty acid oxidation in liver homogenates and isolated hepatocytes from control and clofibrate-treated rats. ." Journal of Biochemistry 254(11): 4585-95.

Marouga, R., David, S., Hawkins, E. (2005). "The development of the DIGE system: 2D fluorescence diference gel analysis technology." Analytical and Bioanalytical Chemistry 382(3): 669-678.

Matuda, S., Kodama, J., Goshi, N., Takase, C., Nakano, K., Nakagawa, S., Ohta, S. (1997). "À polypeptide derived from mitochondrial dihydrolipoamide succinyltransferase is located on the plasma membrane of skeletal muscle. ." Biochem Biophys Res Commun(241): 151-156.

McBride, H., Neuspiel, M., Wasiak, S. (2006). "Mitochondria:More than just a powerhouse." Current Biology(16): R551-R560.

Miao, L., St Clair, DK. (2009). "Regulation of superoxide dismutase genes: implications in disease." Free Radical Biology and Medicine 47(4): 344-356.

Mitchell, P. (1961). "Coupling of phosphorylation to electron and hydrogen transfer by a chemi-osmotic type of mechanism." Nature 191: 144-148.

Mogensen, M., Sahlin, K., Fernstroem, M., Glintborg, D., Vind, BF., Beck-Neilsen, H., and Hojlund, K. (2007). "Mitochondrial respiration is increased in skeletal muscle of patients with type 2 diabetes.
." Diabetes(56): 1592-1599.

Moore, P., Huxley, HE., DeRosier, DJ. (1970). "3D reconstruction of F-actin, thin filaments and decorated thin filaments." Journal of Mlecular Biology(50): 279-297.

Mullen, E., Ohlendieck, K. (2010). "Proteomic Profiling of non-obese type 2 diabetic skeletal muscle." International Journal of Molecular Medicine 25: 45-458.

Mulvey, C., Harno, E., Keenan, A., Ohlendieck,K. (2005). "Expression of the skeletal muscle dystrophin-dystroglycan complex and syntrophin-nitric oxide synthase complex is severly affected in the type 2 diabetic Goto-Kakizaki rat." European Journal of Cellular Biology 85: 867-883.

Mulvey, C., Mullen, E., Ohelndieck, K. (2008). "The pathobiochemical role of the dystrophin-dystrpglycan complex and the Ca2+-handling apparatus in diabetes-related muscle weakness (Review)." Molecular Medicin Reports(1): 297-306.

Murin, R., Schaer, A., Kowwtharapu, BS., Verieysdonk, S., Hamprecht, B. (2008). "Expression of 3-hydroxy-isobutyrate dehydrogenase in cultured neural cells." Journal of Neurochemistry(105): 1176-1186.

Neuhoff, V., Arold, N., Taube, d., and Ehrhardt, W. (1988). "Improved staining of proteins in polyacrylamide gels including isoelectric focusing gels with clear backrounds at nanogram sensitivity using Coomssie Brilliant Blue G-250 and R-250." Electrophoresis(9): 255-262.

Nicholl, I., Quinlan, RA. (1994). "Chaperone activity of alpha-crystallins modulates intermediate filament assembly." EMBO Journal 13(4): 945-953.

Nigg, B., Herzog, W. (1994). "Biomechanics of the musclo-skeletal system." England John Wiley and Sons.

Nishimura, R., Sharp, FR. (2005). "Heat shock proteins and neuromuscular disease " Muscle & Nerve 32(6): 693-709.

O'Connell, K., Gannon, J., Doran, P., Ohlendieck, K. (2007). "Proteomic Profiling reveals a severly perturbed protein expression pattern in aged skeletal muscle." International Journal of Molecular Medicine(20): 145-153.

O'Connell, K., Ohlendieck, K. (2009). "Proteomic DIGE analysis of the mitochondria-enriched fraction from aged rat skeletal muscle." Proteomics(9): 5509-5524.

O'Farrell, P. (1975). "High resolution two-dimensional gel electrophoresis of proteins." Journal of Biological Chemistry 250: 4007-4021.

Ohlendieck, K. (2010). "Proteomics of skeletal muscle differentiation, neuromuscular disorders and fibre aging." Biochimica et Biophysica Acta(1804): 2089-2101.

Ohlendieck, K. (2010). "Proteomics of skeletal muscle glycolysis." Biochimica et Biophysica Acta 1804(11): 2089-2101.

Okumura, N., Hashida-Okumura, A., Kita, K., Matsubae, M., Takao, T., Nagai., K. (2005). "Proteomic analysis of slow- and fast-twitch skeletal muscles." Proteomics(6): 321-340.

Pagel-Langenickel, I., Bao, J., Pang, L., Sack, MN. (2010). "The role of mitochondria in the pathophysiology of skeletal muscle in insulin resistance." Endocrine Reviews(31): 25-51.

Park, S. W., Goodpaster, B.H, Strotmeyer, E.S, de Rekeneire, N, Harris, T.B, Schwartz, A.V, Tylavaky, F.A, Newman, A.B. (2006). "Decrased muscle strength and quality in older adults with type 2 diabetes." Diabetes 55: 1813-1818.

Park, S. W., Goodpaster, B.H, Lee,JS., Kuller, LH., Boudreau, R., de Rekeneire, N, Harris, T.B, Kritchevsky, S., Tylavsky, FA., Nevitt, M., Cho, YW., Newman, A.B. (2009). "Health, aging and body composition study: Excessive loss of skeletal muscle mas in older adults with type 2 diabetes." Diabetes Care 32(1): 1993-1997.

Pennington, S., Wilkins, MR., Hochstrasser, DF., Dunn, MJ. (1997). "Proteome analysis: from protein characterization to biological function." Trends in Cell Biology 7(4): 168-173.

Perseghin, G., Ghosh, S., Gerow, K., Shulman, GI. (1997). "Metabolic defects in lean nondiabetic offspring of NIDDM parents: a cros-sectional study. ." Diabetes 46: 1001-1009.

Petersen, K., Shulman, GI. (2002). "Pathogenesis of skeletal muscle insulin resistance in type 2 diabetes mellitus." American Journal of Cardiology 90(G11-G18).

Pheilix, E., Mensink, M. (2008). "Type 2 diabetes mellitus and skeletal muscle metabolic function." Physiol Behav(94): 252-258.

Piec, I., Listrat, A., Alliot, J., Chambon, C., Taylor, RG., Bechet, D. (2005). "Differential proteome analysisof aging in rat skeletal muscle." Federation of American Societies for experimental Biology 19: 1143-1145.

Porte, D., Kahn, SE. (2001). "beta-cell dysfunction and failure in type 2 diabetes: potential mechanisms." Diabetes 50(1): S160-S163.

Portha, B., Serradas, P., Bailbe, D., Suzuki, K., Goto, Y., Giroix, MH. (1991). "Beta-cell insensitivity to glucose in the GK rat, a spontaneous non-obese model for type 2 diabetes. ." Diabetes 40: 486-491.

Portha B. Transmitted beta-cell dysfunction as a cause for type 2-diabetes. Med Sci (Paris) 2003; 19: 847–853.

Prentki, M., Nolan, CJ. (2006). "Islet b cell failure in type 2 diabetes. ." Journal of Clinical Investigation 116(7): 1802-1812.

Proenza, C., O'Brien, J., Nakai, J., Mukherjee, S., Allen, PD., Beam, KG. (2002). "Identification of a region of the RyR1 that participates in allosteric coupling with alpha1s(Cav1.1) 2-3 loop." Journal of Biological Chemistry 227(8): 6530-6535.

Punkt, K. (2002). "Fibre types in skeletal muscles." Adv Anat Embryol Cell Biol 162: 1-109.

Rabilloud, T., Strub, JM., Luche, S., van Dorselaer, A., Lunardi, J. (2001). "A comparison between Sypro Ruby and ruthenium 2 tris(bathophenanthroline disulfonate) as fluorescentstains for protein detection in gels." Proteomics(1): 699-704.

Rabilloud, T., Vaezzadeh, AR., Potier, N., Lelong, C., Leize-Wagner, E., Chevallet, M. (2009). "Power and limtations of electrophoretic separations in proteomic strategies." Mass Spectrometry Reviews 28(5): 816-843.

Reedy, M. (2000). "Visualising myosins power stroke in muslce contraction." Journal of Celular Science 113(20): 3551-3562.

ROBERT E. DAVIS, S. M., CORINNA HERRNSTADT, SOUMITRA S. GHOSH, EOIN FAHY,, D. G. L. J. T. LESLIE A. SHINOBU, M. FLINT BEAL, NEIL HOWELL,, et al. (1997). "Mutations in mitochondrial cytochrome c oxidase genes segregate
with late-onset Alzheimer disease." PNAS 94(9): 7.

Ruiz-Romero, C., Blanco, FJ., (2009). "Mitochondrial proteomicsand its application in biomedical research." Molecular BioSystems(5): 1130-1142.

Sadowski, P., Groen, AJ., Dupree, P., Lilley, KS. (2008). "Sub-cellular localisation of membrane proteins
" Proteomics 8: 3991-4011.

Sander, G., Giles, TD. (2003). "Diabetes Melliyus and heart failure." Am Heart Hosp J 1: 273-280.

Sano, S., S. Inoue, Y. Tanabe, C. sumiya, and S.koike. (1959). "Significance of mitochondria for porphyrin and heme biosynthesis." Science 129(3344): 275-6.

Saraste, M. (1999). "Oxidative phosphorylation at the fin de siecle." Science 283(5407): 1488-93.

Scheen., A. (2003). "Pathophysiology of type 2 diabetes." Acta Clin Belg(58): 335-341.

Schejter, E., Baylies, MK (2010). "Born to run: creating the muscle fibre." Current Opinion in Cell Biology 22: 566-574.

Shen, W., Hao, J., Tian, C., Ren, J., Yang, L., Li, X., Luo, C., cotma, CW., Lui, J. (2008). "A combination of nutrients improves mitochondrial biogenesis and

function in skeletal muscle of type 2 diabetic Goto-Kakizaki rats." PloS One(3): E2328.

Smithies, O., Poulik, MD. (1956). "Two Dimensional electrophoresis of serum proteins." Nature 177: 1033.

Sohal, R., Forster, MJ. (2007). "Coenzyme Q oxidative stress and aging." Mitochondrion(7): S103-S111.

Staples, G. O., Bowman, M.J., Costello, Hitchcock, A.M., Lau, J.M., Leymarie, N., Miller, C., Naimy, H., Shi, X., Zaia, J. (2009). "A chip-based amide-HILIC LC/MS platform for glycosaminoglycan glycomics profiling." Proteomics 9: 686-695.

Steil, G. (2001). "Adaptation of beta-cell mass to substrate oversupply: enhanced function with normal gene expression." American journal of Physiology and Endocrinology Metabolism 280: E788-E796.

Steiler, T., Galuska, D., Leng, Y., Chibalin, AV., Gilbert, M., Zierath, JR. (2003). "Effect of hyperglycemia on signal transduction in skeletal muscle from diabetic Goto-Kakizaki rats. ." Endocrinology(144): 5259-5267.

Stentz, F., Kitabchi, AE. (2007). "Transcriptome and proteome expressions involved in insulin resistance in muscle and activated T-lymphocytes of patients with type 2 diabetes." Genomics Proteomics Bioinformatics(5): 216-235.

Stevens, T., Arkin, IT. (2000). "Do more complex organisms have a greater proportion of membrane proteins in their genomes?" Proteins 39: 417-422.

Straub, F. (1942). "Actin." Stud Inst Med Chem Univ Szeged 2: 3-15.

Sundsten, T., Ortsaeter, H. (2009). "Proteomics in diabetes research." Molecular Cell Endocrinology(297): 93-103.

Suzuki N, Aizawa T, Asanuma N et al. An early insulin intervention accelerates pancreatic beta-cell dysfunction in young Goto-Kakizaki rats, a model of naturally occur- ring noninsulin-dependent diabetes. Endocrinology 1997; 138: 1106–1110.

Szent-Gyorgyi, A. (1953). "Meromyosins, the subunits of myosin." Arch of Biochem and Biophys 42: 305-320.

Tabb, D., MacCoss, MJ., Wu, CC., Anderson, SD., Yeats, JR. (2003). "Similarity amoung tandem mass spectra from proteomic experiments, detection, significance and utility." Analytical Chemistry 75: 2470-2477.

Tan, S., Tan, HT., Chung, MC. (2008). "Membrane proteins and membrane proteomics." Proteomics 8: 3924-3932.

Tanford, C., Reynolds, JA. (1976). "Characterisation of membrane proteins in detergent solutions." Biochimica et Biophysica Acta 26(457): 13-170.

Tao, T., Gong, BJ., Leavis, PC. (1990). "Calcium-induced movement of troponin-1 relative to actin in skeletal muscle thin filaments." Science 247(4948): 1339-1341.

Tonge, R., Shaw, J., Midleton, B., Rowlinson, R., Rayner, S., Young, J., Pognan, F., Hawkins, E., Currie, I., Davison, M. (2001). "Validation and development of fluorescence two-dimensional diferential gel electrophoresisproteomics technology." Proteomics 1(3): 377-396.

Towbin, H., Staehelin, T., Gordon, J. (1979). "Electrophoretic transfer of proteins from polyacrylamide gels to nitrocellulose sheets, procedure and some applications." Proceedings of the National Academy of Sciences 76: 4350-4354.

Tusie-Luna, M. (2005). "Genes and type 2 diabetes mellitus." Archives of Medical Research 36(3): 210-222.

Unger, R. (1995). "Lipotoxicity in the pathogenesis of obesity dependent NIDM. Genetic and Clinical Implications." Diabetes 44: 863-870.

Unlu, M., M. E. Morgan., J. S. Minden. (1997). "Difference gel electrophoresis. A single gel method for detecting changes in protein extracts." Electrophoresis 18(11): 2071-2077.

van Montfort, R., Slingsby, C., Vierling, E. (2001). "Structure and function of the smal heat shcok protein/alpha-crystallinfamily of molecular chaperones." Advances in Protein Chemistry 59: 105-156.

Viswanathan, S., Unlu, M., Minden, JS., (2006). "Two-dimesnsional difference gel electrophoresis." Nature Protocols 1: 1351-1358.

Waterlow, J. (1976). "The relative importance of muscle protein synthesis and breakdown in the regulation of muscle mass." Journal of Biochemistry(156): 185-188.

Weiss, W., Gorg, A. (2009). "High-resolution two-dimensional electrophoresis." Methods in Molecular Biology 564: 13-32.

Westermeier, R., Schickle, H. (2009). "The current state of the art in high-resolution two-dimensional electrophoresis." Archives of Physiology and Biochemistry 115(5): 279-285.

Wild, S., Roglic, G., Green, A., Sicre, R., King, H. (2004). "Global prevalence of diabetes: estimates for the year 2000 and projections for 2030." Diabetes Care 27(5): 1047-1053.

Wilkins, M. R., Sanches, J.C., Gooley, A.A., Appel, R.D., Humphery-Smith, I., Hochstrasser, D.F. and Williams, K.L. (1996). "Progress with proteome projects, why all proteins expresed by a genome should be identified and how to do it." Biotechnol Genet Engin Rev 13: 19-50.

Witte, K., Jacke, K., Stahrenberg, R., Arlt, G., Reitenbach, I., Schilling, L., Lemmer, B. (2002). "Dysfunction of soluble guanylylcyclase in aorta and kidney of Goto-Kakizaki rat: influence of age and diabetic state." Nitric Oxide 6(1): 85-95.

Wittmann-Liebold, B., Graack, HR., Pohl, T. (2006). "Two-dimensional gel electrophoresis as a tool for proteomics studies in combination with protein identification by mass spectrometry. ." Proteomics 6(17): 4688-4703.

Yan, J., Harry, RA., Wait, R., Welson, SY., Emery, PW., Preedy, VR., Dunn, MJ. (2001). "Separation and identification of rat skeletal muscle proteins using two-dimesional gel electrophoresis and mass spectrometry." Proteomics(1): 424-434.

Yasuda, K., Nishikawa, W., Iwanaka, N., Nakamura, E., Seino, Y., Tsuda, K., Ishihara, A. (2002). "Abnormality in fibre type distribution of soleus and plantaris muscles in non-obese diabetic Goto-Kakizaki rats." Clinical Experimental Pharmacology and Physiology(29): 1001-1008.

Zechner, R., Kienesberger, PC., Haemmerle, G., Zimmermann, R., Lass, A. (2009). "Adipose triglyceride lipase and the lipolytic catabolism of cellular fat stores." Journal of Lipid Research(50): 3-21.

Zimmet, P., Alberti, KG., Shaw, J. (2001). "Global societal implications of the diabetes epidemic." Nature.(414): 782-787.

Zorzano, A., Liesa, M., Palacin, M. (2009). "Mitochondrial dynamics as a bridge between mitochondrial dysfunction and insulin resistance." Arch Physiol Biochem(115): 1-12.

Zuo, X., Speicher, DW. (2002). “Comprehensive analysis of complex proteomes using microscale solution isoelectric focusing prior to narrow pH range two-dimensional electrophoresis.

Publications

Mulvey C, **Mullen** E, Ohlendieck K. 2008. The pathobiochemical role of the dystrophin-dystroglycan complex and the Ca^{2+}-handling apparatus in diabetes-related muscle weakness (Review). Mol Med Rep., 1: 297-306.

Mullen E, Ohlendieck K. 2009. Proteomic profiling of non-obese type 2 diabetic skeletal muscle. Int. J Mol Med., 25: 445-58.

Donoghue P, Staunton L, **Mullen E**, Manning G, Ohlendieck K. 2010. DIGE analysis of rat skeletal muscle proteins using non-ionic detergent phase extraction of young adult versus aged gastrocnemius tissue. Journal of Proteomics. 73: 1441-53.

Mullen E, Ohlendieck K. 2010. Skeletal muscle from the Goto-Kakizaki rat model of type 2 diabetes exhibit increased levels of the small heat shock protein Hsp27. Journal of Intergratedomics.

Mullen E, Ohlendieck K. 2010. Proteomics analysis of the mitochondria-enriched fraction fromdiabetic rat skeletal muscle. (In press)

Presentations

Waters Postgraduate Prize

2009 “The membrane proteome of diabetic skeletal muscle from the non-obese Goto-Kakizaki rat.”

3rd EuPA Congress

2009 “The proteomic profiling of skeletal muscle tissue from the Goto-Kakizaki rat.

Departmental Seminars

2008 “Proteomic profiling of type 2 diabetes.”

2009 “The sub-proteomes of type 2 diabetes”

Publications